

AN ABSTRACT OF THE THESIS OF

Jatila Ranasinghe for the degree of Master of Science
in Mechanical Engineering presented April 16, 1986 .

Title: Analysis of Ceramic Heat Exchangers for Use in a
Combined-Cycle, Wood-Fired Power Plant

Abstract approved: _____ **Redacted for Privacy**
Gordon M. Reistad

This report presents the analysis of ceramic heat exchangers for use in a combined-cycle, wood-fired power plant. The combined-cycle system investigated is characterized by having a wood-fueled combustor, an indirect-fired gas turbine, and a Rankine steam cycle.

The direct use of low-grade fuels, such as wood, in present gas turbines will present difficulties due to corrosion and erosion of the turbine components from the particulate matter in the exhaust gases. This difficulty can be overcome by indirectly firing the gas turbine with the transfer of energy from the combustion gases to the compressor air by means of a heat exchanger. Gas turbines suitable for this type of power plant operate at their maximum efficiency at the rated turbine inlet temperature, typically in the range of 1750 F. Modern ceramics exhibit excellent high temperature strength, and hence a ceramic heat exchanger is considered a very suitable candidate for

such applications.

In the power plant considered, air enters the heat exchanger at 540 F where it is heated to the turbine inlet temperature. Since a compact unit with low leakage was desired, a multiple gas-side pass, cross-flow heat exchanger was selected for the present application.

A model was developed to simulate the ceramic heat exchanger. This model was used to size a heat exchanger for the power plant.

The influence of the ceramic heat exchanger on the overall power plant performance were analyzed. The other plant components were simulated by using a computer code developed during previous studies of this power plant. The ceramic heat exchanger system was compared with a metallic heat exchanger system. Since leakage was recognized as a major difficulty in ceramic heat exchangers, the effects of leakage on the overall plant performance was analyzed. Finally, the ceramic heat exchanger system was compared to other possible methods of obtaining a high turbine inlet temperature.

The results of the study indicate that the use of a ceramic heat exchanger has good potential for this type of power plant. It was also observed that losses due to heat exchanger leakage justify further research towards the development of better sealing arrangements, for high temperature and high pressure applications.

ANALYSIS OF CERAMIC HEAT EXCHANGERS FOR USE IN A
COMBINED-CYCLE, WOOD-FIRED POWER PLANT

by

Jatila Ranasinghe

A THESIS

submitted to

Oregon State University

in partial fulfillment of
the requirement for the
degree of

Master of Science

Completed April 16, 1986

Commencement June 1986

APPROVED:

Redacted for Privacy

Professor of Mechanical Engineering in charge of major

Redacted for Privacy

Head of department of Mechanical Engineering

Redacted for Privacy

Dean of Graduate School

Date thesis is presented April 16, 1986

ACKNOWLEDGEMENT

I would like to thank my major professor, Dr. Gordon Reistad for the valuable advise given to me during this study.

I would also like to thank my co-workers in the biomass project, Abbas Dadkhah-nikoo, Jerry Stephenson, John Robbins, Jai-Hyo Lee, and fellow graduate students, Sigurdur Brynjólfsson and Don Elger for their support and friendship during the past year.

Last but defenitely not the least, I thank my late father Karunaratne and my mother Marlene for their love and faith in me throughout my life.

TABLE OF CONTENTS

	Page
Chapter 1 - INTRODUCTION	1
Chapter 2 - CERAMIC HEAT EXCHANGER TECHNOLOGY.....	7
2.1 Ceramic Materials.....	7
2.2 Current Limitations.....	8
2.3 Some Practical Units.....	10
2.4 Conclusions.....	15
Chapter 3 - EROSION OF CERAMICS.....	16
3.1 Post Erosive Strength.....	16
3.2 Conditions to Prevent Erosion.....	19
3.3 Maximum Gas Velocity.....	20
Chapter 4 - MATHEMATICAL MODELS.....	25
4.1 Ceramic Cross-Flow Heat Exchanger.....	25
4.1.1 Model Development.....	25
A. Energy Balance.....	29
B. Correction Factor F.....	29
C. UA required.....	30
D. Inside Heat Transfer Coefficient.....	31
E. Outside Heat Transfer Coefficient.....	31
F. Overall Heat Transfer Coefficient.....	33
G. Pipe Length.....	33
H. Modelling of Leakage.....	35
4.1.2 Controls.....	35
A. Maximum Velocity.....	37
B. Maximum Shell-Side Pressure Drop.....	37
C. Maximum Pressure Drop Inside the Pipes.....	38
D. Maximum Tube Length.....	39
E. Minimum Velocity and Pressure Drop on Shell-Side...	39
F. Minimum Pipe Length and Pressure Drop Inside the Pipe.	40
4.1.3 Comments.....	40
4.2 Segmentally-Baffled Shell-and-Tube Heat Exchanger.....	41
4.2.1 Model Development.....	41
A. Basic Heat Exchanger Parameters.....	43

	B. Evaluation of LMTD.....	47
	C. Heat Transfer Coefficient Inside the Pipes.....	48
	D. Shell-Side Heat Transfer Coefficient.....	49
	E. Pipe length.....	53
	F. Modelling of Leakage.....	53
4.2.2	Controls.....	53
	A. The Velocity and Pressure Drop on Shell-Side.....	53
	B. Tube Length and Pressure Drop Inside the Pipe.....	57
Chapter 5	- RESULTS FROM HEAT EXCHANGER SIMULATIONS..	58
5.1	Model Behavior.....	58
	5.1.1 Shell-and-Tube Heat Exchanger....	58
	5.1.2 Cross-Flow Heat Exchanger.....	61
5.2	A Ceramic Heat Exchanger for the Biomass Power Plant.....	65
5.3	Conclusions.....	67
Chapter 6	- ANALYSIS OF PLANT PERFORMANCE.....	71
6.1	Plant Description.....	71
6.2	Computer Models Used.....	74
6.3	The Ceramic Heat Exchanger System.....	75
	6.3.1 Influence of Wood Moisture.....	75
	6.3.2 Influence of Leakage.....	81
	6.3.3 Turbine Inlet Temperature.....	84
6.4	Comparison with Alternative Systems....	84
6.5	Conclusions.....	88
BIBLIOGRAPHY	89
APPENDICES		
A.	DESCRIPTION OF SYSTEMS.....	91
B.	HEAT EXCHANGER MODELS.....	96
C.	INPUT DATA TO HEAT EXCHANGER MODEL.....	119

LIST OF FIGURES

<u>Figure</u>	<u>Page</u>
1.1 Operating boundaries for heat exchanger materials.....	3
2.1 Multiple gas-side pass ceramic cross-flow heat exchanger developed by Hauge International.....	11
2.2 Ceramic cross-flow Heat exchanger under development by Garret-Airesearch.....	13
2.3 Multiple air-side pass ceramic cross-flow heat exchanger being developed by Airsearch Manufacturing Co. of California....	14
3.1 The post-erosion strength of ceramics as a fuction of the kinetic energy of the impacting particles.....	18
3.2 Typical Particle sizes and ranges of effective operation of various collectors....	22
3.3 The maximum allowable velocity of the flue gas as a function of the diameter of the dust particles.....	24
4.1 A schematic diagram of a 'U' tube.....	27
4.2 Typical tube arrangement in an inline, cross-flow heat exchanger.....	28
4.3 Flow diagram for the ceramic cross-flow heat exchanger model.....	34
4.4 Model used to simulate the leakage in the ceramic heat exchanger.....	36
4.5 A schematic diagram of a segmentally-baffled shell-and-tube heat exchanger.....	44
4.6 Tube length definitions for the segmentally-baffled shell-and-tube heat exchanger.....	44
4.7 Basic baffle geometry relations.....	45
4.8 Relationship between the baffle cut height (Lbch) and baffle cut (Bc).....	45

4.9	Flow diagram for the segmentally-baffled shell-and-tube heat exchanger.....	54
5.1	Correction factor F for a segmentally-baffled shell-and-tube heat exchanger.....	59
5.2	Typical results obtained from the multiple air-side pass, ceramic cross-flow heat exchanger model, controls(dPamax = 6 psi, lmax = 11 ft, Dersn = 500 microns).....	62
5.3	Typical results obtained from the multiple air-side pass, ceramic cross-flow heat exchanger model (dPamax = 6 psi, lmax = 11 ft, Dersn = 500 microns).....	63
5.4	A schematic diagram of a multiple air-side pass, ceramic cross-flow heat exchanger.....	66
5.5	Typical results obtained from the multiple gas-side pass, ceramic cross-flow heat exchanger model.....	68
6.1	A schematic diagram of the biomass power plant.....	72
6.2	The yearly variation of the average wood moisture content.....	76
6.3	The plant net efficiency as a function of the fuel moisture content, at leakage flow rates of 1.5, 3.0 and 6.0 percent.....	77
6.4	The plant net power as a function of the fuel moisture content, at leakage flow rates of 1.5, 3.0 and 6.0 percent.....	77
6.5	Flue gas inlet temperature to the heat exchanger as a function of the wood moisture content.....	79
6.6	Flue gas outlet temperature from the combustor as a function of the amount of excess air used, at wood moisture contents of 10, 30 and 50 percent.....	80
6.7	Gas turbine power as a function of the wood moisture content, at leakage flow rates of 1.5, 3.0 and 6.0 percent.....	82

6.8	Steam turbine power as a function of the wood moisture content, at leakage flow rates of 1.5, 3.0 and 6.0 percent.....	82
6.9	Plant net efficiency as a function of the turbine inlet temperature.....	85
6.10	Plant net efficiency as a function of the wood moisture content, for the alternate systems of the power plant.....	87
6.11	Plant net Power as a function of the wood moisture content, for the alternate systems of the power plant.....	87

LIST OF TABLES

<u>Table</u>		<u>Page</u>
2.1	Typical engineering properties of ceramic materials.....	9
4.1	Correlational coefficients for j_i and f_i	50
6.1	System components for biomass plant.....	73

ANALYSIS OF CERAMIC HEAT EXCHANGERS FOR USE IN A COMBINED-CYCLE, WOOD-FIRED POWER PLANT

Chapter 1

INTRODUCTION

Gas turbines can be directly fired when high-grade fuels are used. However, economic factors are forcing the examination of lower-grade fuels, such as wood, in gas turbine power cycle applications. The direct use of these low-grade fuels in present gas turbines will present difficulties due to corrosion and erosion of the turbine components, from the particulate matter in the exhaust gases. This difficulty can be overcome by indirectly firing the gas turbine, with the transfer of energy from the combustion gases to the compressor air by means of a heat exchanger. The energy in the exhaust gases from the heat exchanger can be utilized by using a waste heat recovery boiler and a steam turbine.

Presently a feasibility study on a wood-fueled, combined-cycle power plant is being carried out at the Department of Mechanical Engineering, Oregon State University. In this power plant, the hot combustion gases flow through a heat exchanger heating the pressurized air supplied by the compressor. The hot compressed air stream is then expanded through the gas turbine. The turbine

exhaust is then used as combustion air. After leaving the heat exchanger, the combustion gases flow into a waste heat recovery steam generator of a conventional Rankine cycle. The plant is nominally rated at 10 MW, and is designed to be relocatable. This power plant will be here referred to as the biomass power plant. The equipment layout diagrams and the descriptions of some alternative systems of the above power plant being investigated in this report are presented in Appendix A.

Computer simulated evaluations of the base case and a number of alternative arrangements of the biomass power plant are given in reference [1]. Eleven systems have been considered in this study, and are designated as systems 1 through 11. Based on the results obtained from this study, it has been concluded that the net efficiency and net power of the systems were a strong function of the turbine inlet temperature, regardless of the systems considered. The most attractive of these systems had a turbine inlet temperature of 1800 F.

However, the heated air for the turbine will be limited in temperature by the materials in the heat exchanger. The approximate operating boundaries for various heat exchanger materials are shown in Figure 1.1. These limits correspond to comparatively clean conditions, and a reduction in these limits can be expected in a dust laden combustion gas environment. From Figure 1.1, it can

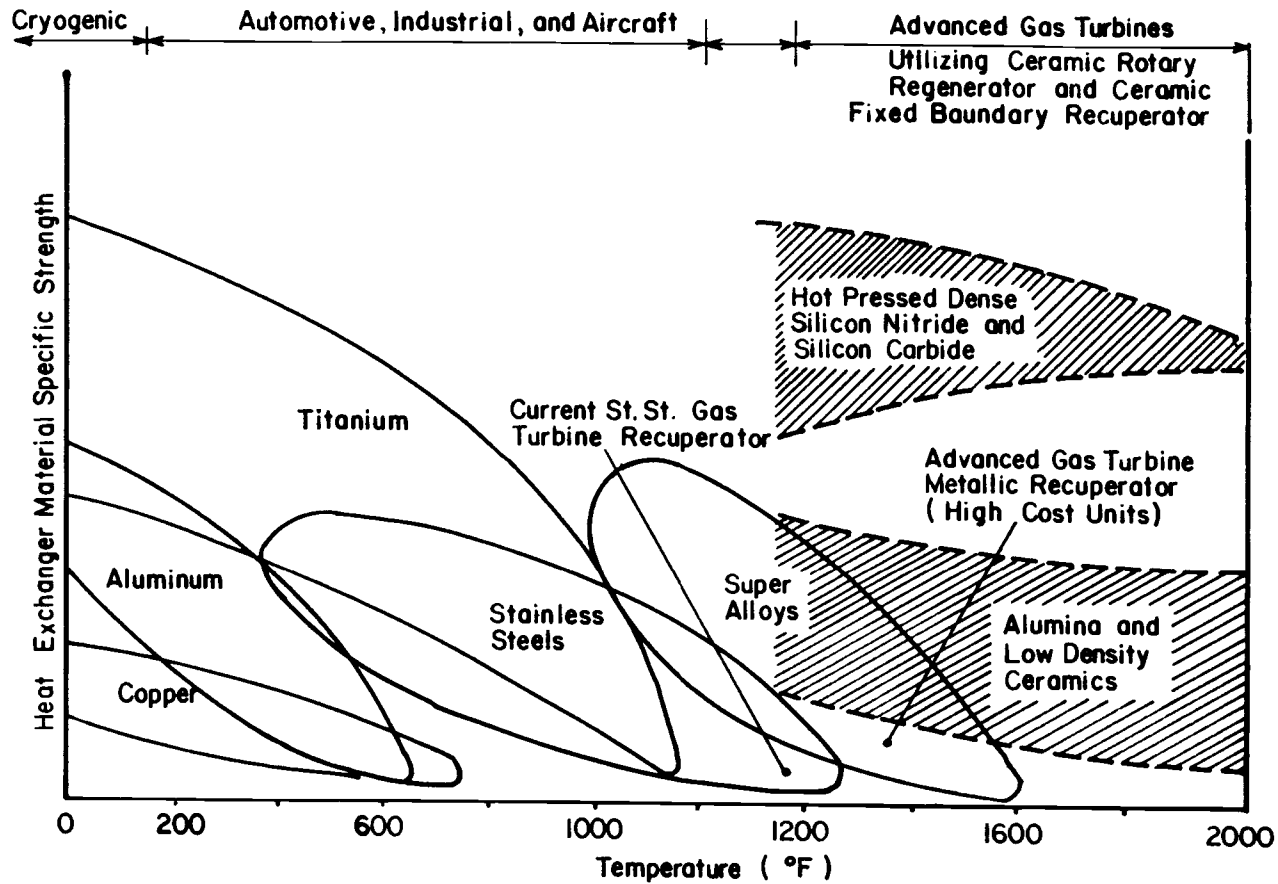


Figure 1.1 Operating boundaries for heat exchanger materials, (from [3]).

be seen that the specific strength of the metallic materials decreases very rapidly at elevated temperatures. Though 1750 F is considered to be an upper limit for practical metallic heat exchanger design [2], the highest temperature achieved in a long life metallic heat exchanger has been 1300 F, according to reference [3]. From the upper shaded portion of Figure 1.1, it can be seen that the silicon based ceramics exhibit excellent high temperature strength. Therefore a ceramic heat exchanger is considered a very suitable candidate for high temperature applications. Hence, the objective of the work presented in this report is to investigate ceramic heat exchangers for application in indirect-fired, combined-cycle power plants, fired with wood.

Sigurdur Brynjolfsson [4], carried out an investigation of heat exchangers for application in indirect-fired, combined-cycle power plants, fired with wood. The heat exchangers emphasized in that work were for low temperature applications, and hence made of metallic materials. In the mathematical model developed to simulate the heat exchanger, the type and the geometry, except the length, is user specified and the length is calculated based on the thermal rating of the heat exchanger. The flow velocities and pressure drops were hence fixed for a given flow condition and heat exchanger geometry. The development of the mathematical model to

simulate the ceramic heat exchanger is a continuation of the work done by Brynjolfsson. Some changes which were required to model a ceramic heat exchanger, and some improvements which were desired over the previous model will be explained next.

Since the power plant is wood-fired, the combustion gases will contain some solid dust particles. Although a cyclonic separator is used between the combustor and the heat exchanger, some dust particles will still go through the cyclone into the heat exchanger. Therefore the maximum velocity in the heat exchanger has to be controlled to prevent the erosion of the ceramic tubes. The minimum velocity too has to be kept above a certain value to prevent fouling and a low overall heat transfer coefficient. The maximum pressure drops have to be controlled to prevent excessive frictional power losses, and should not be too small since it would result in a low overall heat transfer coefficient. The length of the ceramic tubes has to be controlled due to strength and geometric considerations. The objective was to develop a mathematical model incorporating the above stated conditions, which was also insensitive to any initial guesses. Cross-flow heat exchangers and segmentally-baffled shell-and-tube heat exchangers will be investigated in this study.

The current status of the ceramic heat exchanger

technology and some commercially available heat exchangers, which are of interest to the present study, were investigated in Chapter 2. The erosion behavior of ceramics were investigated and an equation for the maximum allowable shell-side gas velocity was developed in Chapter 3. The mathematical models necessary to simulate a multiple tube-side pass cross-flow heat exchanger, and a segmentally-baffled shell-and-tube heat exchanger are described in Chapter 4. The results obtained from some computer simulations of the above models, and hence the type of heat exchanger which is most suitable for the biomass power plant are presented in Chapter 5. The influence of the ceramic heat exchanger on the performance of the biomass power plant, and a comparison of the ceramic heat exchanger system with a metallic heat exchanger system and trimburner system (which was an alternative method to obtain a high turbine inlet temperature) was done in Chapter 6.

Chapter 2

CERAMIC HEAT EXCHANGER TECHNOLOGY

The objective of this chapter is to investigate the current status of the ceramic heat exchanger technology. The desired properties of ceramic materials for high temperature and high pressure heat exchanger applications, and the ceramics satisfying these conditions will be initially discussed. Some disadvantages in the present generation of commercial ceramic heat exchangers will be discussed next. Finally, some commercially available ceramic heat exchangers, and some ceramic heat exchangers under development at the present time will be investigated.

2.1 Ceramic Materials

The ceramic materials for high temperature and high pressure heat exchanger applications should have the following properties,

- . high specific strength
- . low permeability
- . high thermal conductivity
- . low thermal expansion coefficient
- . good erosion and oxidation resistance
- . ability to be fabricated in practical heat exchanger geometries

- . adaptability to economic fabrication processes
- . low cost

Silicon carbides and silicon nitrides are the highest strength engineering ceramics available, and are suitable for high temperature applications, [2]. These materials are either hot pressed or reaction bonded into shape. Some typical engineering properties of these materials are presented in Table 2.1. Silicon nitride has a low thermal expansion coefficient than silicon carbide, but the thermal conductivity of silicon carbide is much higher than silicon nitride. Silicon carbides also have a good erosive resistance. Therefore silicon carbides become the preferred material for the ceramic heat exchanger tubes, and silicon nitride can be used for the construction of the tube-sheets and the enclosures. Due to its low gas permeability, reaction bonded silicon carbide is preferred over pure silicon carbide for the construction of ceramic heat exchanger tubes, [5].

2.2 Current Limitations

One of the major disadvantages in commercial ceramic heat exchangers is the limitation on the maximum operating pressure. This has been due to the difficulties encountered in designing sealing arrangements to operate efficiently at high temperatures and pressures. Ceramic heat exchangers have been tested successfully for long

Table 2.1 Typical engineering properties of ceramic materials, (from [5]).

Property	Alumina (Dense, Sintered)	Silicon Nitride (Hot Pressed)	Silicon Nitride (Reaction Bonded)	Silicon Carbide (Hot Pressed)	Silicon Carbide (Recrystallized)	Silicon Carbide / Silicone Nitride (Reaction Bonded)
Flexural strength (10 psi)						
at 70 F	46-50	130	30-35	110	16-65	115
at 2,250 F	21-44	45	40-45	80	20-40	45
Compressive strength (10 psi)	340	500	100	500	100	400
Hardness, Knoop	2,500	2,200	—	2,500	2,400	2,200
Modulus of elasticity, tension (10 psi)	45-55	45	25	62	35	52
Maximum use temperature (F)	3,092	3,000	2,600	3,360	3,200	—
Coefficient of thermal expansion, 70-2,000 F (10 in./in.-F)	4.2-4.3	1.7	1.7	2.7	2.7	2.4
Thermal conductivity, 70 F (Btu-in./hr-ft-F)	120-225	101	101	290	290	—
Density (lb/in.)	0.13-0.14	—	—	—	—	—
Electrical resistivity (ohm-cm)						
at 70 F	10^{14}	10^{11}	10^{15}	10	10^2	10^6
at 1,500 F	10^8-10^{10}	10^4	10^7	10^{-1}	10^{-1}	10^6

periods of time at pressure values of approximately 100 psi. A multiple gas-side pass ceramic heat exchanger, with an operating pressure of 176 psi, has been developed by Hauge Intl. [6], and is commercially available. Some short term test have been performed successfully, at an operating pressure of 150 psi, on multiple air-side pass heat exchanger by Airesearch Manufacturing Company [7], but it has been concluded that long term test under operating conditions will be necessary to prove the stability of the sealing system.

Another limitation in the present ceramic heat exchangers is the minimum allowable tube wall thickness. The minimum tube wall thickness of ceramic tubes, which have been operated successfully for long periods of time, is approximately 1/4 inches. Test carried out to use relatively thin walls (1/8 inch) has not been successful, and severe manufacturing defects was thought to be the reason for it, [7].

2.3 Some Practical Units

(1) A multiple gas-side pass ceramic cross flow heat exchanger has been developed by Hauge International [6], and is commercially available. A schematic diagram of the above heat exchanger is shown in Figure 2.1. The heat exchanger is capable of operating at a temperature of 2400 F. Units with two and three gas-side passes are

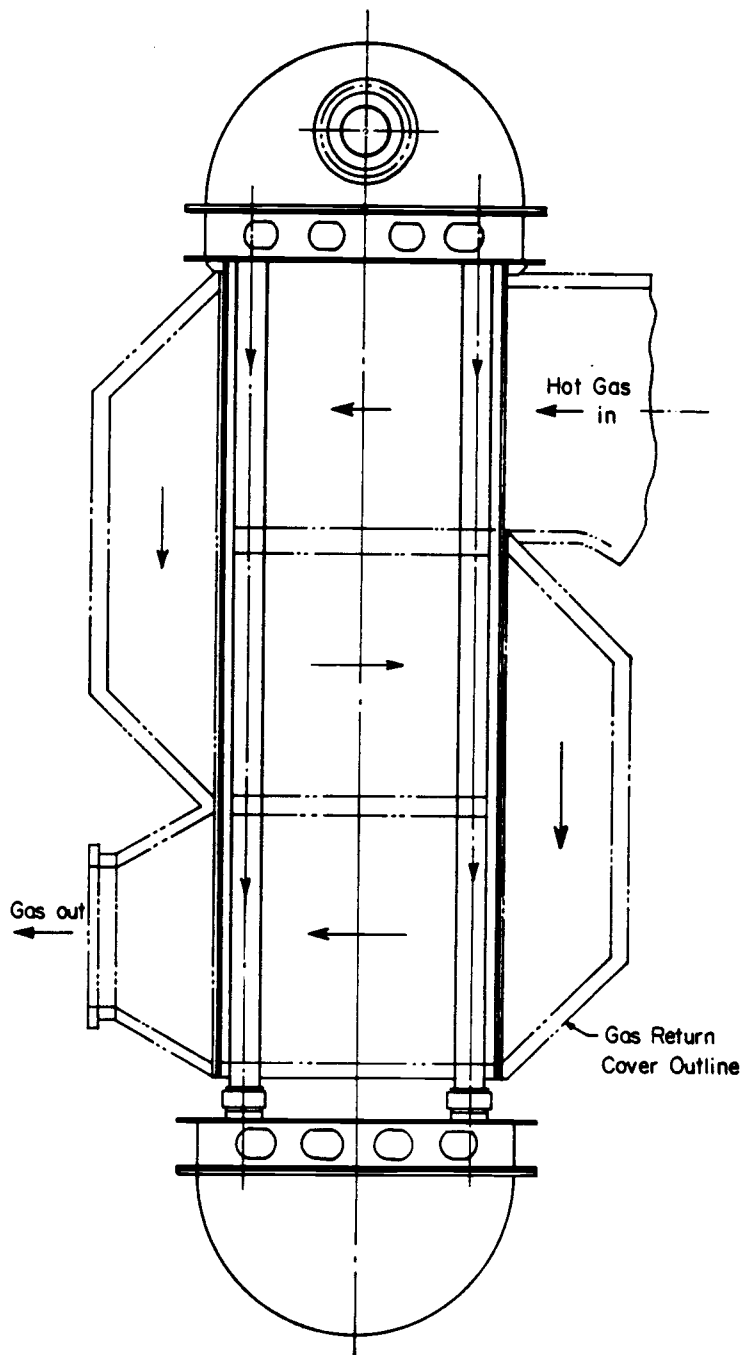


Figure 2.1 Multiple gas-side pass ceramic cross-flow heat exchanger developed by Hauge International, (from [6]).

commercially available at the present moment. The three gas-side pass unit has 36 tubes normal and 20 tubes parallel to the direction of the gas flow. The two gas-side pass unit has 20 tubes normal and 20 tubes parallel to the direction of the gas flow. The operating pressure of the second unit is 176 psi with a leakage flow rate of 1.5%. A 12 month warranty against material defects is offered by the manufacturer at this time. From the manufactures quotations [6], the cost for a two gas pass unit is \$1,820,000 and for a three gas pass unit is \$2,800,000.

(2) A ceramic cross-flow heat exchanger under development by Garret-Airesearch [8] is shown in Figure 2.2. This design is a tube-and-header ceramic recuperator in series with a plate and fin metallic recuperator. Silicon carbide is the ceramic material used, and there are two tube passes. The tube sheets and enclosures are silicon nitride bonded silicon carbide. Leakage at the tube-to-tubesheet joints, and the high air-side pressure drop has been the major difficulties faced in this design.

(3) A multiple air-side pass heat exchanger, using ceramic 'U' tubes, is being developed by Airsearch Manufacturing Company of California, [7]. Figure 2.3 shows a schematic diagram of such a heat exchanger. Siliconized silicon carbide is the ceramic material used for the heat exchanger tube construction. This unit has

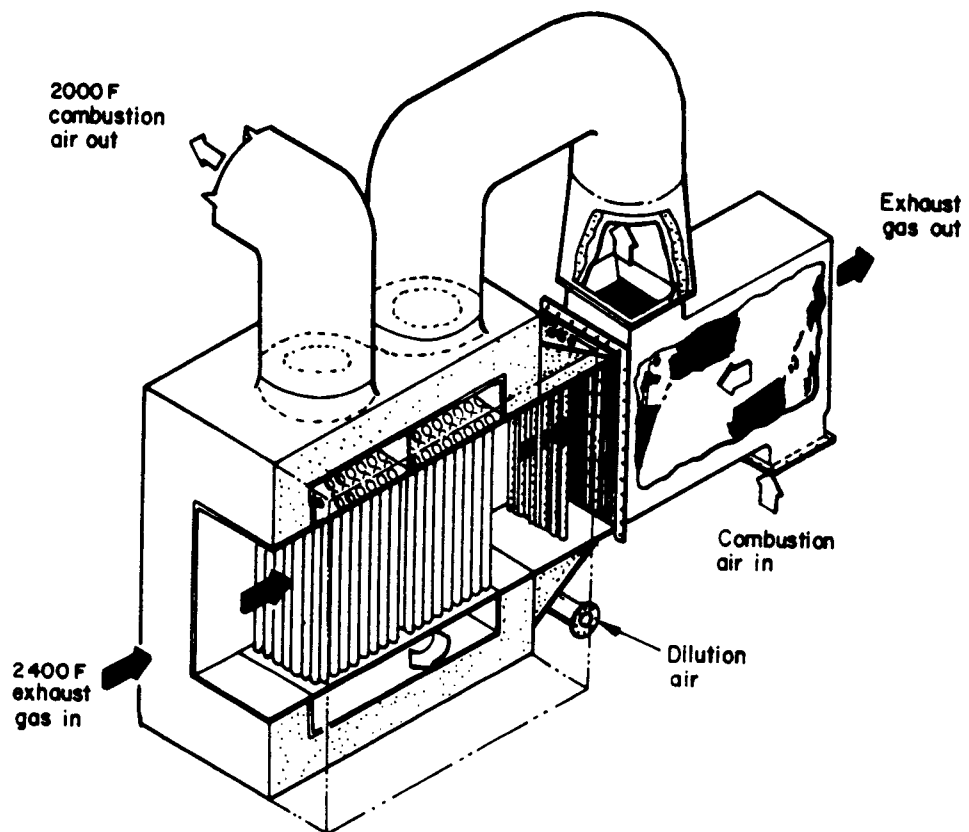


Figure 2.2 Ceramic cross-flow Heat exchanger under development by Garret-Airesearch, (from [8]).

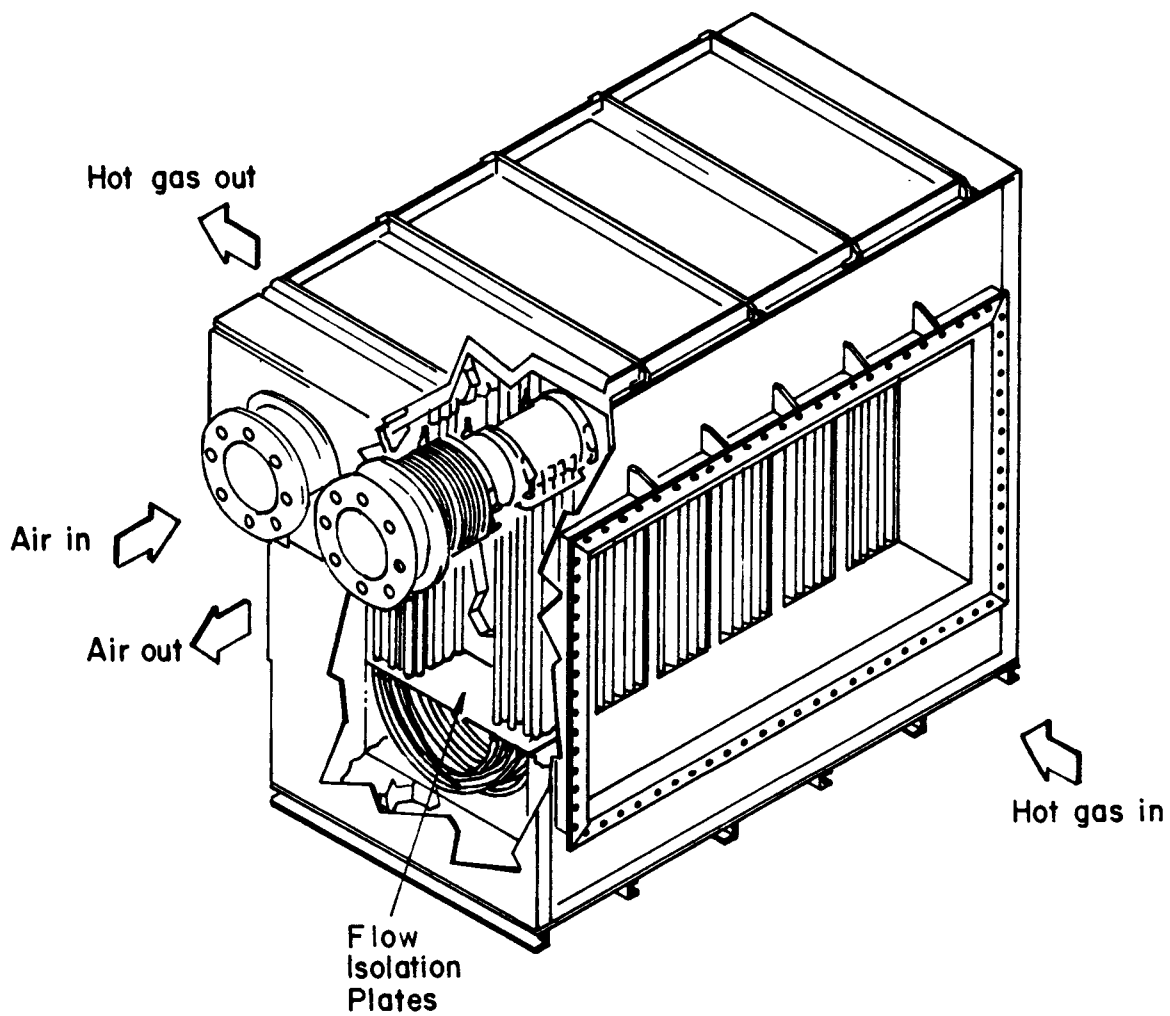


Figure 2.3 Multiple air-side pass ceramic cross-flow heat exchanger being developed by Airsearch Manufacturing Co. of California, (from [7]).

been successfully tested up to 10 hours at 150 psi. The minimum tube wall thickness, for successful operation, was limited to 1/4 inches. A maximum operating temperature of 2000 F is recommended for the ceramic material used.

2.4 Conclusions

From the above discussion it is apparent that Silicon carbide is the preferred ceramic for high temperature ceramic heat exchanger tube construction while silicon nitride can be used for the construction of the tube-sheets and the enclosures. The minimum tube wall thickness has to be approximately 1/4 inch at high operating temperatures and pressures. An operating pressure of approximately 150 psi can be considered to be a possibility at the present moment, at a leakage flow in the range of 1.5%-5%, depending on the number of joints. The maximum use temperature is approximately 2400 F.

Chapter 3

EROSION OF CERAMICS

Due to the impact of hard, sharp particles it is possible that localized surface cracking would occur in ceramics. This impact damage can lead to material losses through erosive wear, resulting in strength degradation and subsequent failure of the ceramic component. In a ceramic heat exchanger this type of failure would be due to the excessive velocities of the dust-laden shell-side gases, and has to be avoided. In this work, an equation was developed for the maximum velocity of the shell-side gases, to prevent the erosion and strength degradation of the ceramic tubes.

3.1 Post Erosive Strength

The post erosive strength can be modeled after Ritter, et al. [9,10]. In these references the effect of multiparticle impact at various temperatures and angles on the erosion rate and strength degradation has been determined. It has been concluded that the erosion rate is a function of the kinetic energy of the impacting particles, and that the erosion rate increased with increasing kinetic energy of the particles but the strength degradation leveled off to a constant value. They observed that neither erosion rate nor strength

degradation for normal impingement depended strongly on the temperature. The normalized strength after erosion (P_f/P_i) as a function of the kinetic energy of the impacting particles (U) is shown in Figure 3.1. The strength after erosion is denoted by (P_f) while (P_i) is the strength of the as received material, which is a constant. An increase in strength can be observed at higher temperatures, and was thought to be due to stress relief annealing. The erosion rate and strength degradation for normally oriented impact has been observed to be more than that at other angles. The kinetic energy is based on the maximum particle size, since it was these particles that were thought to be responsible for strength controlling flaw.

The dependency of the post-erosion strength on the kinetic energy of the impacting particles is given by,

$$\frac{P_f}{P_i} = \frac{\text{sqrt}(C_0/L)}{z*(1.+1.23\exp(-3.94x))*(1.12-.22\text{atan}(x))}$$

where, $x = K_1/(U^{1/3})$

and K_1 is a constant. The size of an annular crack is L and C_0 corresponds to the initial strength-controlling flaw size.

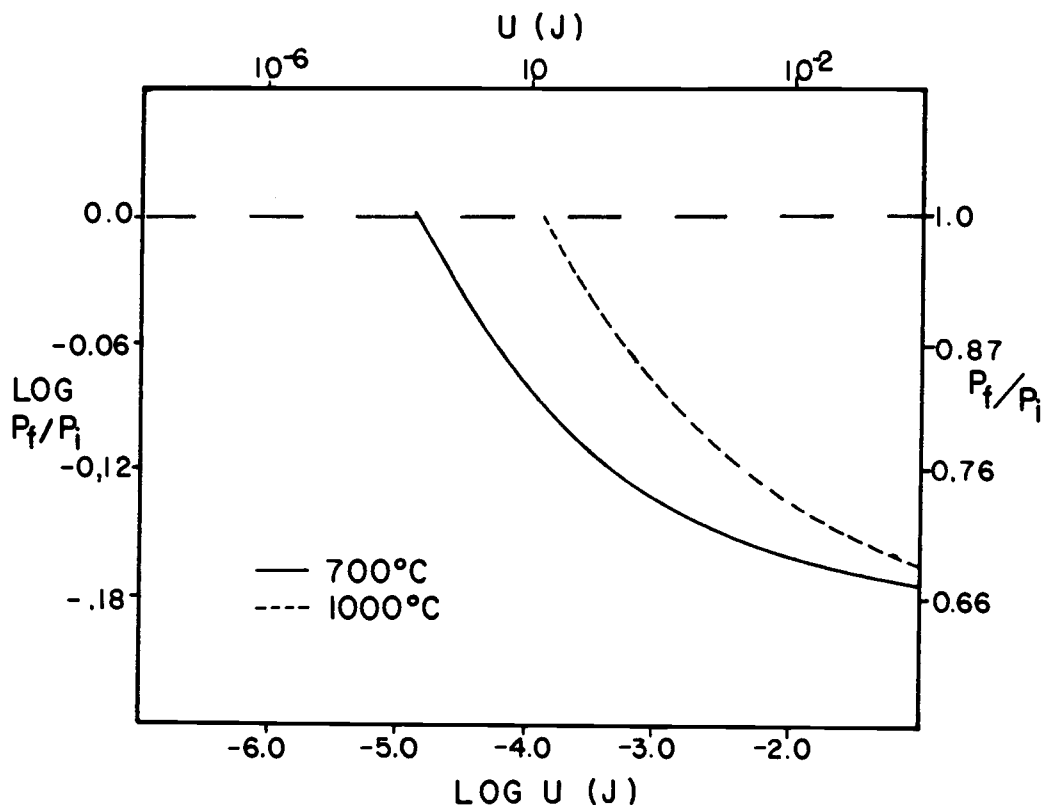


Figure 3.1 The post-erosion strength of ceramics as a function of the kinetic energy of the impacting particles, (from [9]).

3.2 Conditions to Prevent Erosion

If there is no erosion damage, the strength of the ceramic should remain equal to the initial strength. Therefore for no strength degradation, P_f/P_i should be approximately equal to 1.

The quantity $(\sqrt{C_0/L})/z$ can be evaluated by considering the results at high kinetic energies. At high kinetic energies the post erosive strength approaches a constant value which is independent of the temperature. For large values of U , at 25C,

$$\frac{P_f}{P_i} = \frac{\sqrt{C_0/L}}{2.5*z}$$

and this equal to a constant. Reference [9] gives this value of the constant as equal to 0.65.

This yields $(\sqrt{C_0/L})/z = 1.625$, which is applicable to all temperatures. From the above equations and results,

$$x = \frac{-1}{3.94 * \ln(1/1.23 * (1.625 / (1.12 - .22 \tan(x)) - 1))}$$

and solving numerically,

$$x = .2207$$

The value of the threshold constant K_1 is given in Reference [9] as,

$$K_1 = .00538 \quad \text{at 23C and 700C}$$

$$K_1 = .0115 \quad \text{at 1000C}$$

Since, $x = k_1/(U^{1/3})$ and $U = 0.5*(M)*(V_{ersn}^2)$ the maximum velocity, not to cause any erosion of the ceramic tubes can be calculated as,

$$V_{ersn} = \{(2/M)^{.5}\}*\{(k_1/x)^{1.5}\}$$

and substituting for x and k_1 ,

$$V_{ersn} = \frac{.005382}{\sqrt{M}} * F_1 \quad \text{at 23C and 700C, and}$$

$$V_{ersn} = \frac{.016821}{\sqrt{M}} * F_1 \quad \text{at 1000C.}$$

In the above equation, (V_{ersn}) is in m/s and the mass of the impacting particles (M) is in kg. To take into account any manufacturing defects which could be present on the ceramic tubes, a safety factor F_1 was introduced in the equation for the maximum velocity. The value of F_1 is assumed to be equal to 0.7 for the remaining calculations.

3.3 Maximum Gas Velocity

The above analysis was based on data obtained for alumina. It was concluded in Chapter 2 that silicon carbide was the most suitable ceramic material for heat exchanger tube construction. Information on the erosion behavior of silicon carbide was not found in the literature. However, the hardness of silicon carbide and alumina are approximately equal (see Table 2.1), and hence

the results obtained for alumina can be used with confidence for silicon carbide.

It is evident from the above equations that the maximum velocity to cause erosion, V_{ersn} , is higher at 1000 C than at 700 C. For design purposes the value of the velocity at the lower temperatures will be taken, since then it will be valid at the higher temperature too.

Multiple Cyclones are used in the Biomass Power plant to remove particulate material before the gas stream enters the ceramic Heat exchanger. The material caught will consist of coarse and very fine particles, while the material passing the collector will be predominantly fine with some coarse material [11]. Typical particle sizes and ranges of effective operation of various collectors are shown in Figure 3.2. The majority of the dust particles passing through the collector would be ash, but there is a possibility of some unburnt wood particles escaping through it. For a reliable heat exchanger design, the design should be based on the most adverse operating conditions. Hence, the maximum allowable velocity should be calculated corresponding to the largest and most dense dust particle escaping through the collector. An unburnt wood particle (Douglas-Fir) was assumed to be the most dense particle which can escape through the collector. Hence, the maximum allowable velocity in the heat exchanger was calculated

corresponding to such a dust particle. The variation of the above velocity for a diameter range of Douglas-Fir wood is shown in Figure 3.3. The density of the wood was taken to be equal to 44 lbm/cu.ft, which is for a high moisture content.

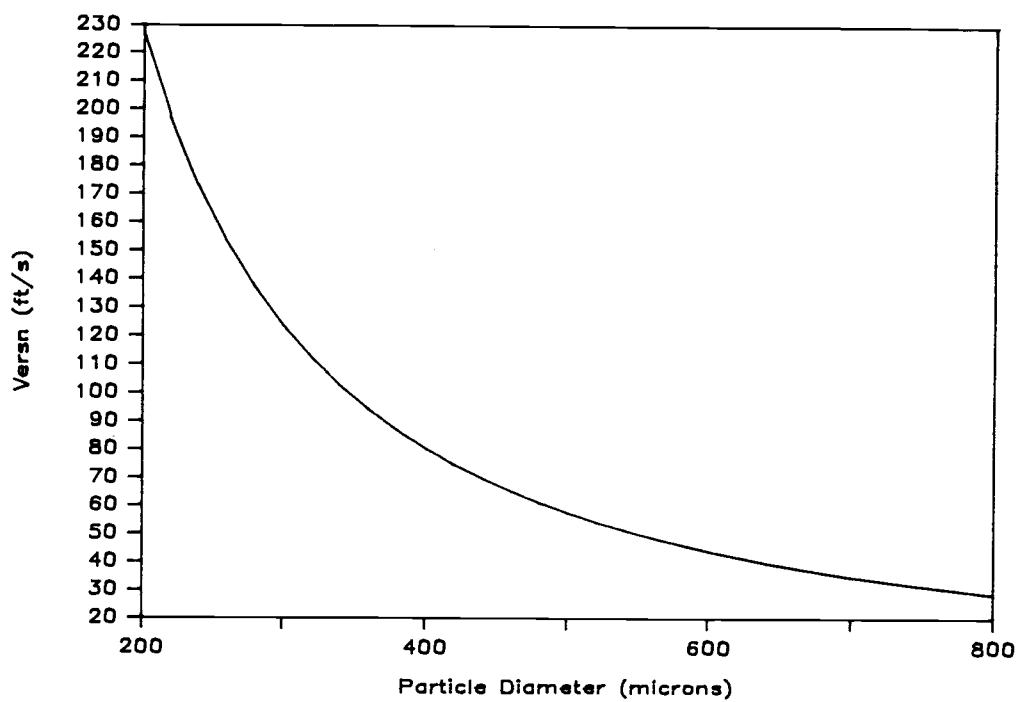


Figure 3.3 The maximum allowable velocity of the flue gas as a function of the diameter of the dust particles.

Chapter 4

MATHEMATICAL MODELS

It was decided to investigate two types of heat exchangers in this study, namely, a cross-flow heat exchanger and a segmentally-baffled shell-and-tube heat exchanger. The objective of this chapter is to develop the necessary mathematical models to simulate the above heat exchangers.

4.1 Ceramic Cross-Flow Heat Exchanger

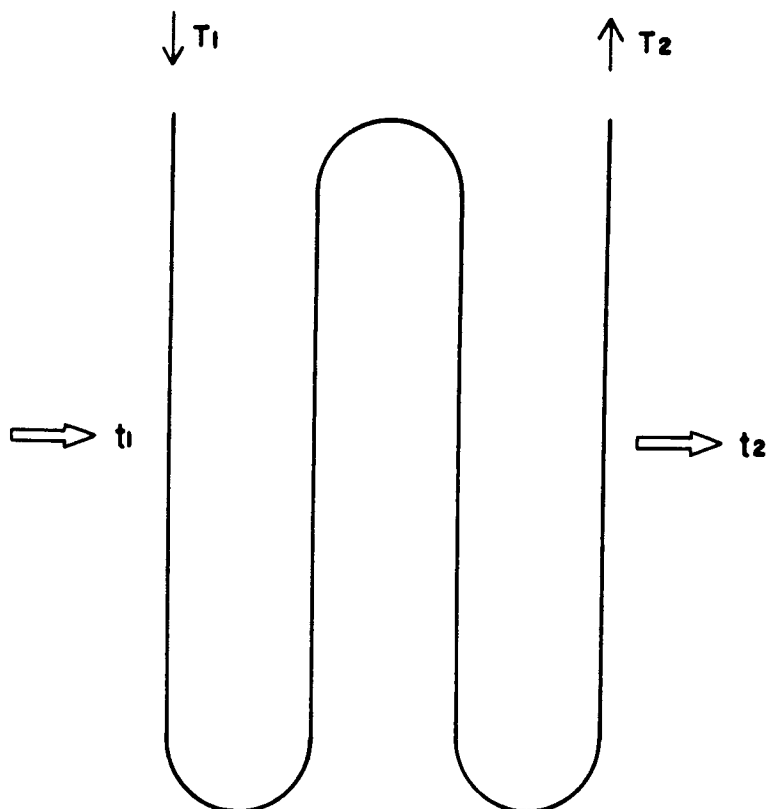
This section describes the mathematical model developed to simulate the ceramic cross-flow heat exchanger. The input data, the procedure used to calculate the total heat transfer area and the method employed to model the leakage is explained under model development. The control actions employed in the model are described under controls. Finally, some assumptions made during the model development are presented under comments.

4.1.1 Model Development

The cross-flow heat exchanger can have single or multiple passes on the air-side, and is specified by the user. For the single-pass case the number of 'U's (noU) should be specified as equal to zero. For a multipass tube arrangement the number of passes is given by

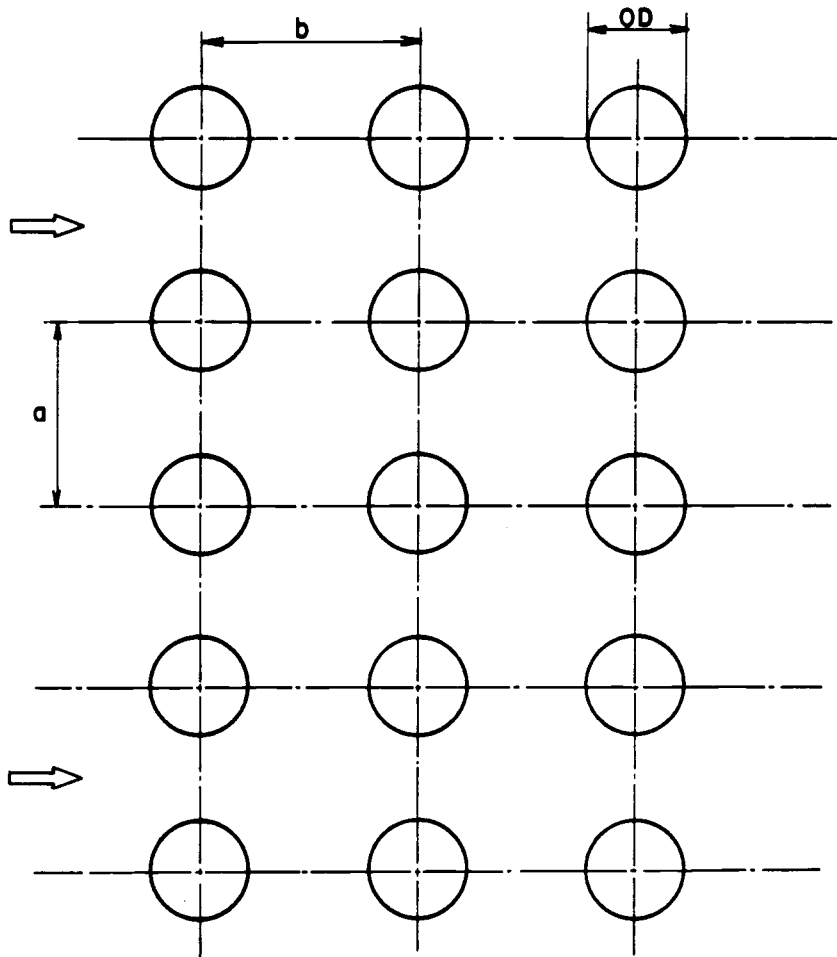
specifying noU , and an example of this is given in Figure 4.1. The number of tube passes is equal to $2*noU$. The tube arrangement is specified by the user as staggered or inline. The normalized pipe spacings normal (SnD) and parallel (SpD) to the flow direction are equal, and variables in the program. These parameters control the velocity and pressure drop on the shell-side. The number of pipes parallel to the flow direction (npp) in a single-pass is given as a constant, and an initial guess for the number of pipes normal (npn) is given by the user. An example on the use of the above parameters is shown in Figure 4.2. The pressure drop inside the pipes and the pipe length is controlled by varying npn . The inside diameter (ID) and outside diameter (OD) of the pipes, the thermal conductivity (K) of the pipe material, the roughness ($rough$) and any fouling which might be present are specified as constants. The diameter ($Dersn$) and density ($Roash$) of the eroding particles and the percentage leakage ($leakge$) in the heat exchanger are specified by the user.

In the model, initially an energy balance is done to obtain the exit temperature of the gas from the heat exchanger. The deviation of the flow through the heat exchanger from a pure countercurrent flow situation is then accounted for by introducing a correction factor F . The thermal rating of the heat exchanger is then



$$noU = 2$$

Figure 4.1 A schematic diagram of a 'U' tube.



$$a = S_n \theta * OD$$

$$b = S_p \theta * OD$$

$$n_p n = 5.$$

$$n_{pp} = 3$$

Figure 4.2 Typical tube arrangement in an inline, cross-flow heat exchanger.

established by calculating the product of the overall heat transfer coefficient and the total heat transfer area. The heat transfer coefficients on both the shell and tube sides are calculated by using experimentally established correlations, and then the necessary pipe length is obtained by an iterative procedure.

A. Energy Balance

Given the temperature of the inlet air (T_{ain}), and the exit temperature of the air (T_{ao}) the total heat transfer rate can be calculated as,

$$Q = MRa(H_{a,out} - H_{a,in})$$

Knowing the inlet temperature of the flue gas (T_{gin}) and the total heat transfer rate (Q), the exit temperature of the gas (T_{go}) can be calculated from an energy balance.

B. Correction Factor F

The correction factor F is calculated from the correlations given in reference [12] as follows,

For a single pass case,

$$p = (T_1 - T_2)/(T_1 - t_1)$$

$$q = (t_2 - t_1)/(T_1 - t_1)$$

$$r_0 = \frac{p - q}{\ln((1 - q)/(1 - p))}$$

$$r = \frac{q}{\ln(1/(1 - q/p \cdot \ln(1/1 - p)))}$$

$$F = r/r_0$$

Figure 4.1 illustrate T_1, T_2, t_1 and t_2 .

For a multipass tube arrangement the correction factor F is calculated from,

$$1/1-p = (\exp(x))(\cosh(x) + (1-p)\sinh(x))$$

$$x = kp/q$$

$$k = 1 - \exp(-q/2r)$$

$$F = r/r_0$$

where p and q are as defined above. The above equations are solved using an iteration procedure as described in reference [4].

C. UA Required

The log mean temperature difference for a countercurrent flow ($LMTD_{cc}$) is calculated as follows,

$$dt_1 = T_{gin} - T_{ao}$$

$$dt_2 = T_{go} - T_{ain}$$

$$LMTD_{cc} = \frac{dt_1 - dt_2}{\ln(dt_1/dt_2)}$$

To get the true log mean temperature difference ($LMTD$) the $LMTD_{cc}$ should be multiplied by the correction factor F . Hence the true log mean temperature difference

and UA required are given by,

$$\text{LMTD} = F \cdot \text{LMTD}_{cc}$$

$$UA_{req} = Q / \text{LMTD}$$

where U and A are the overall heat transfer coefficient and the total heat transfer area respectively.

D. Inside Heat Transfer Coefficient

The heat transfer coefficient on the inside pipe surface is calculated from the correlations suggested in reference [13] as follows,

$$\text{Nu} = .0214 (\text{Re}^{.8} - 100) \text{Pr}^{.4} (1 + (\text{ID}/\text{length})^{2/3})$$

for $0.5 < \text{Pr} < 1.5$, and

$$\text{Nu} = .012 (\text{Re}^{.87} - 280) \text{Pr}^{.4} (1 + (\text{ID}/\text{length})^{2/3})$$

for $1.5 < \text{Pr} < 500$. Hence the inside heat transfer coefficient (h_{in}) is given by,

$$h_{in} = \text{Nu} \cdot k_a / \text{ID}$$

where k_a is the conductivity of the air flowing inside the pipes. The fluid properties are to be evaluated at the mean fluid temperature. The method employed to calculate the pipe length (length) is described later.

E. Outside Heat Transfer Coefficient

The heat transfer coefficient on the shell-side (h_{out}) is calculated from the correlations given in

reference [13], as follows,

$$h_{out} = Nu \cdot K_f / L$$

$$Nu = f \cdot Nu_{1row}$$

The characteristic length (L) is equal to half the outer perimeter of the tube, and K_f is the conductivity of the shell-side gas. The arrangement factor f is given by,

$$f = 1 + \frac{.7(SpD/SnD - .3)}{(PHY^{**1.5}(SpD/SnD+.7)**2)}$$

for an inline tube bank and,

$$f = 1 + 2/(3 \cdot SpD)$$

for a staggered tube bank.

The void fraction PHY and the Nusselt number of a single row of tubes (Nu_{1row}) are calculated as follows,

$$PHY = 1 - PI/SnD$$

$$Nu_{1row} = Nu_{0row} \cdot c$$

$$c = (T_b/T_w)^{**.12}$$

$$Nu_{0row} = .3 + \sqrt{Nu_{lam}^{**2} + Nu_{turb}^{**2}}$$

$$Nu_{lam} = .664 \cdot (\sqrt{Re}) Pr^{**1/3}$$

$$Nu_{turb} = .037 \cdot Re^{**.8} \cdot Pr / (1 + 2.443 \cdot Re^{**-.1} \cdot (Pr^{**2/3} - 1))$$

$$Re = \frac{V_b \cdot \text{length}}{PHY \cdot ETA}$$

Factor c takes into account the temperature

dependence of the fluid properties. The fluid properties are evaluated at the mean fluid temperature, and V_b and η are the velocity of gas coming into the heat exchanger and the dynamic viscosity respectively.

F. Overall Heat Transfer Coefficient

The overall heat transfer coefficient, based on the outside surface, is now calculated as follows,

$$1/U = R_O + R_c + R_i + R_{foul}$$

where,

$$R_O = \frac{1}{h_{out}}$$

$$R_c = \frac{OD}{24K/\ln(OD/ID)}$$

$$R_i = OD/(ID \cdot h_{in})$$

$$R_{foul} = \text{user supplied.}$$

and K is the conductivity of the pipe material.

G. Pipe Length

The required pipe length is given by,

$$\text{length} = UA_{req}/(U \cdot \pi \cdot OD \cdot n_{pp} \cdot n_{pn})$$

for a single pass case and,

$$\text{length} = UA_{req}/(U \cdot \pi \cdot OD \cdot n_{pp} \cdot n_{pn} \cdot 2 \cdot n_oU)$$

for a multipass tube arrangement.

A guess for U is specified in the program, and the corresponding tube length is initially calculated. The flow diagram for the ceramic cross-flow heat exchanger is shown in Figure 4.3. The correct length is hence

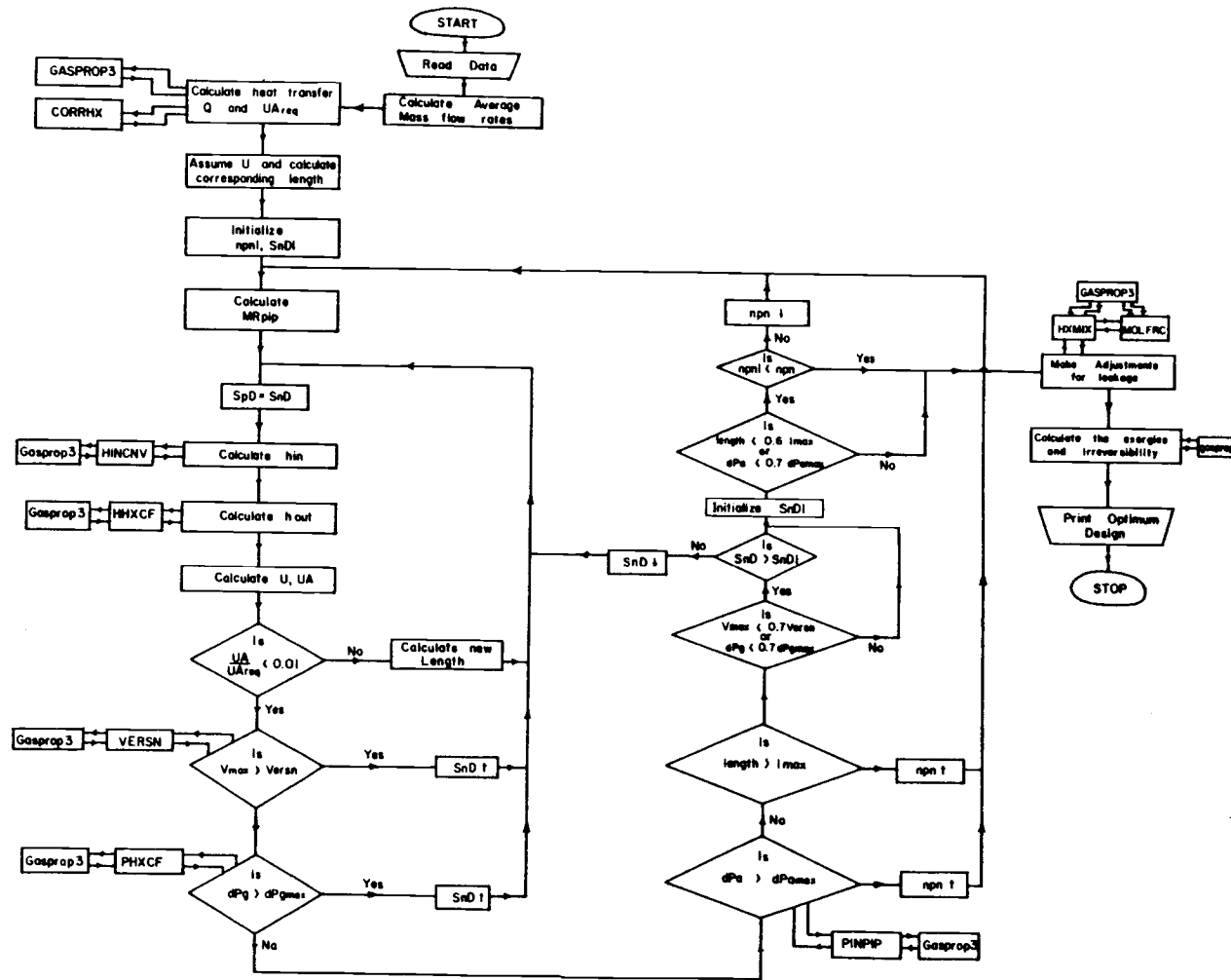


Figure 4.3 Flow diagram for the ceramic cross-flow heat exchanger model.

calculated by employing an iterative procedure, as shown in the flow diagram.

H. Modelling of Leakage

Leakage is an important factor in modelling a ceramic heat exchanger, since it accounts for a direct system loss. The leakage in the ceramic heat exchanger was modelled as shown in Figure 4.4, using a splitter and mixer on the air and gas sides respectively. The percentage leakage (leakge) is supplied by the user. Adjustments for the change in mass flow rates and the corresponding changes in pressure drop are accounted for by using the average mass flow rates for the calculations.

4.1.2 Controls

There are many parameters being controlled in the model. The maximum velocity of the shell-side gas is controlled to prevent the erosion of the ceramic tubes. The frictional power losses are controlled in the model by specifying the upper bounds for the pressure drops on the shell and tube sides respectively. The upper and lower limits of the pipe length is specified due to strength and geometric considerations. Finally the model checks for the lower limits of the pressure drops and the shell-side velocity in order to have a sufficiently large overall heat transfer coefficient. The model is insensitive to the initial guesses of the variables, and the final design

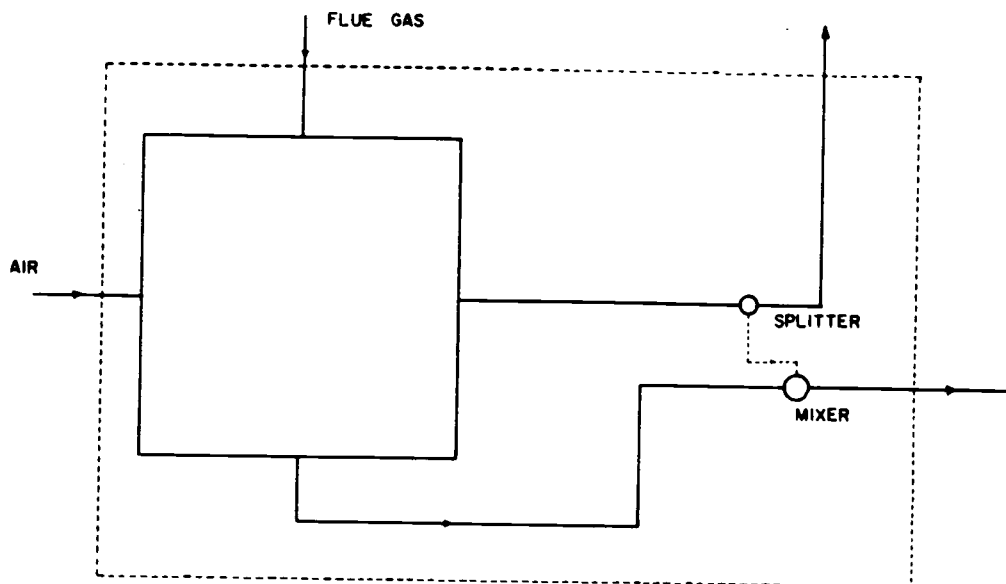


Figure 4.4 Model used to simulate the leakage in the ceramic heat exchanger.

would satisfy all the above mentioned criteria.

A. Maximum Velocity

The maximum velocity on the shell-side of the heat exchanger was selected as one of the limiting factors for the design. This was to prevent the erosion of the ceramic tubes. An equation for the maximum allowable shell-side velocity (Versn) was developed in Chapter 3 as,

$$\text{Versn} = \frac{.005382 * 0.7 * 3.28}{\text{sqrt}(\text{Mash})}$$

the value of Versn is in ft/s and (Mash) is the mass of a dust particle in Kg. If the maximum velocity in the heat exchanger exceeded Versn the intertube spacings SnD and SpD are increased in steps of 0.1, and hence the maximum velocity reduced. With the new SnD and SpD values the heat transfer coefficients and the length of the tubes are then recalculated, as shown in Figure 4.3.

B. Maximum Shell-Side Pressure Drop

The program ensures that the maximum pressure drop on the shell-side does not exceed a value which is specified by the user. If the pressure drop is too large a large amount of power will be used for overcoming the friction. The pressure drop is controlled by adjusting the intertube spacings SnD and SpD. The value of SnD is increased in steps of 0.1, and hence decreases the pressure drop. With

the new value of SnD the new values of the heat transfer coefficient and pipe length are calculated. The pressure drop on the shell-side is calculated as given in [4], as follows,

$$dPg = f \cdot (Ro \cdot V_{max}^2) \cdot z \cdot (\mu_{wall} / \mu_{ave})^y \cdot 0.03613$$

where (z) is the number of tube rows perpendicular to the direction of flow and friction factor f is given by,

$$f = (Re^{-.16}) \cdot (.25 + .1175 / (SnD - 1)^{1.08})$$

for a staggered tube arrangement and,

$$f = (Re^{-.15}) \cdot (.044 + .08 \cdot SpD / (SnD - 1)^{.43 + 1.13 / SpD})$$

for an inline tube arrangement, and factor y is given by,

$$y = .776 \cdot \exp(-.545 \cdot Re^{.256})$$

C. Maximum Pressure Drop Inside the Pipes

The maximum pressure drop inside the pipes is user specified and controlled in the program to, avoid the use of too much pumping power. The pressure drops inside the pipe could be controlled by varying npn, npp or ID. It was decided to keep npp fixed as the variation of this value by one would result in the total number of pipes being increased by npn*noU. The tube diameter ID was also kept as a constant in the program. However, the user can change the value of the pipe diameter, depending on the application. Thus the pressure drop on the shell-side is controlled by varying npn in steps of 1, as shown in

Figure 4.3. With the new value of n_{pn} the new pipe length is calculated and the maximum velocity and pressure drop on the shell-side is checked. The pressure drop inside a pipe (dPa) is calculated from,

$$dPa = f \cdot (L/D) \cdot R_o \cdot (V^{**2}/2)$$

$$f = 1/X^{**2}$$

$$X = 1.74 - 2 \cdot \log(2k/D + 18.7 \cdot X/Re)$$

Friction factor f is calculated by implicitly solving the above equations as described in reference [4], and hence the pressure drop is calculated.

D. Maximum Tube Length

The maximum tube length (l_{max}) is specified by the user. The length is decreased if necessary by increasing n_{pn} . The new pipe length is then calculated and checks are made for the maximum pressure drop and velocity on the shell-side.

E. Minimum Velocity and Pressure Drop on Shell-Side

The program ensures that either the minimum pressure drop or the velocity on the shell-side does not decrease below a pre-specified value in the program. This value is currently set as equal to 0.7 of the maximum value. Since the pressure drop is a function of the velocity, only one of the above values will satisfy the specified lower limit. The specification of the lower limits are

important to prevent very low heat transfer coefficients, resulting in large heat transfer surface areas and high cost. Also, very low velocities could cause fouling. The control is done by decreasing S_nD . Before the new S_nD value is calculated the program compares the current value with the previously calculated value, and if the current value is greater than the previously calculated value it means that an adjustment has been done for either the maximum velocity and pressure drop, and this value of S_nD is the appropriate value.

F. Minimum Pipe Length and Pressure Drop Inside the Pipe

The minimum pressure drop is specified to avoid very low velocities which could result in a low inside heat transfer coefficient. The minimum pipe length is specified due to geometric considerations. These two quantities too are interrelated and thus one of the values would be adjusted to the limit and the other to the corresponding value. The controlling is done by adjusting $n_p n$ and the control loop is similar to the one described for the shell-side.

4.1.3 Comments

In the multipass cross-flow heat exchanger only the straight portions of the ceramic pipes are used for heat transfer purposes. This is done by using flow diverters. The 'U' section of the ceramic tubes are not used due to

the following reasons:

(i) The 'U' section of the ceramic tube would be the weakest section and thus to prevent erosion of this part, lower velocities will have to be used. This would cause lower heat transfer coefficients. Presently, the strength behavior of such sections are not known and hence it is not possible to decide whether the loss in heat transfer would be compensated by the added surface area.

(ii) The cost of manufacturing ceramic tubes with 'U' sections can be quite costly. Therefore straight ceramic tubes might have to be used with the return bend being in the housing.

4.2 Segmentally-Baffled Shell-and-Tube Heat Exchanger

The mathematical model developed to simulate a segmentally-baffled shell-and-tube heat exchanger is described in this section. A schematic diagram of such a heat exchanger is shown in Figure 4.5. The input data to the model, the restrictions imposed on some heat exchanger dimensions, the evaluation of the basic heat exchanger parameters and the method used to calculate the total heat transfer area are described under model development. Finally, some controls used in the model will be explained under controls.

4.2.1 Model Development

The heat exchanger has a single shell pass and two

tube passes. The thermodynamic states of the incoming gases, the pipe diameters, conductivity and roughness of the pipe material, the density and diameter of the eroding particles, the percentage leakage and any fouling which might be present in the heat exchanger are inputs to the program. The inner shell diameter (D_{shell}), the normalized tube pitch (L_{tpD}) and the baffle spacing (L_{bc}) are variables in the program. Initial guesses for the above variables have to be provided by the user. A tube layout angle of 90 degrees was selected to achieve easy external cleaning.

The tube layout pitch (L_{tp}) is equal to $L_{tpD} \cdot OD$ where OD is the outer diameter of the tubes. The tube layout pitch determines the cross-flow area. The smaller the value, more tubes can be accommodated within a given shell diameter. The limitation, however, is determined by the minimum necessary web thickness between adjacent tube holes in the tube-sheet, and cleaning requirements. Shell-side pressure drop too could be effectively adjusted by the tube layout pitch variation. A compromise between the above factors is achieved by keeping L_{tpD} between the values of 1.25 as a minimum and 1.5 as a maximum, [13].

The central baffle spacing L_{bc} is subjected to two limitations, based on established practices, for good flow distribution and adequate support of the tubes [13]. The smallest acceptable baffle spacing is required for reasons

of good flow distribution, so that a steady flow pattern of the cross-flow and baffle window flow would result. The minimum baffle spacing is kept equal to 20% of the shell diameter. The maximum permissible baffle spacing to achieve good flow distribution calls for this parameter not to exceed the shell diameter. Therefore the maximum baffle spacing is kept at 90% of the shell diameter or 80% of the overall tube length, depending on which of the two is the smaller value.

A. Basic Heat Exchanger Parameters

The basic heat exchanger parameters are evaluated as given in reference [13]. Figures 4.6-4.8 shows some of these parameters.

The number of holes in the tubesheet (N_{tt}) is calculated as follows,

$$N_{tt} = \frac{0.78(D_{ct1}^{**2})}{L_{tp}^{**2}}$$

$$D_{ct1} = D_{ot1} - OD \quad (\text{mm})$$

$$D_{ot1} = D_{shell} - L_{bb} \quad (\text{mm})$$

$$L_{bb} = D_{shell}/200. + 13.5 \quad (\text{mm})$$

Some basic heat exchanger parameters and equations to evaluate them are given below.

B_c - Segmental baffle cut as a percentage of the shell diameter.

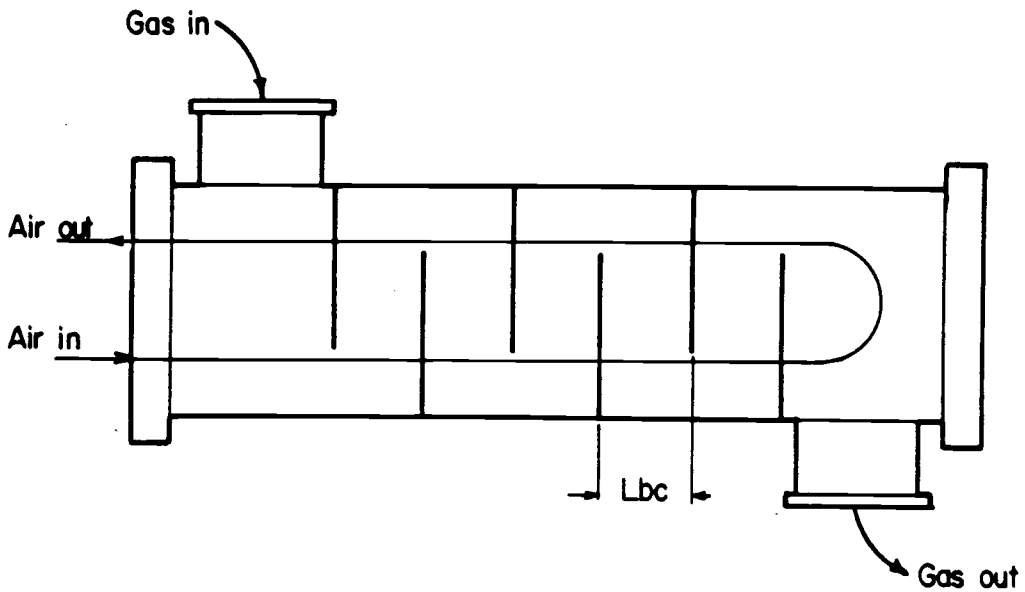


Figure 4.5 A schematic diagram of a segmentally-baffled shell-and-tube heat exchanger.

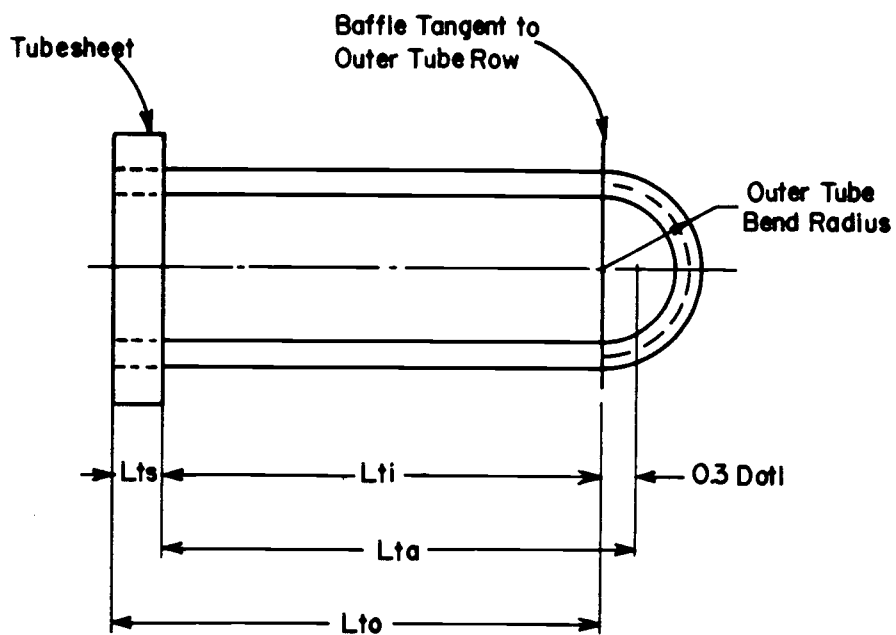


Figure 4.6 Tube length definitions for the segmentally-baffled shell-and-tube heat exchanger, (from [13]).

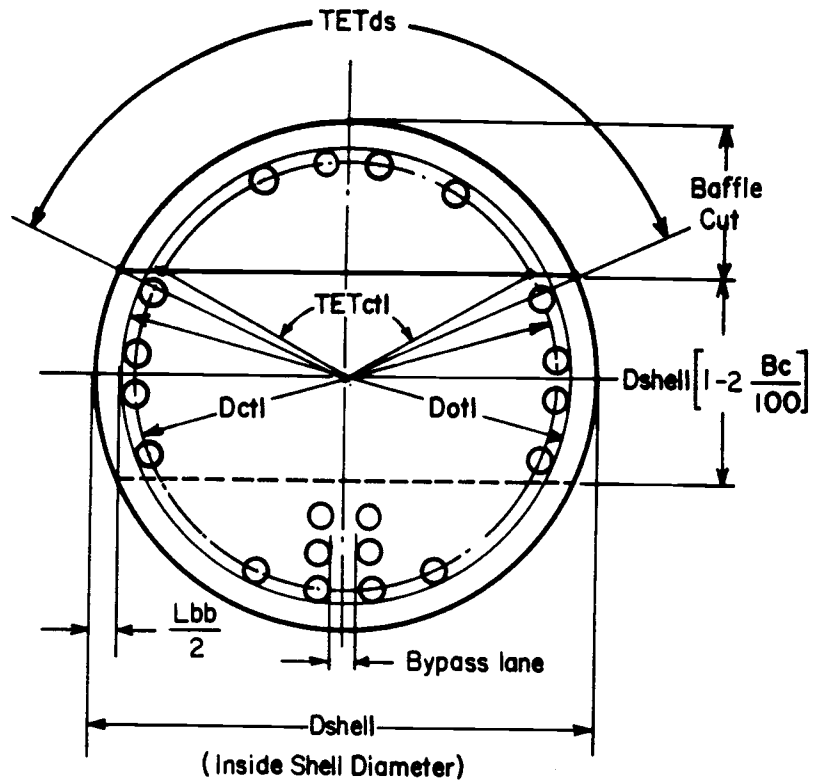


Figure 4.7 Basic baffle geometry relations, (from [13]).

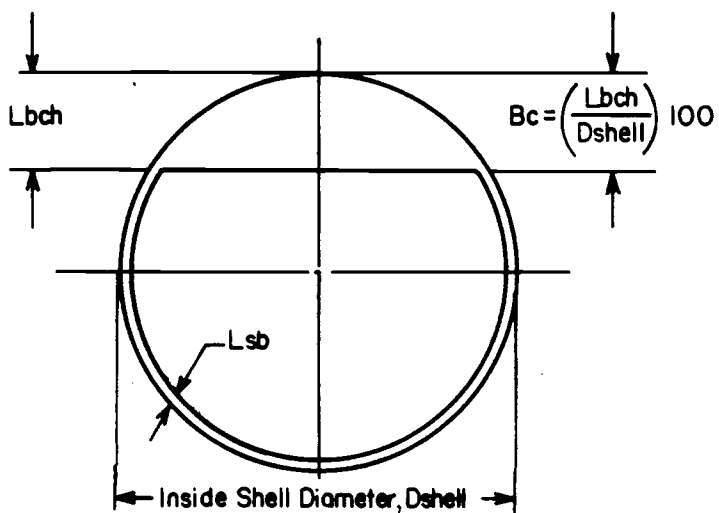


Figure 4.8 Relationship between the baffle cut height (L_{bch}) and baffle cut (Bc), (from [13]).

$$Bc = 20(Lbc/Dshell) + 16.$$

Ltb - Tube to baffle-hole diametral clearance. (mm)

$$Ltb = .8 \quad Lbc < 450 \text{ mm}$$

$$Ltb = .4 \quad Lbc > 450 \text{ mm}$$

Sm - Cross-flow area at the shell center line within one baffle spacing. (sq.mm)

$$Sm = Lbc[Lbb + Dctl(1-1/LtpD)]$$

TETds - Centri-angle of the baffle cut intersection with the inside shell wall, (deg)

$$TETds = 2*\text{acos}[1 - 2(Bc/100)]$$

TETctl - Centri-angle of the baffle cut intersection with the diameter Dctl, (deg)

$$TETctl = 2*\text{acos}(Dshell/Dctl*[1 - 2(Bc/100)])$$

Swg - The gross baffle window flow area. (sq.mm)

$$Swg = \text{PI}/4*(Ds**2)[TETds/360 - (\sin TETds)/2\text{PI}]$$

Fw - The fraction of number of tubes in one window.

$$Fw = TETctl/360 - (\sin TETctl)/2\text{PI}$$

Fc - The fraction of number of tubes in pure cross-flow between baffle tips.

$$Fc = 1-2(Fw)$$

Ntw - The number of tubes in the window.

$$Ntw = Ntt*Fw$$

Swt - The segmental baffle window area occupied by the tubes. (sq.mm)

$$Swt = Ntw(\text{PI}/4*OD**2)$$

Sw - The net cross-flow area through one baffle window. (sq.mm)

$$Sw = Swg - Swt$$

Ntcc - Number of effective rows crossed in one cross-flow section.

$$Ntcc = Ds/Lpp[1 - 2(Bc/100)]$$

Ntcw - The number of effective tube rows crossed in the baffle window.

$$Ntcw = 0.8/Ltp[Ds(Bc/100) - (Ds-Dct1)/2]$$

Nb - Number of baffles.

$$Nb = Lti/Lbc - 1$$

Sb - Bypass area within one baffle. (sq.mm)

$$Sb = Lbc[(Ds-Dot1) + Lp1]$$

Fsbp - The ratio of the bypass area ,Sb, to the overall cross-flow area.

$$Fsbp = Sb/Sm$$

Lsb - Inside shell to baffle clearance. (mm)

$$Lsb = 3.1 + .004*Dshell$$

Ssb - Shell to baffle leakage area. (mm)

$$Ssb = .00436*Dshell*Lsb*(360 - TETds)$$

Stb - Tube to baffle hole leakage area. (mm)

$$Stb = \{PI/4*[(OD+Ltb)**2-OD**2]\}(Ntt)(1-Fw)$$

B. Evaluation of LMTD

Given the temperature of the inlet air (Tain), and the exit temperature of the air (Tao) the total heat transfer rate (Q) and the exit temperature of the gas

(Tgo) can be calculated as described under the ceramic cross-flow heat exchanger. Knowing all four temperatures, the log mean temperature difference for a countercurrent flow (LMTD,cc) too can be calculated as explained under the cross-flow heat exchanger.

The correction factor F, which accounts for the flow not being countercurrent is given in reference [14], and is calculated as follows,

$$R = (T_{gin} - T_{go}) / (T_{ao} - T_{ain})$$

$$P = (T_{ao} - T_{ain}) / (T_{gin} - T_{ain})$$

$$\Delta = \frac{R - 1}{\ln[(1-P)/(1-PR)]} \quad \text{for } R \text{ not equal to } 1, \text{ and}$$

$$\Delta = (1 - P) / P \quad \text{for } R = 1.$$

$$ETA = \sqrt{R^2 + 1} \quad \text{and,}$$

$$F = \frac{ETA}{\Delta * \ln[[2 - P(1 + R - ETA)] / [2 - P(1 + R + ETA)]]}$$

Now the true log mean temperature difference and UA,req can be calculated as described under the cross-flow heat exchanger.

C. Heat Transfer Coefficient Inside The Pipes

The heat transfer coefficient on the inside pipe surface was modelled as described under the cross-flow heat exchanger.

D. Shell-Side Heat Transfer Coefficient

The shell-side heat transfer coefficient is calculated by initially calculating the ideal tube bank heat transfer coefficient and then correcting it for the nonidealistics of the flow in the baffled exchanger, [13].

Ideal Tube Bank Heat Transfer Coefficient:

The heat transfer coefficient for an ideal tube bank is obtained from,

$$h_{ideal} = j_i(C_p s)G_s(Pr_s^{*-2/3})$$

where factor j_i is given by,

$$j_i = (a_1)(1.33/L_{tp}D)^{**a}(Re_s^{**a_2})$$

and, $a = a_3/[1+0.14(Re_s^{**a_4})]$

Constants a_1, a_2, a_3 and a_4 are given in Table 4.1. The specific heat of the shell-side gas is denoted by $C_p s$ and G_s (kg/sq.ms) is the shell-side mass velocity. Pr_s is the prandtl number of the shell-side fluid.

Segmental Baffle Window Correction (J_c):

This factor takes into account the effects of the baffle window flow on the heat transfer coefficient. An approximate expression for J_c based on a straight line fit on to the experimental data is given by,

$$J_c = 0.55 + 0.72F_c$$

Correction factor for baffle leakage (J_l):

The pressure difference between two adjoining baffle

Table 4.1 Correlational coefficients for j_i and f_i ,
(from [13]).

Layout angle	Reynolds number	a_1	a_2	a_3	a_4	b_1	b_2	b_3	b_4
30°	10^5-10^4	0.321	-0.388	1.450	0.519	0.372	-0.123	7.00	0.500
	10^4-10^3	0.321	-0.388			0.486	-0.152		
	10^3-10^2	0.593	-0.477			4.570	-0.476		
	10^2-10	1.360	-0.657			45.100	-0.973		
	<10	1.400	-0.667			48.000	-1.000		
45°	10^5-10^4	0.370	-0.396	1.930	0.500	0.303	-0.126	6.59	0.520
	10^4-10^3	0.370	-0.396			0.333	-0.136		
	10^3-10^2	0.730	-0.500			3.500	-0.476		
	10^2-10	0.498	-0.656			26.200	-0.913		
	<10	1.550	-0.667			32.000	-1.000		
90°	10^5-10^4	0.370	-0.395	1.187	0.370	0.391	-0.148	6.30	0.378
	10^4-10^3	0.107	-0.266			0.0815	+0.022		
	10^3-10^2	0.408	-0.460			6.0900	-0.602		
	10^2-10	0.900	-0.631			32.1000	-0.963		
	10	0.970	-0.667			35.0000	-1.000		

compartments forces part of the flow to penetrate in the gap between the shell and the baffle edge circumference, and tube and baffle tube holes. This decreases the effective cross-flow stream and hence the heat transfer coefficient. From the two leakage streams the shell to baffle stream is the most important, as it does not exchange heat with any tubes. The correlation suggested in the reference for computer applications is as follows,

$$r_{lm} = \frac{S_{sb} + S_{tb}}{S_m}$$

$$r_s = \frac{S_{sb}}{S_{sb} + S_{tb}}$$

$$J_1 = 0.44(1-r_s) + [1 - 0.44(1-r_s)] \exp(-2.2r_{lm})$$

The value of J_1 should preferably be within 0.7-0.9, and not less than 0.6. If the value of J_1 is too small it would result in a low heat transfer efficiency. The value of J_1 could be increased by using wider baffle spacings or increasing the tube pitch.

Correction factor for Bundle bypass effects (J_b):

The flow resistance in the shell to tube-bundle bypass is much lower than through the tube field, and therefore part of the flow will seek this path. This stream is only partially effective for heat transfer as it touches the tubes only on one side. The correction factor J_b is calculated as follows,

$$J_b = \exp[-C_{bh} \cdot F_{sbp}]$$

where,

$$C_{bh} = 1.35 \text{ for laminar flow, } Re_s < 100.$$

$$C_{bh} = 1.25 \text{ for turbulent and transition flow.}$$

Correction factor due to laminar flow (J_r):

Due to the adverse temperature gradient developed through the boundary layer in laminar flow, there could be a large decrease in the heat transfer coefficient. In the heat exchanger this will not be an important factor as the flow is mostly turbulent. The correction factor J_r is calculated as follows,

$$J_r = J_{rr} = 1.51 / N_c^{**0.18} \quad \text{for } Re_s < 20$$

$$J_r = J_{rr} + [(20 - Re_s) / 80] [J_{rr} - 1] \quad \text{for } 100 > Re_s > 20$$

$$J_r = 1 \quad \text{for } Re_s > 100$$

Correction factor due to unequal baffle spacing (J_s):

This factor takes into account the unequal baffle spacing at the inlet or exit. This factor was taken as equal to one, as unequal baffle spacings were not employed in the model.

Shell Side Heat Transfer Coefficient:

Hence the total shell-side heat transfer coefficient is calculated from,

$$h_{out} = h_{ideal} \cdot J_c \cdot J_l \cdot J_b \cdot J_r \cdot J_s$$

E. Pipe Length

The overall heat transfer coefficient and the pipe length is calculated as described under the cross-flow heat exchanger.

F. Modelling of Leakage

The leakage in the heat exchanger is modelled as explained under the cross-flow heat exchanger.

4.2.2 Controls

The variables controlled in the segmentally-baffled shell-and-tube heat exchanger are same as in the cross-flow heat exchanger.

A. The Velocity and Pressure Drop on Shell-Side

The shell-side velocity and pressure drop is controlled by varying L_{tpD} , L_{bc} and D_{shell} as shown on the flow chart presented in Figure 4.9. When adjusting for the maximum conditions, initially L_{tpD} and L_{bb} are increased one at a time in that order till they reach their upper limits. Finally the shell diameter is increased, to decrease either the maximum velocity or pressure drop on the shell-side.

The minimum allowable values of the pressure and velocity is set as equal to 0.7 of the maximum value. If either of the above values is less than the minimum value, L_{tpD} , L_{bc} and D_{shell} would be decreased in that order till the necessary conditions are satisfied. Here the

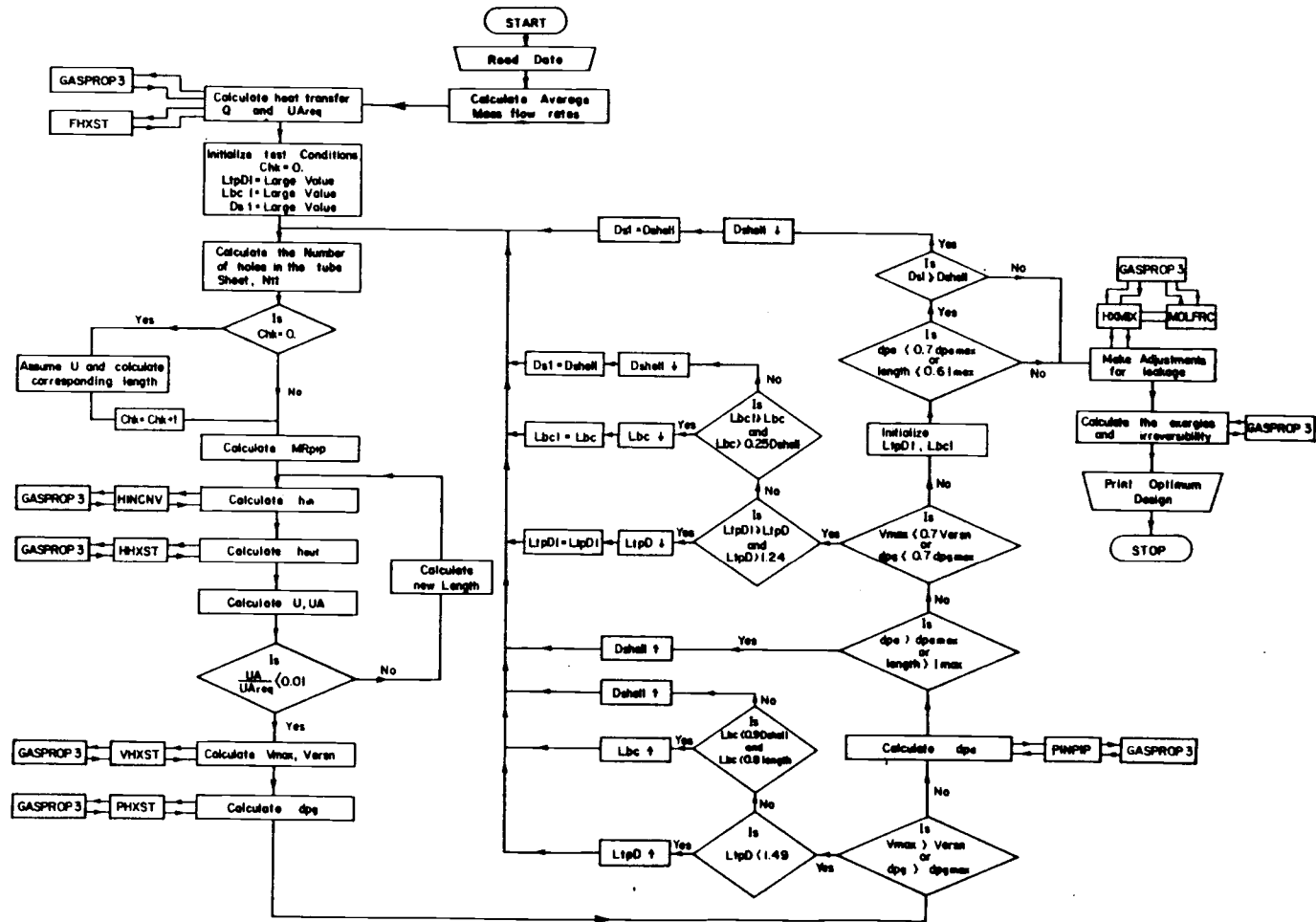


Figure 4.9 Flow diagram for the segmentally-baffled shell-and-tube heat exchanger.

variables are decreased till they reach their lower limits.

Once L_{tpD} , L_{bc} or D_{shell} are adjusted, the pipe length is recalculated and the other conditions are checked. When making adjustments to the lower limit a check is made to see if the upper limit of either the velocity or pressure has been reached, and if so the iteration is stopped. The control action is shown in Figure 4.9.

The shell-side pressure drop was calculated using the modified Bell correlation, [13]. The shell-side pressure drop could be divided into three distinct parts. They are the pressure drops in pure cross-flow (d_{Pc}), in the baffle window (d_{Pw}), and the end zones (d_{Pe}).

Pressure Drop in Cross-Flow Between the Baffle Tips:

The pressure drop in cross-flow between the baffle tips d_{Pc} (KPa) is calculated as follows,

$$d_{Pc} = d_{Pbi}(N_b - 1)(R_b)(R_l)$$

where d_{Pbi} is the ideal tube bank pressure drop in one baffle compartment, and R_b and R_l are the bypass and leakage correction factors respectively. The ideal tube bank pressure drop d_{Pbi} (KPa) is given by,

$$d_{Pbi} = 2(10^{-3})f_i N_{tcc} (G_s^2) / \rho_s$$

where ρ_s (Kg/cu.m) is the density of the shell-side

gases and the friction factor f_i is calculated from,

$$f_i = b_1[(1.33/LtpD)^{b_2}][REs^{b_2}]$$

$$b = b_3/[1+0.14(REs^{b_4})]$$

where constants b_1, b_2, b_3 and b_4 are given in table 4.1.

The bypass and leakage correction factors are given by,

$$R_b = \exp[-C_{bp} \cdot F_{sbp}]$$

$$R_l = \exp[-1.33(1+r_s)(r_{lm})^p]$$

where,

$$p = [-0.15(1+r_s)+0.8]$$

$$C_{bp} = 4.5 \quad \text{for laminar flow, } REs < 100$$

$$C_{bp} = 3.7 \quad \text{for turbulent and transition flow.}$$

The Baffle Window Pressure Drop:

The baffle window pressure drop dP_w (KPa) is calculated from,

$$dP_w = N_b[(2+0.6N_{tcw})(G_w^{**2})/(2 \cdot 10^{**3} \cdot RO_s)]R_l$$

The End Zone Pressure Drop:

The pressure drop in the two end zones dP_e (kPa) is given by,

$$dP_e = (dP_{bi})(1+N_{tcw}/N_{tcc})(R_b)(R_s)$$

and the end zone correction factor R_s is equal to 2 when all the baffle spacings are equal.

The Total Pressure Drop:

Finally, the total shell-side pressure drop dPs (kPa) is calculated from,

$$dPs = dPc + dPw + dPe$$

B. Tube Length and Pressure Drop Inside the Pipe

The tube length and pressure drop inside the pipe is adjusted by varying the shell diameter. The shell diameter is increased to decrease either the tube length or the pressure drop, and increased to decrease them. Here too a control loop is introduced as shown in Figure 4.9, when adjusting for the lower limit. The pressure drop inside the pipe is calculated as explained under the cross-flow heat exchanger.

Chapter 5

RESULTS FROM HEAT EXCHANGER SIMULATIONS

The development of the heat exchanger models, and their desired characteristics were discussed in chapter 4. The objective of this chapter is to investigate the behavior of the above models, and to decide on a specific heat exchanger to be used in the biomass power plant.

5.1 Model Behavior

Computer simulated results obtained from the cross-flow heat exchanger, and the segmentally-baffled shell-and-tube heat exchanger will be presented in this section. The operating conditions for the simulations were obtained from previous results generated during the study of the biomass power plant [1,4], and are given in Appendix C. The objective of presenting these results is to investigate the behavior of the models against that desired, and to select the heat exchanger which would be most suitable for the present application.

5.1.1 Shell-and-Tube Heat Exchanger

The temperature of the flue gas leaving the heat exchanger can be calculated from an energy balance, and is approximately equal to 849 F at a flue gas flow rate of 51 lbm/s (this is the approximate mass flow rate of flue gas in the biomass power plant). Figure 5.1 shows the

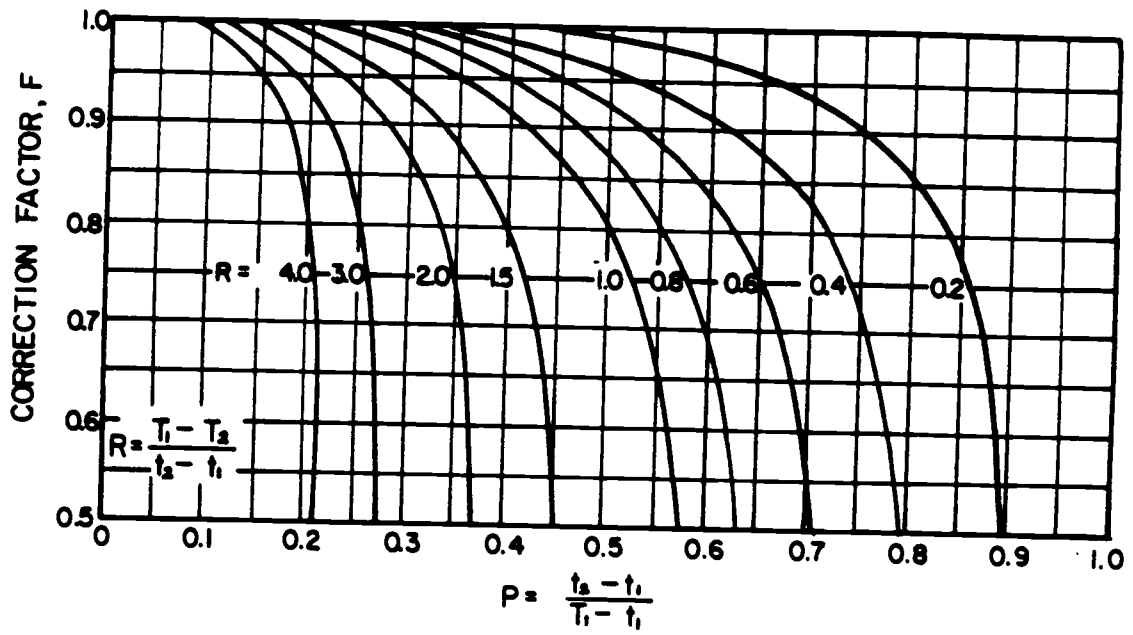


Figure 5.1 Correction factor F for a segmentally-baffled shell-and-tube heat exchanger, (from [12]).

variation of the correction factor F , for various values of P and R . The values of P and R can be calculated for the present case as,

$$\begin{aligned} P &= (T_{ao} - T_{ain}) / (T_{gin} - T_{ain}) \\ &= (1730 - 540) / (2250 - 540) = .696 \\ R &= (T_{gin} - T_{go}) / (T_{ao} - T_{ain}) \\ &= (2250 - 849) / (1730 - 540) = 1.177 \end{aligned}$$

It is evident from Figure 5.1 that the value of the correction factor F , for the above values of P and R , is very small. This means that the temperature rise on the air-side is too high for a single shell-and-tube heat exchanger to operate efficiently. Therefore at least two of these heat exchangers will have to be used to obtain a high enough correction factor. The cost associated with an additional heat exchanger is very high, and hence is a major disadvantage in using a baffled shell-and-tube heat exchanger.

It was also observed that the low density shell-side gases caused very high velocities at the intertube spacings. The velocity can be controlled by varying the tube pitch, L_{tpD} , the baffle spacing, L_{bc} , or the shell diameter. The restrictions on the variation of L_{tpD} and L_{bc} were discussed in chapter 4. Therefore it was necessary to increase the shell diameter by a considerable amount to obtain allowable velocities. A large shell diameter results in a large number of total tubes N_{tt} , low

velocities on the air-side, and hence a low overall heat transfer coefficient.

From the above discussion it is apparent that this type of heat exchanger is only suitable when the temperature rise on the air-side is low, and for high density shell-side fluids. Therefore a segmentally-baffled shell-and-tube heat exchanger is not suitable for the present study, and will not be investigated any further.

5.1.2 Cross-Flow Heat Exchanger

The computer simulated results obtained from the ceramic cross-flow heat exchanger are presented in this section. The objective of presenting these results is to investigate the behavior of the model.

This model has various restrictions imposed on the maximum and minimum allowable pressure drops, shell-side gas velocity and tube lengths respectively. These restrictions were discussed in detail in Chapter 4. The mass flow rate and the maximum allowable pressure drop on the shell-side were used as variables, and the corresponding variation of some heat exchanger and flow parameters are shown in Figures 5.2 and 5.3. The above variables were chosen to obtain different flow conditions. The maximum allowable pressure drop and mass flow rate on the air-side were fixed.

The model ensures that the maximum limits of any

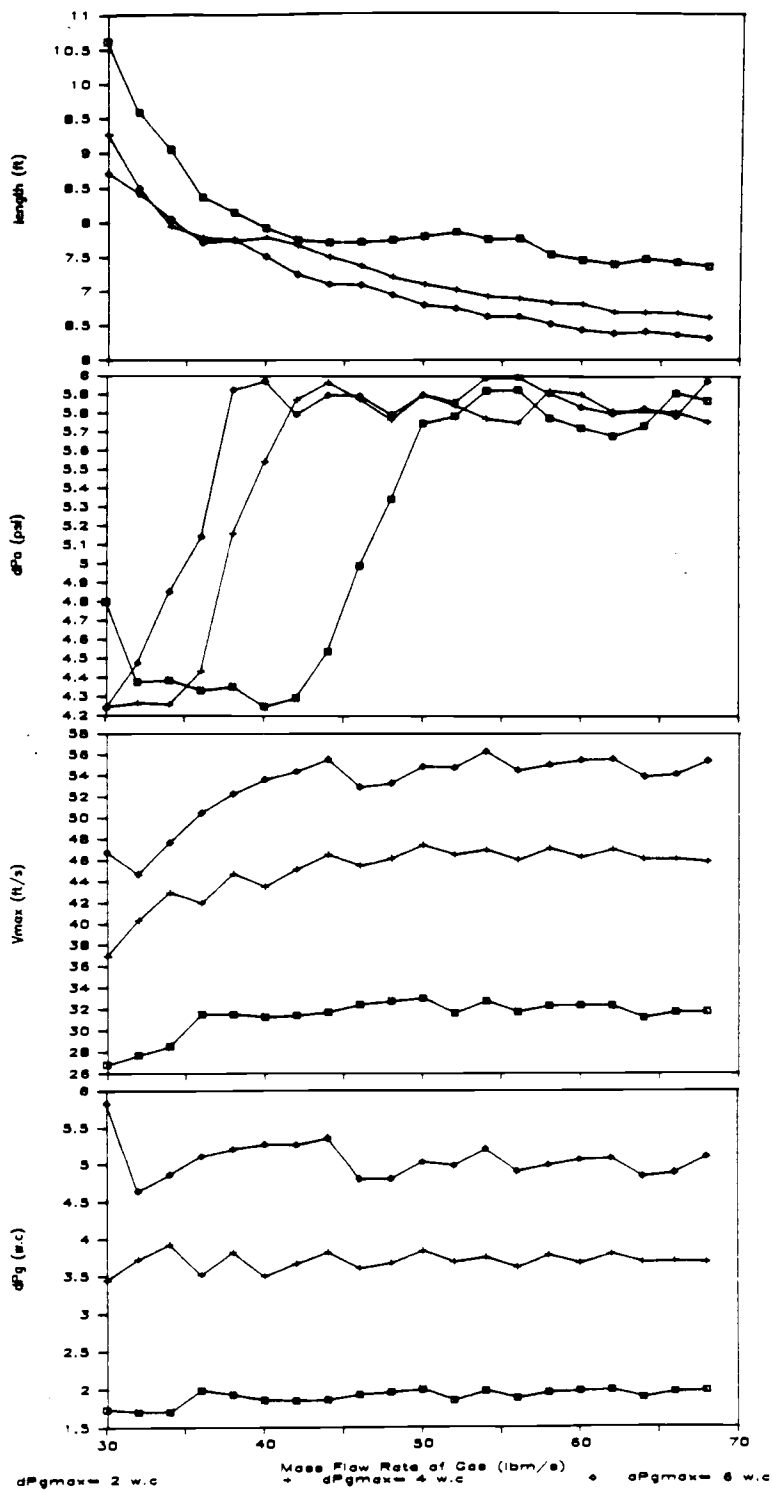


Figure 5.2 Typical results obtained from the multiple air-side pass, ceramic cross-flow heat exchanger model, controls (dPmax = 6 psi, lmax = 11 ft, Dersn = 500 microns).

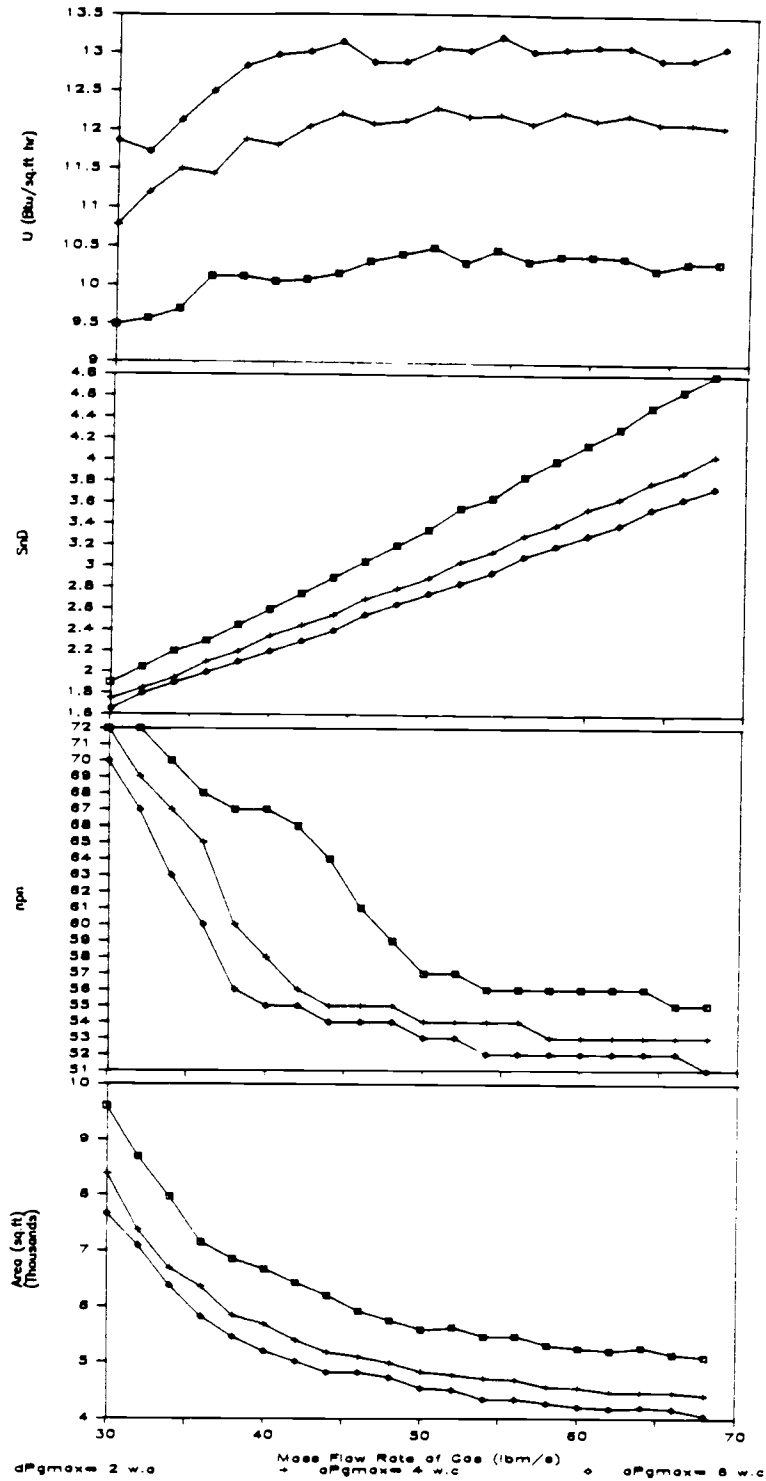


Figure 5.3 Typical results obtained from the multiple air-side pass, ceramic cross-flow heat exchanger model ($dP_{max} = 6 \text{ psi}$, $l_{max} = 11 \text{ ft}$, $D_{ersn} = 500 \text{ microns}$).

specified parameter is not exceeded. This has been confirmed by Figure 5.2. The minimum limits for all of the above specified parameters were set as equal to 0.7 of the maximum value. Some of the variables can have values less than the specified minimum, and the reasons were discussed in Chapter 4. For example, the minimum allowable pipe length should be 7.7 ft, but the pipe length drops below this value at some points since a greater pipe length will violate the maximum air-side pressure drop condition. This can also be observed in the shell-side velocity, which drops below the minimum value to prevent the pressure drop exceeding its maximum limit. Since the control variables are bounded, a non-linear behavior within these bounds can be observed. The convergence of the pressure drop inside the pipe was observed to be sensitive to the specified pipe diameters. This problem would only occur if the specified pipe diameter is too large or small, for the specified maximum pressure drop on the air-side. Therefore the user will have to use a trial and error procedure to decide on the pipe diameter during the initial design stage. From Figure 5.3, it can be seen that the sizes of the cross-flow heat exchanger are within practical bounds.

5.2 A Ceramic Heat Exchanger For the Biomass Power Plant

From the above analysis it is apparent that a cross-flow heat exchanger is the most suitable for the biomass power plant. In the multiple air-side pass heat exchanger discussed earlier, there are 6 air-side passes (noU is equal to 3). The fabrication of a single ceramic tube with 5 'U' bends will not be very practical. By having a tube arrangement as shown in Figure 5.4, the above difficulty can be overcome. It is also possible to have an arrangement with three banks of single U tubes with the air mixing between the tube banks. As discussed in Chapter 2, one of the main difficulties in using a ceramic heat exchanger for high temperature and high pressure applications is the inefficiency of the sealing arrangement. Therefore the best arrangement should have a minimum number of tube to tube-sheet joints. Due to the high number of tube to tube-sheet joints, a high leakage flow rate can be anticipated from the arrangement described in Figure 5.4.

Since the efficiency of the air-side has a greater influence on the overall plant efficiency, a heat exchanger with a low leakage, few tube to tube-sheet joints, and low air-side pressure drop will be most suitable for the biomass power plant. A schematic diagram of a multiple gas-side pass, cross-flow heat exchanger was

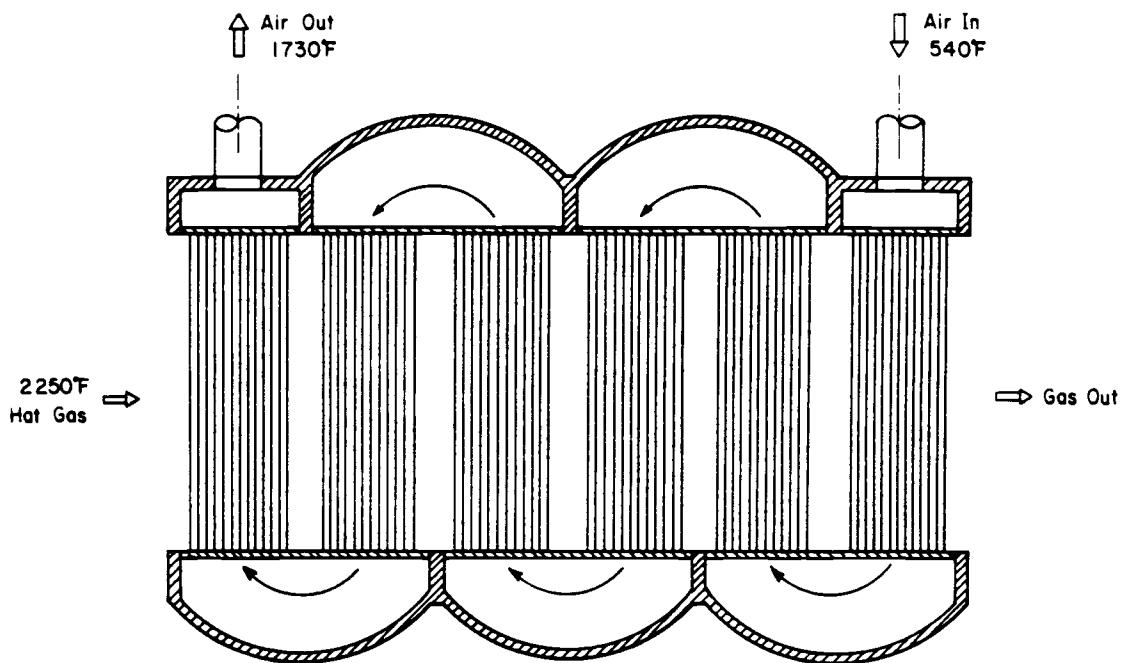


Figure 5.4 A schematic diagram of a multiple air-side pass, ceramic cross-flow heat exchanger.

presented in Figure 2.1. This unit has a lower pressure drop on the air-side and a higher pressure drop on the gas-side when compared with the multiple air-side pass heat exchanger. Due to the low tube to tube-sheet joints, a low leakage flow rate can be expected. Such a unit, which is commercially available, was described in chapter 2. Therefore the multiple gas-side pass, ceramic cross-flow heat exchanger is the most promising candidate for the use in the biomass power plant.

The heat exchanger shown in Figure 2.1 can be modelled similar to the multiple air-side pass unit, with a few minor adjustments. A program listing of the model developed to simulate the multiple gas-side pass heat exchanger is presented in Appendix B. The flow in this heat exchanger arrangement can be assumed to be pure counterflow, when using more than two passes on the gas side. The results obtained from this model can be used to size a fixed size ceramic heat exchanger, to be used in the biomass power plant. Typical results obtained from this model are shown in Figure 5.5.

5.3 Conclusions

It was evident from this analysis that a multiple gas-side pass ceramic cross-flow heat exchanger is the most suitable candidate for use in a wood-fueled combined-cycle power plant.

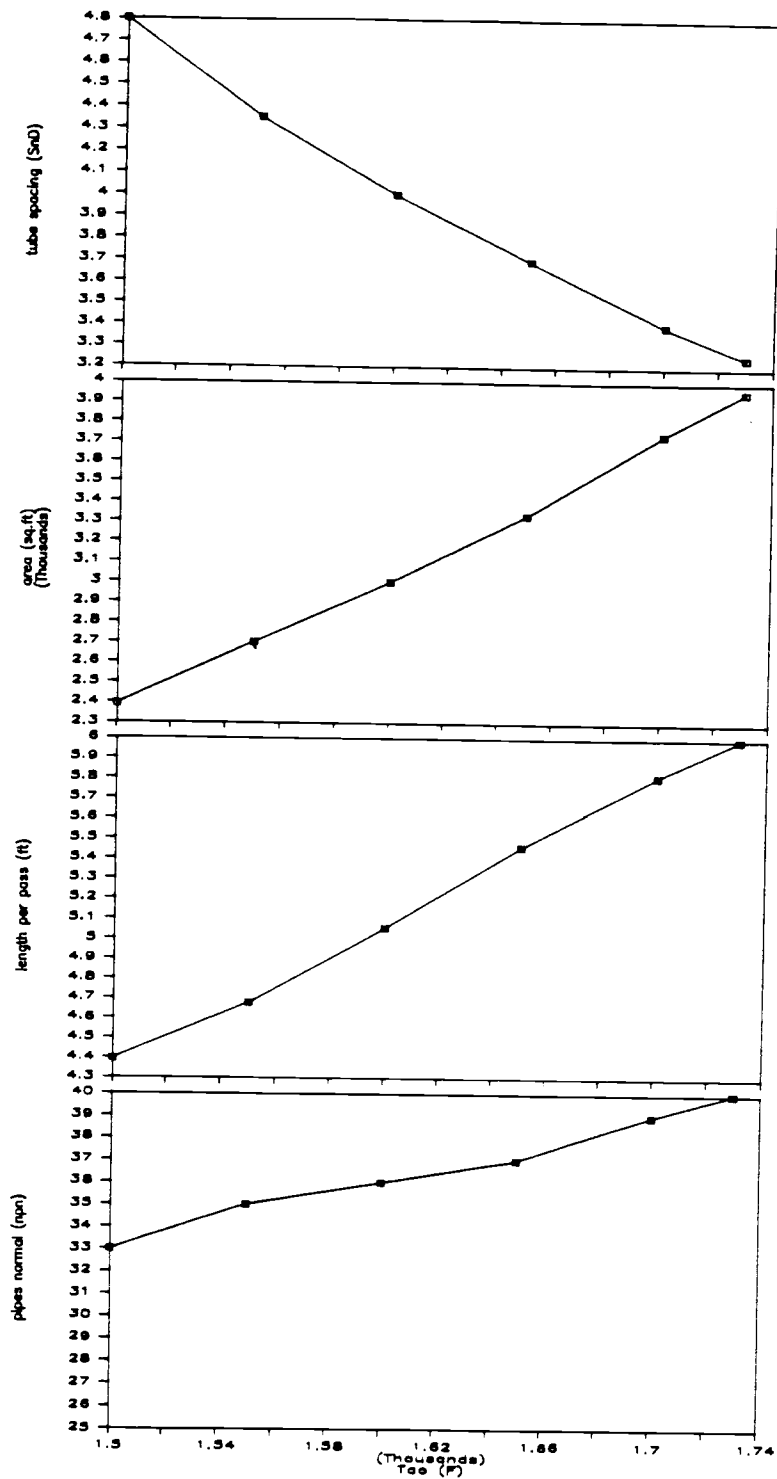


Figure 5.5 Typical results obtained from the multiple gas-side pass, ceramic cross-flow heat exchanger model.

In selecting heat exchangers for a particular operation, it is advisable to find the approximate temperatures at the inlets and outlets and then check on the correction factor F for the various units being investigated. If this was done initially, it would have been evident that a segmentally-baffled shell-and-tube heat exchanger was not suitable for the present application. In this work the heat exchanger model was developed before this was realized. However, it was decided to include the model development in this report, since the development of a computer code for such a model with reliable correlations was not well documented in the literature.

The heat exchanger sized by the model, developed during this study, would be an appropriate design for the specified conditions. However, it should be noted that this will not be an optimum design. To have an optimum design it would be necessary to minimize the irreversibilities in the heat exchanger. Theoretical studies on the minimization of irreversibilities in heat exchangers have been done, and the results are documented in the literature. However, these results are for fixed area or fixed volume conditions. Irreversibility minimization for a variable size heat exchanger model was not documented in the literature. The necessity to develop such a technique has been recognized by

Bejan [15]. Therefore it was not possible to develop a heat exchanger model to obtain an optimum design.

Chapter 6.

ANALYSIS OF PLANT PERFORMANCE

The development of the ceramic heat exchanger model, and the type of heat exchanger most suitable for the use in the biomass power plant were discussed in the previous chapters. The objective of this chapter is to investigate the influence of a ceramic heat exchanger on the overall power plant performance, and to compare the ceramic heat exchanger system to some other systems which have been considered in previous studies.

6.1 Plant Description

A schematic diagram of the power plant being analyzed is shown in Figure 6.1. The list of plant components are given in Table 6.1. The distinguishing features of this power plant are,

- (1) the wood undergoes direct combustion
- (2) the gas turbine system is of the indirect-fired type
- (3) the system is of the combined-cycle type, with a gas turbine cycle and a steam cycle.

More detailed descriptions of the power plant are given in Appendix (A).

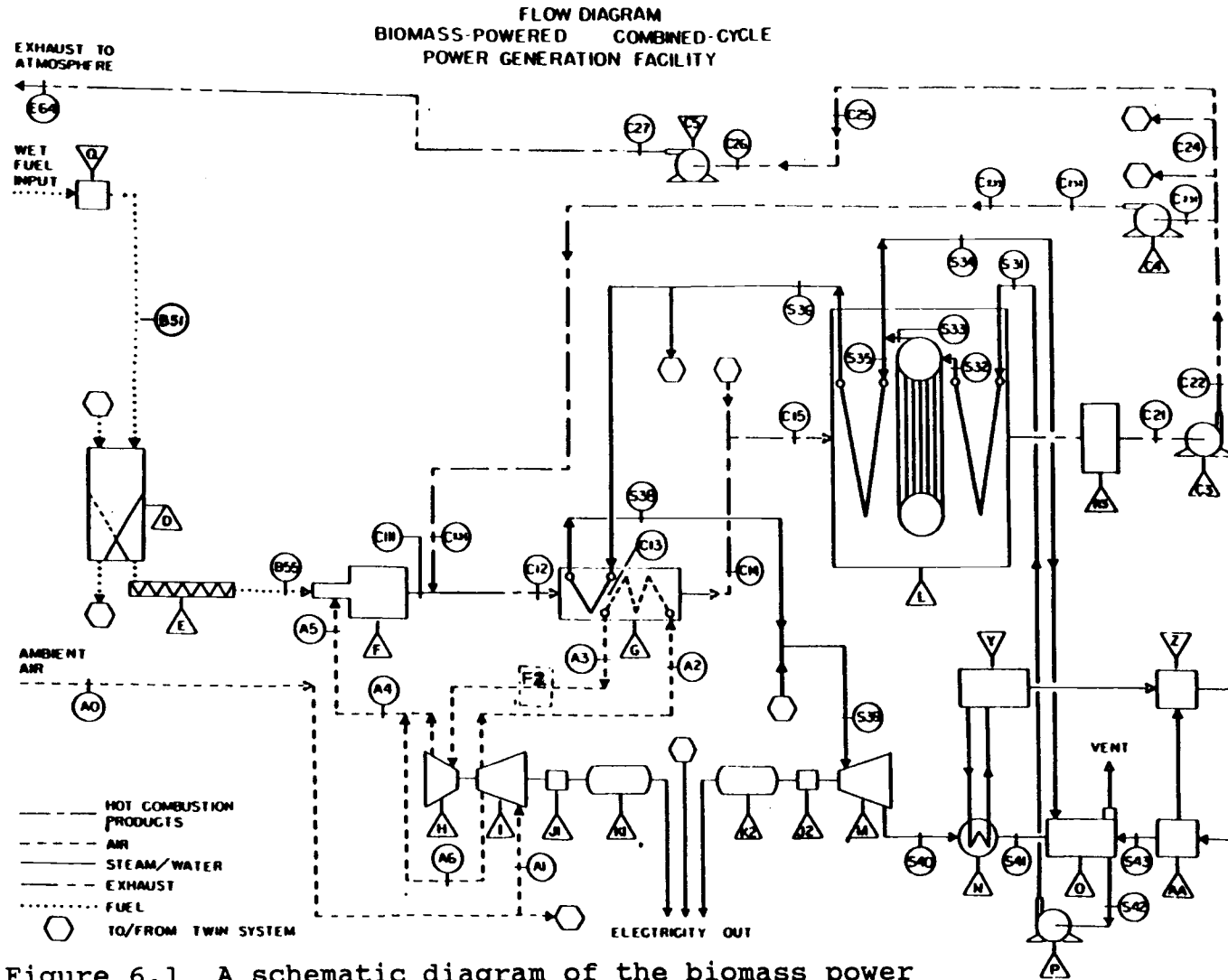


Figure 6.1 A schematic diagram of the biomass power plant.

Table 6.1 System Components for Biomass Plant

Dryer - A
Water Treatment Package - AA
Cyclones - B1, B2, B3
Fans - C1, C3, C4, C5
Storage Bins - D
Screw Feeders - E
Combustor - F1
Heat Exchangers - G
Trimburner - F2
Gas Turbine - H
Compressor - I
Gear boxes - J1, J2
Generators - K1, K2
Heat Recovery Steam Generator - L
Throttling Valve - T
Desuperheater - V
Steam Turbine - M
Condenser - N
Deaerator - O
Pump - P
Hammermill - Q
Air Pollution Devices - R
Cooling Tower - Y
Solid Waste Treatment Package - Z

6.2 Computer Models Used

The computer model used to simulate the biomass power plant was developed during previous studies of this power plant [16,17]. All components of the power plant are fixed in size. A fixed size ceramic heat exchanger model was developed for this analysis, and a program listing is given in Appendix (B). The values of the various geometric parameters of the heat exchanger such as the pipe spacing normal to the flow direction, the number of pipes normal and parallel to the flow direction, the tube length and the pipe diameters will be inputs to the fixed size model. These values were evaluated using the previously developed variable size heat exchanger model, for specified flow conditions.

In the model used to simulate the power plant, each component of the power plant is a separate module, essentially a subroutine. These subroutines are combined by an executive program that reads the input data, passes the intermediate calculations to each subroutine, and creates the output file. An iterative technique, using successive substitution, is used in the main program to calculate the various unknown plant parameters. The unknown variables are initially estimated and then improved upon during intermediate calculations, for use in the next iteration. The executive program controls the iteration process and checks for convergence. Program

listings of the executive program, the subroutine which calls the various component models and the subroutines representing the various plant components are given in reference [17].

6.3 The Ceramic Heat Exchanger System

The influence of some ceramic heat exchanger parameters on the performance of the biomass power plant will be investigated in this section. For these simulations, a maximum temperature of 2250 F was specified for the ceramic heat exchanger. If the flue gas exit temperature from the combustor increases above the maximum allowable heat exchanger inlet temperature, a low temperature mixing stream (c234 in Figure 6.1) is used to reduce this temperature.

6.3.1 Influence of Wood Moisture

The typical yearly variation of the Wood moisture content is given in reference [17], and shown in Figure 6.2. Since there is no control over the moisture content in the wood, moisture contents between 25% and 50% (wet basis) will be considered for the remainder of the power plant analysis.

The variation of the plant net efficiency and power with the wood moisture content is shown in Figures 6.3 and 6.4. It can be seen that there is a significant drop in the net efficiency and power at high moisture contents

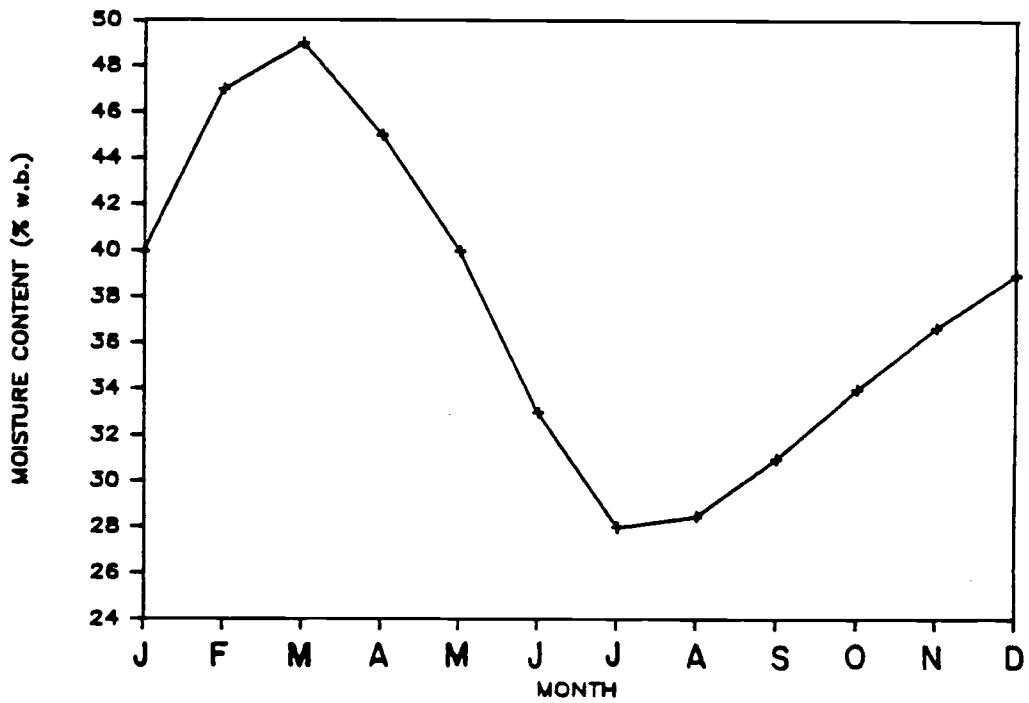


Figure 6.2 The yearly variation of the average wood moisture content, (from [16]).

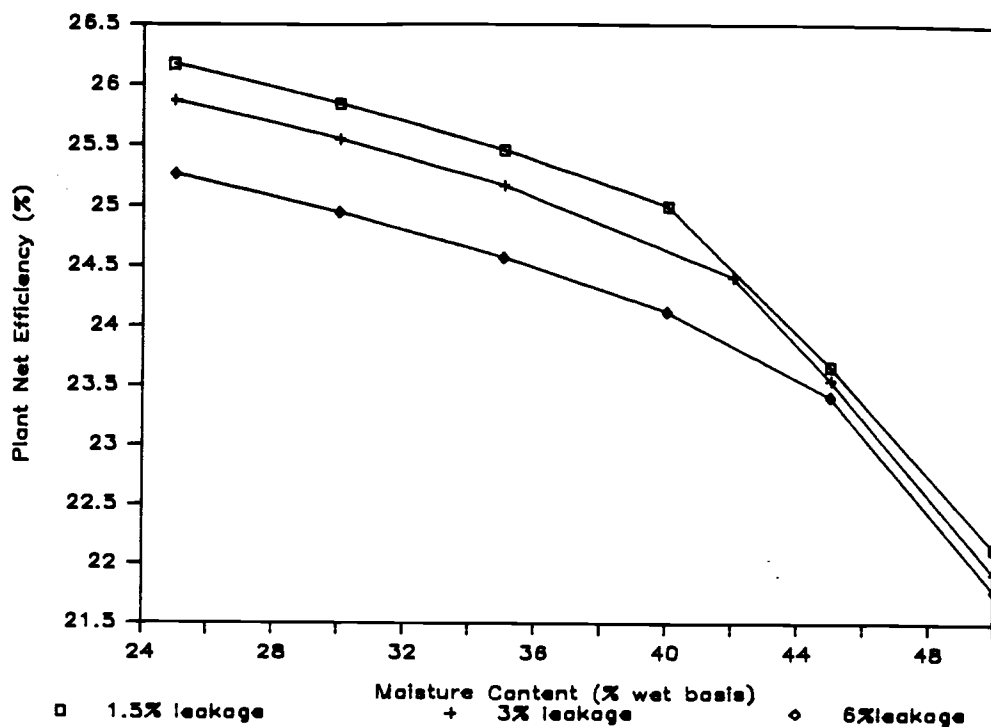


Figure 6.3 The plant net efficiency as a function of the fuel moisture content, at leakage flow rates of 1.5, 3.0 and 6.0 percent.

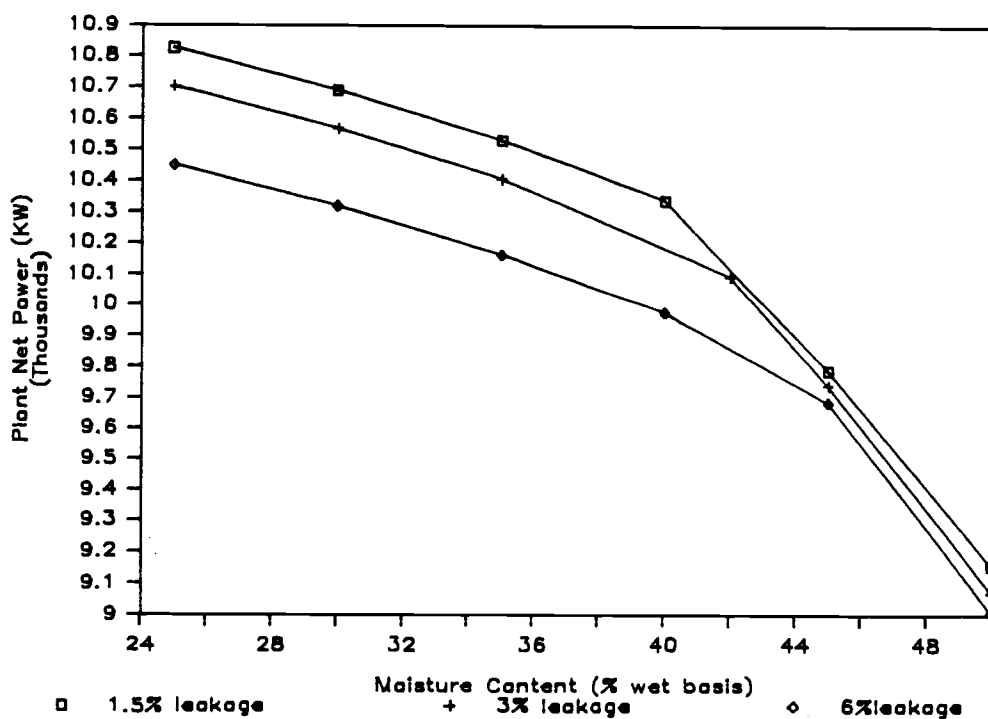


Figure 6.4 The plant net power as a function of the fuel moisture content, at leakage flow rates of 1.5, 3.0 and 6.0 percent.

(greater than 40%). This can be explained by considering the variation of the heat exchanger inlet temperature with the moisture content, as shown in Figure 6.5. From this figure, a significant drop in the inlet temperature to the heat exchanger is observed at moisture contents greater than 40%. This results in a decrease in the turbine inlet temperature below its rated value. The resulting decrease in the gas cycle efficiency accounts for the drop in the performance of the power plant.

The drop in performance, at high moisture contents, is not desirable for the efficient operation of the ceramic heat exchanger system. The drop in the flue gas inlet temperature is due to a reduction of the flue gas outlet temperature from the combustor. Since there is no control over the wood moisture content, the best power plant arrangement should have a maximum heat exchanger inlet temperature for the entire range of wood moisture contents. The variation of the flue gas exit temperature from the combustor as a function of the amount of excess air used for the wood combustion, for various moisture contents, is given in reference [18] and shown in Figure 6.6. These results are for combustion air at 600 F, which is a typical value in the biomass power plant. During previous studies of this power plant, and for the present simulation 162.5% of excess air (air fuel ratio of approximately 17) is used for wood combustion.

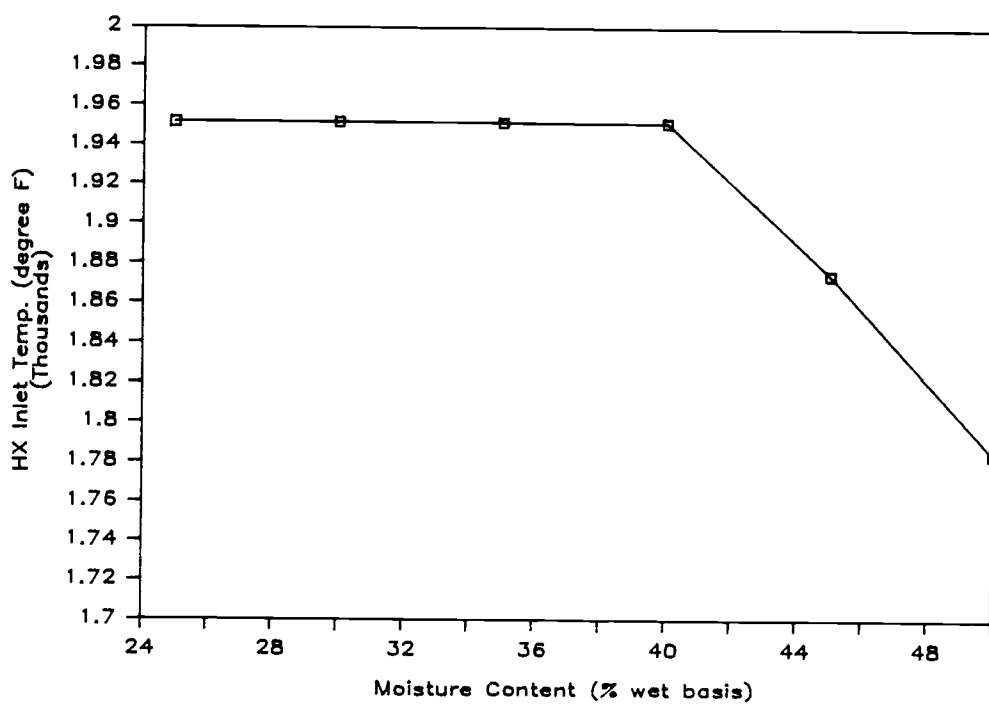


Figure 6.5 Flue gas inlet temperature to the heat exchanger as a function of the wood moisture content.

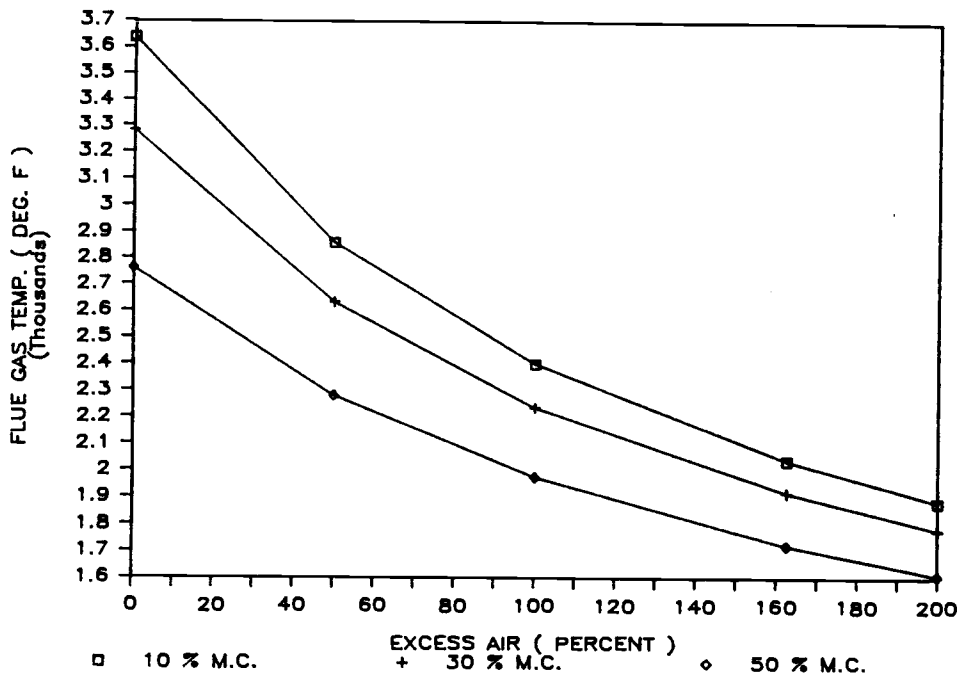


Figure 6.6 Flue gas outlet temperature from the combustor as a function of the amount of excess air used, at wood moisture contents of 10, 30 and 50 percent, (from [17]).

From Figure 6.6, it can be observed that the percent excess air used has to be decreased to approximately 50 percent to obtain the necessary heat exchanger inlet temperature for the entire range of moisture contents. Therefore the reduction of the percent excess air used can be recognized as a necessary change, for the efficient operation of the ceramic heat exchanger system.

6.3.2 Influence of Leakage

Leakage was recognized to be one of the problems associated with the present generation of ceramic heat exchangers. Since the leakage accounts for a direct system loss, the effects of the heat exchanger leakage on the biomass power plant performance was investigated. The results of this investigation are presented in Figures 6.3, 6.4, 6.7 and 6.8. From Figure 6.3, a decrease in net efficiency of about 1% can be observed when the leakage increases from 1.5% to 6%. This difference remains almost constant up to a moisture content of about 40%, and the influence of leakage at high moisture contents is not very significant. A similar behavior can be observed in the variation of the net power (see Figure 6.4), with a power loss of about 400 kW at moisture contents less than 40%.

Leakage results in a mass and energy transfer from the gas turbine cycle to the steam turbine cycle. This can be clearly seen from Figure 6.7 and Figure 6.8. As

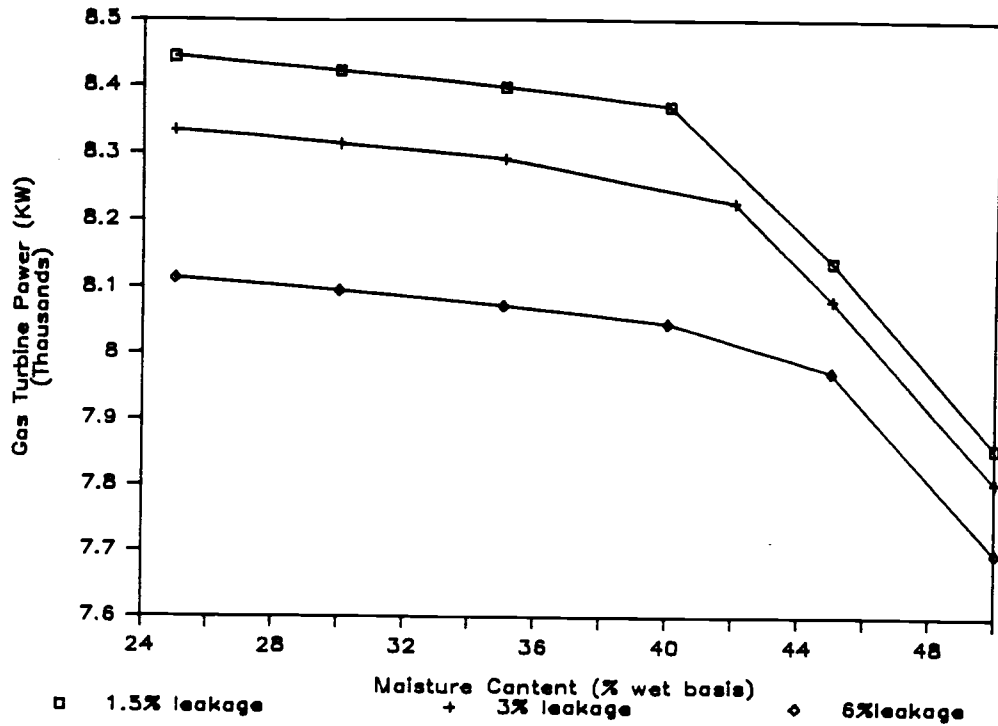


Figure 6.7 Gas turbine power as a function of the wood moisture content, at leakage flow rates of 1.5, 3.0 and 6.0 percent.

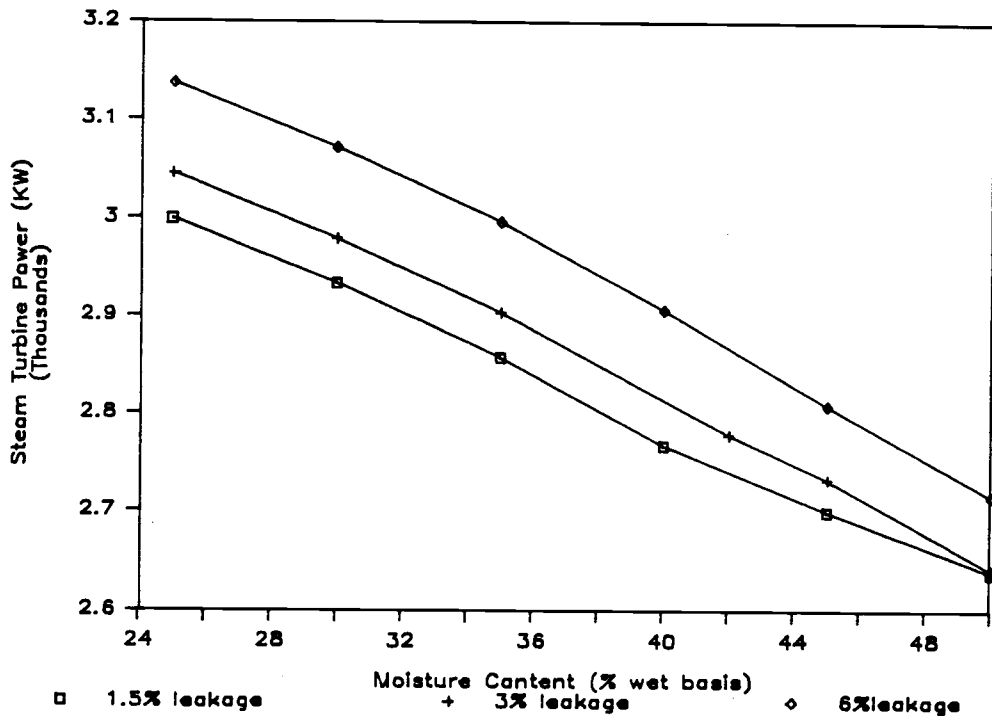


Figure 6.8 Steam turbine power as a function of the wood moisture content, at leakage flow rates of 1.5, 3.0 and 6.0 percent.

the leakage increases the power generated by the gas turbine decreases whereas the power generated by the steam turbine increases. The increase in the power generated by the steam turbine is less than the loss of power in the gas turbine, resulting in a power loss in the total system. The above is due to the higher efficiency of the gas turbine cycle compared to that of the steam turbine cycle.

At high moisture contents, there will be a drop in the air outlet temperature from the heat exchanger, as a result of the drop in the flue gas inlet temperature into the heat exchanger. A gas turbine suitable for this type of power plant, with an external combustor and heat exchanger hookup, has a rated turbine inlet temperature of approximately 1730 F, as given in reference [19]. Since the gas turbine operates at its maximum efficiency at the rated turbine inlet temperature, a drop in temperature below this value will result in a drop in the overall efficiency of the gas turbine cycle. Therefore at low turbine inlet temperatures the difference in efficiency of the gas turbine cycle to that of the steam turbine cycle is not very significant. This results in the leakage having a lesser effect on the overall plant performance at high moisture contents.

6.3.3 Turbine Inlet Temperature

The turbine inlet temperature is equal to the temperature of the air leaving the ceramic heat exchanger. In previous studies conducted on many alternative arrangements of this power plant, it has been concluded that the plant net efficiency and power was a strong function of the turbine inlet temperature, regardless of the system. The influence of the heat exchanger air outlet temperature on the plant net efficiency is shown in Figure 6.9. It can be seen that the plant net efficiency is a strong function of the turbine inlet temperature, and hence confirms the earlier results. The area of the heat exchanger, necessary to obtain the rated turbine inlet temperature, is a strong function of the flue gas inlet temperature. Therefore, from an economic and thermodynamic point of view a high flue gas inlet temperature to the heat exchanger is desirable.

6.4 Comparison with Alternative Systems

Two alternative methods have been considered in the biomass power plant to obtain a high turbine inlet temperature. They are,

- i) Using a ceramic heat exchanger
- ii) Using a metallic heat exchanger and a trimburner.

These two systems together with a system using only the metallic heat exchanger will be considered in this

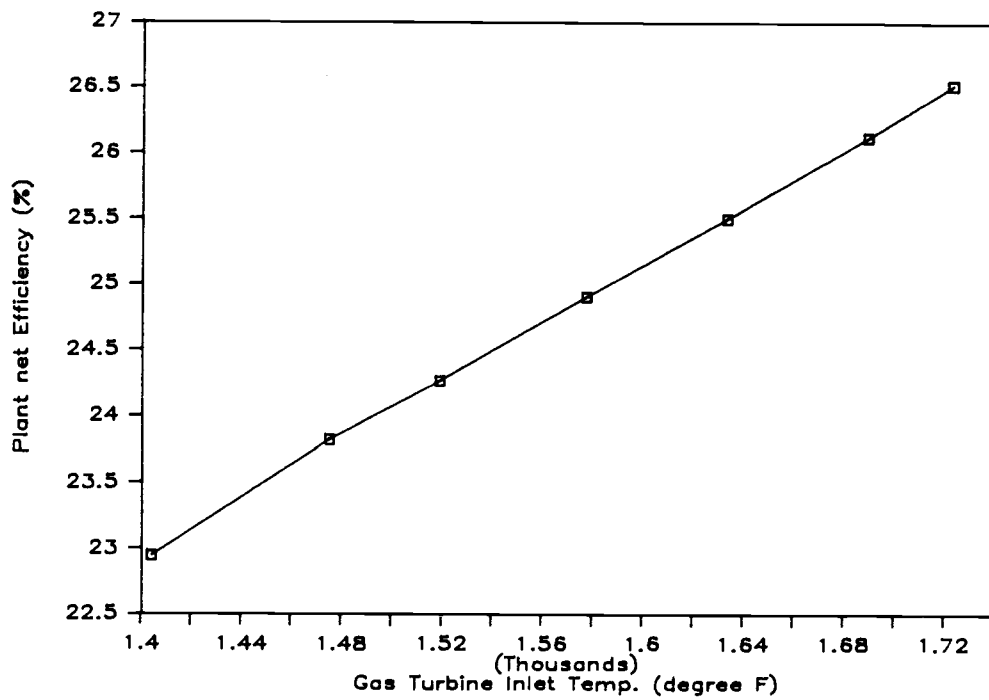


Figure 6.9 Plant net efficiency as a function of the turbine inlet temperature.

section. The ceramic heat exchanger system being considered is assumed to have a leakage flow of 1.5%. The variation of the plant net efficiency and power with the wood moisture content is shown in Figure 6.10 and Figure 6.11 respectively.

The ceramic heat exchanger system is much superior to the metallic heat exchanger system. This is due to the higher turbine inlet temperature in the ceramic heat exchanger system. The difference in efficiency is approximately 3% at moisture contents less than 40%, and is close to 1% at a moisture content of 50%. The variation of the net power exhibits a similar trend to that of the net efficiency, with the ceramic heat exchanger system generating approximately 1000 kW more than the metallic heat exchanger system at wood moisture contents less than 40%.

Comparing the ceramic heat exchanger system with the trimburner system, the ceramic heat exchanger system has a slightly better efficiency at moisture contents up to 40% while the net efficiency of the trimburner system is superior at higher moisture contents. The net power of the trimburner system is higher than the ceramic heat exchanger system. This is mainly due to the additional energy input into the trimburner, and hence is not a good parameter for the purpose of comparison.

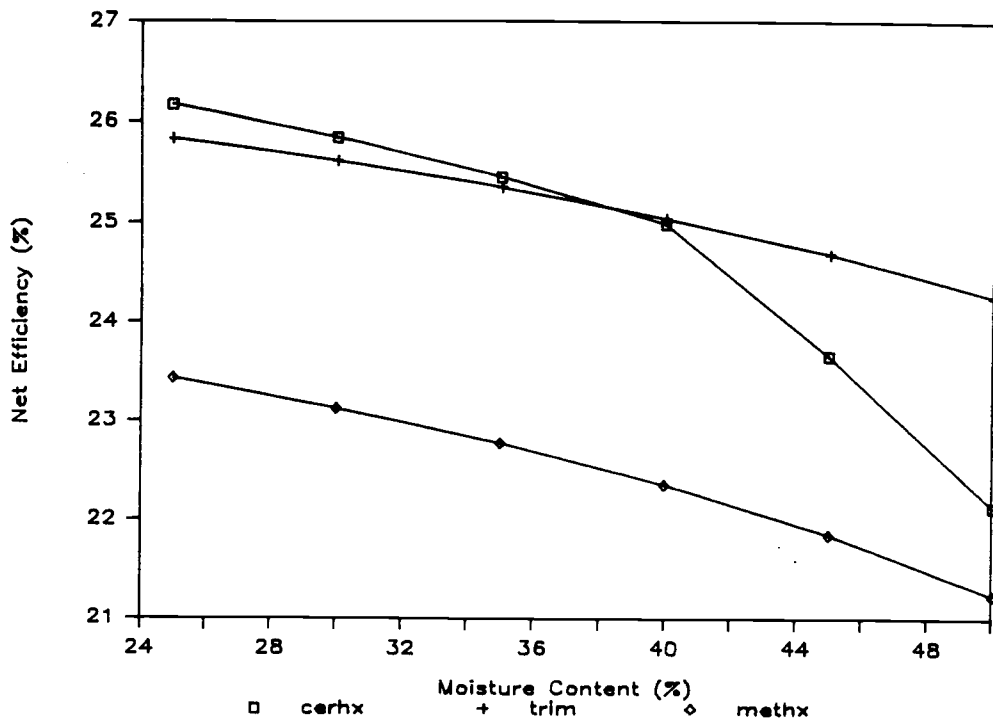


Figure 6.10 Plant net efficiency as a function of the wood moisture content, for the alternate systems of the power plant.

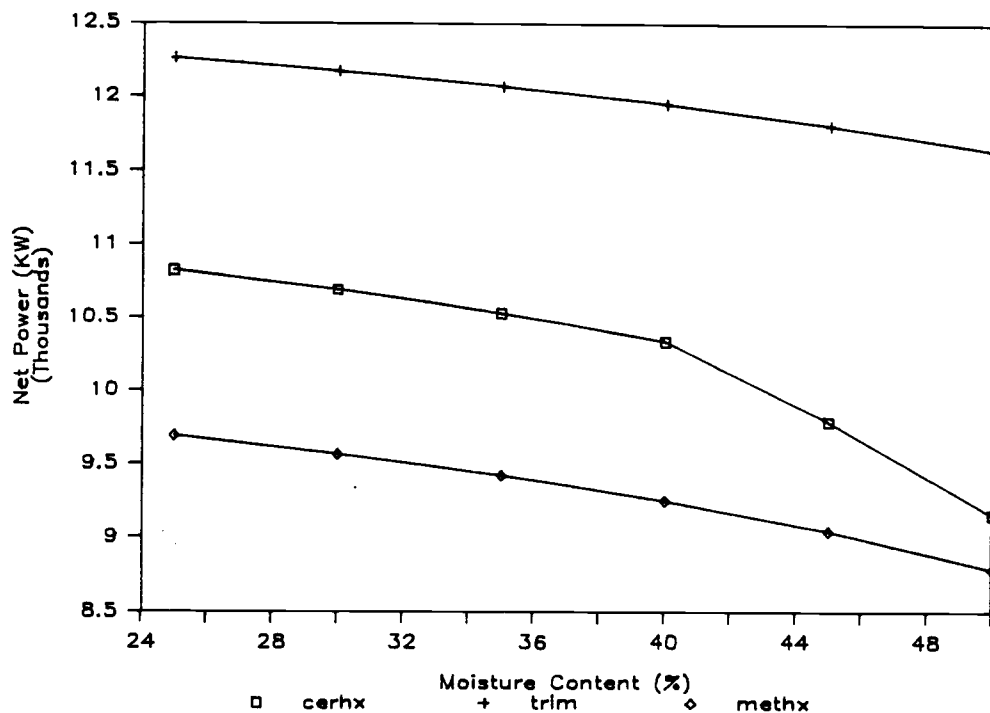


Figure 6.11 Plant net Power as a function of the wood moisture content, for the alternate systems of the power plant.

6.5 Conclusions

In the biomass power plant, the use of a ceramic heat exchanger is much more attractive than a metallic unit. However, the flue gas inlet temperature to the heat exchanger should be kept sufficiently high (approximately 2250 F) to obtain the best results from the ceramic heat exchanger system.

Commercially available trimburners use oil as fuel. Since the present study is to develop a feasible system using wood as fuel, a trimburner using the same source as fuel is the most appropriate. This can be a disadvantage in using a trimburner for this type of power plant. A detailed discussion on trimburners for this type of power plant can be found in reference [20]. It was concluded in section 6.3.1 that the sudden decrease in the net efficiency and power of the ceramic heat exchanger system, at high moisture contents, can be avoided by reducing the percent of excess air used for combustion.

From the above analysis it is apparent that there is no significant advantage of one system over the other thermodynamically. Both the trimburner and ceramic heat exchanger systems are attractive alternatives. Therefore the final decision will have to be based on the reliability and cost of the systems.

BIBLIOGRAPHY

- [1] Reistad, G.M., Bushnell, D.J., Bauer, T.L., Brynjolfsson, S. and Fox, S.J., "Evaluation of Parametric and Selected System Variations of Combined-Cycle Biomass Systems", Report prepared for the U.S. Department of Agriculture, January 1985.
- [2] McDonald, C.F., "The Role of Ceramic Heat Exchanger in Energy and Resource Conversion", Journal of Engineering for Power, Vol.102, April 1980, pp.303-315.
- [3] Ward, M.E., "Development of a Ceramic Tube Heat Exchanger with Relaxing Joint", Report prepared for the U.S. Department of Energy, Report no: FE-2556-30, June 1980.
- [4] Brynjolfsson, S., "Investigation of Heat Exchangers for Application in Indirect-Fired, Combined Cycle Power Plants Fired with Wood", M.S. Project report, Oregon State University, Corvallis, 1983.
- [5] Willamina Project Report, "Indirect-Fired, Biomass-Fueled, Combined-Cycle, Gas Turbine Power Plant Using a Ceramic Heat Exchanger", Vol.1, May 1984.
- [6] Information supplied by Haugue International, for OSU 10MW wood-fired power plant, September 1985.
- [7] Coombs, M., Kotchick, D., and Weidhaas, M., "High Temperature Ceramic Heat Exchanger Development", Airsearch Manufacturing Company, May 1983.
- [8] Report prepared for the US department of energy, "An Assesment of Ceramic Materials Technology for Heat Exchangers", Report no: EGG-SE-6367, January 1984.
- [9] Ritter, J.E., Rosenfeld, L., and Jakus, K., "Erosion and Strength Degradation in Alumina", ASME, 1985.
- [10] Ritter, J.E., Strzepa, P., and Jakus, K., "Erosion and Strength Degradation in Soda-Lime Glass", Physics and Chemistry of Glasses, Vol.25 No.6, December 1984.
- [11] ENFOR project C-258, "A Comparative Assesment of Forest Biomass Conversion to Energy Forms", December 1983.

- [12] Bowman, R.A., Mueller, A.C, and Nagle, W.M, "Mean Temperature difference in design", ASME, 1939.
- [13] Hemisphere Publishing Corp., "Heat Exchanger Design Handbook", Vol 2, 1983.
- [14] Hemisphere Publishing Corp., "Heat Exchanger Design Handbook", Vol 1, 1983.
- [15] Bejan, A., "Entropy Generation Through Heat and Fluid Flow", John Wiley & Sons, 1982.
- [16] Fox, S.J., "Computer Simulation of a Combined-Cycle Biomass-Fueled Power Plant", M.S. Thesis, Oregon State University, Corvallis, April 1984.
- [17] Brawn, R.C., "off-Design Analysis and Control of a Wood-Fired Combined-Cycle Power Plant", M.S. Thesis, Oregon State University, Corvallis, March 1985.
- [18] Dadkhah-Nikoo, A., "Analysis of Wood Combustion and Combustion Systems for a Combined-Cycle Wood-Fired Power Plant", M.S. Thesis, Oregon State University, Corvallis, August 1985.
- [19] Ebasco Services Inc., "Oregon State University 10 MW Biomass-Fired Combined-Cycle Cogeneration Plant", Feasibility Report, Task 5A, September 1985.
- [20] Stephenson, J.D., "Analysis of a Wood-Fueled Trimburner System for use in a Combined-Cycle, Wood-Fired Power Plant", M.S. Thesis, Oregon State University, Corvallis, September 1985.

APPENDICES

Appendix A

DESCRIPTION OF SYSTEMS

Metallic Heat Exchanger System (System 5)

Trimburner System (System 7)

Ceramic Heat Exchanger System (System 8)

Appendix A

DESCRIPTION OF SYSTEMS

Three alternative designs of the biomass power plant will be described in this appendix. The systems described are referred to as system 5 (metallic heat exchanger system), system 7 (trimburner system) and system 8 (ceramic heat exchanger system). The numbering system used is consistent with that defined in reference [1]. A schematic diagram of the biomass power plant is presented in Figure 6.1, and a listing of the plant components is given in Table 6.1.

System 5

The power plant consists of two combustors, two indirect-fired gas turbine systems and a single steam turbine system. In modelling only half of the system has been considered. Therefore all the figures and descriptions will be for half of the actual system.

System 5 has a metallic heat exchanger, and no trimburner. The proposed combined-cycle power plant is nominally rated at 10 MW. Fuel is obtained from forest residues and/or industrial mill wastes. The fuel arrives by truck at the plant site in hogged form, 3 inch minus, with a moisture contents in the range of 35 to 50 percent wet basis. A 30 day supply of fuel is maintained on site. Fuel is removed from storage to the wet-cell combustor

with a screw feeder.

The hot combustion gases leaving the combustor is passed through the heat exchanger where the steam produced in the heat recovery steam generator is super heated. The combustion gases then flow through a second heat exchanger heating the pressurized air supplied by the compressor. The high temperature (1450 F), high pressure (approximately 9 atm) air is expanded through the gas turbine, driving the gas turbine , compressor and generator. The gas turbine exhaust is then used as combustion air. A blend box is supplied at the exit of the combustor so that the inlet temperature into the metallic heat exchangers is maintained at 1675 F. The mixing air for this blend box is returned from the exit of the heat recovery steam generator (HRSG). The hot combustion gases leaving the heat exchangers is passed through the HRSG where much of the available energy of the gases is removed by producing steam. Finally the gas is passed through the pollution devices and then discharged to the atmosphere.

In the steam cycle, 640 psia feedwater is supplied to the economizer by the feedwater pump. The feedwater is heated in the economizer by the exhaust gases thereby supplying the evaporator with saturated makeup water. Excess feedwater flow in the economizer is throttled to 20 psia and returned to the deaerator. Saturated steam

produced in the evaporator flows through the initial superheater in the HRSG before receiving additional superheating in the steam-gas heat exchanger. Before entering the steam turbine, the steam flows through a desuperheater where excessive steam temperatures may be reduced to 900 F by injecting HRSG feedwater. The steam is cooled by the latent heat of vaporization of the feedwater. After passing through the turbine, the steam is condensed by 5200 gpm of cooling water supplied from the cooling tower. The condensate is pumped from the condenser operating at 1.5 psia to the deaerator at 20 psia. Depending on the amount of feedwater recycled from the economizer, some saturated steam is bled from the evaporator and supplied to the deaerator for deaerating purposes.

Makeup water is supplied to the cooling tower and deaerator from the water treatment unit. Waste water is sent to the waste water treatment facilities before discharging.

System 7

The difference between the metallic heat exchanger system (system 5) and system 7 is the addition of a trimburner. The trimburner considered in this study is essentially a duct burner. Using the trimburner, the hot compressed air leaving the metallic heat exchanger is heated to the rated turbine inlet temperature. This

allows the gas turbine to produce its maximum rated power.

System 8

System 8 is the ceramic heat exchanger system. The compressed air is heated up to the rated turbine inlet temperature in the heat exchanger. Hence the difference between system 5 and 8 is the use of a ceramic heat exchanger in place of the metallic unit. Due to the use of a ceramic heat exchanger the inlet temperature into the heat exchanger can be increased upto 2400 F. Systems 7 and 8 were the two alternative systems considered to obtain a high turbine inlet temperature.

Appendix B

HEAT EXCHANGER MODELS

.Multiple Gas-Side Pass Cross-Flow HX (V.S)

.Multiple Gas-Side Pass Cross-Flow HX (F.S)

.Heat Exchanger Subroutines

Appendix B

HEAT EXCHANGER MODELS

```

C***** CERAMIC CROSS-FLOW HEAT EXCHANGER *****
C.....Multiple Gas-Side Pass (U.S).....
C
C   This program calculates the size of the ceramic cross-flow
C   Heat Exchanger. The heat exchanger has multiple passes on the
C   gas-side, and one or more passes on the air-side. The
C   thermodynamic states of the incoming streams and the outlet
C   temperature of the air is given. Air flows inside the pipes,
C   and the combustion products flow on the shell side. The
C   number of passes on the gas-side noPg, and the number of pipes
C   parallel to the flow direction in one air pass npp is
C   specified by the user. The above values are kept constant
C   throught the program. The pipe size is a costant, and is
C   specified by giving the inner and outer diameters, ID and OD,
C   respectively. Initial guesses for the pipe spacing normal to
C   the flow direction, SnD, and the number of pipes nomal to the
C   flow direction, npn, is given by the user, and is varied in
C   the program. The pipe spacing parallel to the flow direction
C   SpD is a variable in the program, but is kept equal to SnD.
C   The maximum velocity on the shell side is kept below a certain
C   value, depending on the diameter of the eroding particles,
C   to prevent pipe erosion. The friction losses are controlled
C   by specifying the upper bounds for the pressure drops. The
C   maximum pipe length is user specified, and is dependant on
C   the material strength. By specifying the lower bounds of the
C   above quantities, it was possible to make the program
C   insensitive to the initial guesses. The amount of leakage
C   should be provided by the user , and thus corrections are made
C   for the pressure drop and the change in the composition of
C   the shell side gases.
C
C                                     Jatila Ranasinghe, November 1985.
C
C Variable names:
C
C   area   - Heat transfer area. (sq.ft)
C   Cp_    - Specific heat. (Btu/lbm F)
C   Derosn - Diameter of the dust particles. (in)
C   dP_    - Pressure drop. (psia,W.C)
C   Ex_    - Exergy. (KW)
C   Fcfhx  - Correction factor F.
C   foul   - Fouling in the heat exchanger.
C   h_     - Heat transfer coefficient. (Btu/sq.ft F)
C   H_     - Enthalpy. (Btu/lbm)
C   height - Height of the heat exchanger. (ft)
C   ID     - Inside tube diameter. (in)
C   IRR    - Irreversibility. (KW)
C   K_     - Thermal conductivity. (Btu/h ft R)
C   leakage - Percentage leakage.
C   length - Effective pipe length. (ft)

```

```

C      lmax - Maximum allowable pipe length. (ft)
C      LMTD - Log mean temperature difference.
C      MR_ - Mass flow rate. (lbm/s)
C      mu_ - Dynamic viscosity. (lbm/s ft)
C      noPg - Number of gas-side passes.
C      noU - Number of passes on the air-side divided by 2.
C      npn - Number of pipes normal to the flow direction.
C      npp - Number of pipes parallel to the flow direction.
C      OD - Outer tube diameter. (in)
C      P_ - Pressure. (psia,W.C)
C      Q - Heat transfer. (Btu/s)
C      Ro_ - Density. (lbm/cu.ft)
C      rough - Pipe roughness.
C      SnD - Normalised pipe spacing normal to the flow direction.
C      SpD - Normalised pipe spacing parallel to the flow direction.
C      T_ - Temperature. (F)
C      totalL - Total pipe length .
C      type - Type of heat exchanger. (inline=1., staggered=2.)
C      U - Overall heat transfer coefficient. (Btu/sqft F)
C      UA - U*area
C      V_ - Velocity. (ft/s)
C      width - Width of the heat exchanger. (ft)

```

Subscripts:

```

C      a - air
C      ab - absolute value.
C      ave - average value.
C      cnv - due to convection.
C      ersn - erosion.
C      fric - due to friction.
C      g - gas.
C      in - at the inlet.
C      lk - due to leakage.
C      loss - total loss.
C      max - the maximum value.
C      o - at the outlet.
C      out - outside.
C      pip - inside the pipe.

```

C*****

```

C
C $TITLE:'Multi-gas pass Hx'
C $storage:2

```

```

      SUBROUTINE CERHXG(Tain,Pain,MRain,yaCO2,yaH2O,yaO2,yaN2,yaAr,yaCO,
>                      Tao,dPamax,Pao,MRao,
>                      Tgin,Pgin,MRgin,
>                      ygCO2,ygH2O,ygO2,ygN2,ygAr,ygCO,
>                      yoCO2,yoH2O,yoO2,yoN2,yoAr,yoCO,
>                      dPgmax,Tgo,Pgo,MRgo,dPa,dPg,
>                      OD,ID,SnD,noU,npp,npn,type,noPg,length,lmax,
>                      K,Derosn,rough,foul,ROasn,leakge,
>                      u,area,Umax,IRR,print)

```

```

C
C      logical*2 print

```

```

real MRa,MRg, ID, lmax,K,LMTD,length,MRpip,12,11,
>   mua,mug,MUGAST,KGAST,ka,kg,IRR,noU,npp,npn,npn1,
>   leakge,MRgin,MRain,MRalk,MRO,MRao,MRgo,noPg
common/DS/Tds,Pds,ydsCO2,ydsH2O,ydsO2,ydsN2,ydsAr,ydsCO
character*10 txt1,txt2

C
C
      PI=acos(-1.)
C
C.....Calculate the average mass flow rates.
C
      MRalk=MRain*leakge/100.
      MRao =MRain-MRalk
      MRgo =MRgin+MRalk
C
      MRa  =.5*(MRain+MRao)
      MRg  =.5*(MRgin+MRgo)
C
C.....Calculate the heat transfer.
C
      Hain=HGAST(Tain,yaCO2,yaH2O,yaO2,yaN2,yaAr,yaCO)
      Hao  =HGAST(Tao,yaCO2,yaH2O,yaO2,yaN2,yaAr,yaCO)
      Q    =MRa*(Hao-Hain)
C
C.....Find the exit temp of the gas.
C
      Hgin=HGAST(Tgin,ygCO2,ygH2O,ygO2,ygN2,ygAr,ygCO)
      Hgo  =Hgin - Q/MRg
      Tgo  =TGASH(Hgo,ygCO2,ygH2O,ygO2,ygN2,ygAr,ygCO)
C
C.....Find the correction factor F.
C
      if(noPg.gt.1.)then
        Fcfhx=1.
      else
        Fcfhx=CORRHX(Tain,Tao,Tgin,Tgo,noU)
      end if
C
C.....Calculate the LMTD,Cp and UAreq.
C
      dt1=Tgin-Tao
      dt2=Tgo-Tain
      LMTD=(dt1-dt2)/alog(dt1/dt2)
C
      Cpa =(Hao-Hain)/(Tao-Tain)
      Cpg =(Hgin-Hgo)/(Tgin-Tgo)
      UAreq=Q/Fcfhx/LMTD*3600.
C
C.....Assume U=8 and estimate pipe length.
C
      if(noU.NE.0.)then
        length=UAreq/00*12./(PI*npn*npp*noU*2.*noPg)/8.
      else
        length=UAreq/00*12./(PI*npn*npp*noPg)/8.
      end if

```

```

totalL=noPg*length
C
C.....Calculate the average temp and initial guess for wall temp.
C
    Tavea=(Tain+Tao)*.5
    Taveg=(Tgin+Tgo)*.5
    Twall=0.25*Taveg+0.75*Tavea
    Pgo  =Pgin-dPgmax/100.*Pgin
    Pao  =Pain-dPamax/100.*Pain
C
C.....Initialize the test conditions.
C
    A=0.
    B=0.
    C=0.
    D=0.
    npn1=10000.
    SnD1=100.
C
C.....Calculate the mass flow rate inside the pipe.
C
    10 MRpip=MRa/(npn*npp)
C
C.....Iterate and calculate the correct length.
C
    12=0.
    UA2=0.
C
    20 do 30 i=1,20
        SpD=SnD
C
        Paveg=(Pgin+Pgo)*.5
        Pavea=(Pain+Pao)*.5
C
        Roavea=ROGAS(Tavea,Pavea,yaCO2,yaH2O,yaO2,yaN2,yaAr,yaCO)
C
C.....Calculate the heat transfer coefficient inside the pipe.
C
        hincnv=HINCON(MRpip,yaCO2,yaH2O,yaO2,yaN2,yaAr,yaCO,Tavea,
            Pavea,ID,totalL)
        hin    =hincnv
C
C.....Calculate the outside heat transfer coefficient.
C
        hout=HHXCF(MRg,ygCO2,ygH2O,ygO2,ygN2,ygAr,ygCO,Taveg,Twall,
            Paveg,length,OD,type,SnD,SpD,npn,npp,noU)
C
C.....Calculate U,A and UA
C
    U=1./((1./((ID/OD)*hin))+1./hout+OD/(2.*K*12.)*alog(OD/ID)+foul)
C
    if(noU.NE.0.)then
        area=OD/12.*PI*totalL*npn*npp*noU*2.
    else
        area=OD/12.*PI*totalL*npn*npp

```

```

        end if
C
        UA=U*area
C
C.....Calculate the wall and film temps
C
        Twall=(hin*Tavea+hout*Taveg)/(hin+hout)
        Tfilmg=(Taveg+Twall)*.5
C
C.....Check for convergence.
C
        if(abs(UA/UAreq-1.)>.01)goto 40
            I1=I2
            UA1=UA2
            I2=length
            UA2=UA
C
        length=(UAreq-UA2)/(UA1-UA2)*(I1-I2)+I2
        if(length>=0.)length=(UAreq-UA2)/UA2*I2+I2
        totalL=length*noPg
    30 continue
C
C.....Check for tube erosion.
C
    40 CONTINUE
        height=totalL*1.2
C
        call VEROSN(Paveg,Taveg,MRg,length,OD,SnD,SpD,nnp,Derossn,ROash,
        >             ygCO2,ygH2O,ygO2,ygN2,ygAr,ygCO,Umax,Versn)
C
        if(Umax>Vern)then
            SnD=SnD+.05
            goto 20
        end if
C
C.....Check for maxm pres drop on gas-side.
C
        dPg=PHXCF(MRg,ygCO2,ygH2O,ygO2,ygN2,ygAr,ygCO,Taveg,Tfilmg,
        >             Paveg,length,OD,type,SnD,SpD,nnp,pp)
C
        if(noU>0.)dPg=dPg*2.*noU
            Pgo=Pgin-dPg
            Paveg=(Pgin+Pgo)*.5
C
C
        if(dPg>=dPpmax)then
            SnD=SnD+.05
            goto 20
        end if
C
C.....Check for maxm pressure drop inside the pipe.(Friction+losses)
C
        call PINPIP(MRpip,yaCO2,yaH2O,yaO2,yaN2,yaAr,yaCO,Tavea,Pavea,
        >             ID,rough,dPfric,fric)
C

```

```

C
  if(noU.NE.0.)then
    dPfric=dPfric*totalL*2.*noU
  else
    dPfric=dPfric*totalL
  end if
C
C.....Pressure loss at entrance exit and bends.
C
  Vpip=MRpip/ROavea/PI/((ID/12./2.)**2)
  dPloss=(Vpip**2)/2.*ROavea*(0.78+1.)/32.174/144.
C
C.....Total pressure loss in pipe.
C
  dPa=dPfric+dPloss
  Pao=Pain-dPa
  Pavea=(Pain+Pao)*.5
  if(dPa.GT.dPamax)then
    npn=npn+1.
    B=B+1.
    goto 10
  end if
C
C.....Check whether maxm length has been exceeded.
C
  if(length.GT.lmax)then
    npn=npn+1.
    B=B+1.
    goto 10
  end if
C
C.....Check whether maximum velocity and Pressure loss on the
C.....gas-side is too small.
C
  if((Umax.LT.0.95*Uersn).or.(dpg.lt.0.95*dpgmax))then
    if(SnD.GT.SnD1)goto 50
    SnD=SnD-.05
    SnD1=SnD
    A=A+1.
    goto 20
  end if
C
C.....Check whether the length and the pressure loss inside the
C.....pipes are too small.
C
50  SnD1=100.
    if((length.LT.0.95*lmax).or.(dpa.lt.0.95*dpamax))then
      if((B.gt.0.).and.(A.gt.0.))then
        npn1=10000.
        if(C.gt.0.)D=D+1.
      end if
      if(npn.GT.npn1)goto 60
      if(D.gt.1.)goto 60
        npn =npn-1.
        npn1=npn

```

```

    A=0.
    B=0.
    C=C+1.
    goto 10
end if
C
C.....Make adjustments for leakage .
C
60  continue
    call HXMIX(MRalk,yaCO2,yaH2O,yaO2,yaN2,yaAr,yaCO,Tao,Pao,
    >          MRgin,ygCO2,ygH2O,ygO2,ygN2,ygAr,ygCO,Tgo,
    >          MRgo,yoCO2,yoH2O,yoO2,yoN2,yoAr,yoCO,To)
C
C.....Calculate the exergies and irreversibility.
C
    Pginab= 14.696 + .03613*Pgin
    Pgoab = 14.696 + .03613*Pgo
C
    Sain=SGASTP(Tain,Pain,yaCO2,yaH2O,yaO2,yaN2,yaAr,yaCO)
    Sao =SGASTP(Tao,Pao,yaCO2,yaH2O,yaO2,yaN2,yaAr,yaCO)
    Sgin=SGASTP(Tgin,Pginab,ygCO2,ygH2O,ygO2,ygN2,ygAr,ygCO)
    Sgo =SGASTP(To,Pgoab,yoCO2,yoH2O,yoO2,yoN2,yoAr,yoCO)
    Exain=(Hain-(Tds+459.67)*Sain)*MRain*1.0552
    Exao =(Hao-(Tds+459.67)*Sao)*MRao*1.0552
    Exgin=(Hgin-(Tds+459.67)*Sgin)*MRgin*1.0552
    Exgo =(Hgo-(Tds+459.67)*Sgo)*MRgo*1.0552
    IRR  = Exain+Exgin-Exao-Exgo
C
C.....Transport properties of both Streams.
C
    kg =KGAST (Taveg,ygCO2,ygH2O,ygO2,ygN2,ygAr,ygCO)
    ka =KGAST (Tavea,yaCO2,yaH2O,yaO2,yaN2,yaAr,yaCO)
    mua=MUGAST (Tavea,yaCO2,yaH2O,yaO2,yaN2,yaAr,yaCO)
    mug=MUGAST (Taveg,ygCO2,ygH2O,ygO2,ygN2,ygAr,ygCO)
C
C.....Print the results.
C
    write(8,1000)'....AIR GAS HEAT EXCHANGER... '
    txt1='flue gas'
    txt2='air'
    call HXPRIN(txt1,txt2,Tgin,Tain,Pginab,Pain,MRg,MRA,Tgo,Tao,
    >          Pgoab,Pao,Cpg,Cpa,mug,mua,kg,ka,Exgin,
    >          Exain,Exgo,Exao,type,SnD,SpD,npn,npp,noPg,noU,OD,IO,K,rough,
    >          length,lmax,height,width,area,Umax,Versn,Fcfhx,hout,
    >          hin,foul,U,UA,LMTD,Tfilmg,Twall,Q,IRR,dPa,dPamax,dPgmax,dPg)
1000 format(1x/10x,a)
    RETURN
    END

```

C***** CERAMIC CROSS FLOW HEAT EXCHANGER *****
 C.....Fixed Size Model.....

C
 C This subroutine simulates a multiple gas-side pass, ceramic
 C cross-flow heat exchanger. The size of the heat exchanger
 C is specified by the user by giving the values of the number
 C of pipes parallel and normal to the flow direction, the number
 C of passes on the gas-side, normalized pipe spacing and the
 C pipe length in a single gas pass. The inlet thermodynamic
 C states of the gas and air are inputs to the subroutine. The
 C outlet thermodynamic states of the air and flue gas is
 C calculated in the model.

C
 C Jatila Ranasinghe, December 1985.

C
 C Variable names:
 C -----

C
 C area - Heat transfer area. (sq.ft)
 C Cp_ - Specific heat. (Btu/lbm F)
 C Derosn - Diameter of the dust particles. (in)
 C dP_ - Pressure drop. (psia,W.C)
 C Ex_ - Exergy. (KW)
 C Fcfhx - Correction factor F.
 C foul - Fouling in the heat exchanger.
 C h_ - Heat transfer coefficient. (Btu/sq.ft F)
 C H_ - Enthalpy. (Btu/lbm)
 C ID - Inside tube diameter. (in)
 C IRR - Irreversibility. (KW)
 C K_ - Thermal conductivity. (Btu/h ft R)
 C leakage - Percentage leakage.
 C length - Effective pipe length. (ft)
 C lmax - Maximum allowable pipe length. (ft)
 C LMTD - Log mean temperature difference.
 C MR_ - Mass flow rate. (lbm/s)
 C mu_ - Dynamic viscosity. (lbm/s ft)
 C noPg - Number of passes on the gas-side.
 C npn - Number of pipes normal to the flow direction.
 C npp - Number of pipes parallel to the flow direction.
 C OD - Outer tube diameter. (in)
 C P_ - Pressure. (psia,W.C)
 C Q - Heat transfer. (Btu/s)
 C Ro_ - Density. (lbm/cu.ft)
 C rough - Pipe roughness.
 C SnD - Normalised pipe spacing normal to the flow direction.
 C SpD - Normalised pipe spacing parallel to the flow direction.
 C T_ - Temperature. (F)
 C totalL - Total pipe length per single air-side pass. (ft)
 C U - Overall heat transfer coefficient. (Btu/sqft F)
 C UA - U*area
 C V_ - Velocity. (ft/s)

```

C      Subscripts:
C      -----
C
C      a      - air
C      ab     - absolute value.
C      ave   - average value.
C      cnv   - due to convection.
C      ersn  - erosion.
C      fric  - due to friction.
C      g     - gas.
C      in    - at the inlet.
C      lk    - due to leakage.
C      loss  - total loss.
C      o     - at the outlet.
C      out   - outside.
C      pip   - inside the pipe.
C
C*****
C
C $TITLE: 'Air-Gas heat exchanger'
C $storage:2
C      SUBROUTINE CRHXFS(Tain,Pain,MRain,yaCO2,yaH2O,yaO2,yaN2,yaAr,yaCO,
C      > Tao,dPa,Pao,MRao,
C      > Tgin,Pgin,MRgin,ygCO2,ygH2O,ygO2,ygN2,ygAr,ygCO,
C      > yoCO2,yoH2O,yoO2,yoN2,yoAr,yoCO,
C      > dPg,Tgo,Pgo,MRgo,
C      > OD,ID,SnD,noU,npp,npn,type,noPg,
C      > length,K,Derosn,rough,foul,ROash,leakge,
C      > Vmax,IRR,print)
C
C      logical*2 print
C      real MRa,MRg,ID,lmax,K,LMTD,length,MRpip,l2,l1,
C      > mua,mug,MUGAST,KGAST,ka,kg,IRR,noU,npp,npn,npn1,
C      > leakge,MRgin,MRain,MRalk,MRO,MRao,MRgo,noPg
C      common/DS/Tds,Pds,ydsCO2,ydsH2O,ydsO2,ydsN2,ydsAr,ydsCO
C      character*10 txt1,txt2
C
C      PI=acos(-1.)
C
C      C.....Calculate the average mass flow rates.
C
C      MRalk=MRain*leakge/100.
C      MRao =MRain-MRalk
C      MRgo =MRgin+MRalk
C
C      MRa  =.5*(MRain+MRao)
C      MRg  =.5*(MRgin+MRgo)
C
C      C.....Calculate the total pipe length in one pass.
C
C      SpD  =SnD
C      totalL=length*noPg
C
C      C.....Calculate the mass flow rate inside the pipe,
C      C.....and total heat transfer area.

```

```

C
  MRpip=MRa/(npn*npp)
C
  if(noU.eq.0.)then
    area=OD/12.*PI*totalL*npn*npp
  else
    area=OD/12.*PI*totalL*npn*npp*noU*2.
  end if
C
C.....Calculate enthalpy at inlets.
C
  Hain=HGAST(Tain,yaCO2,yaH2O,yaO2,yaN2,yaAr,yaCO)
  Hgin=HGAST(Tgin,ygCO2,ygH2O,ygO2,ygN2,ygAr,ygCO)
  Q1 =0.
C
C.....Iterate and find the exit air temperature.
C
  do 10 i=1,20
    Hao =HGAST(Tao,yaCO2,yaH2O,yaO2,yaN2,yaAr,yaCO)
    Qa  =MRa*(Hao-Hain)
    Hgo =Hgin - Qa/MRg
    Tgo =TGASH(Hgo,ygCO2,ygH2O,ygO2,ygN2,ygAr,ygCO)
C
C.....Calculate the fluid properties.
C
  Tavea=(Tain+Tao)*.5
  Taveg=(Tgin+Tgo)*.5
  Twall=0.25*Taveg+0.75*Tavea
  Pavea=(2.*Pain-dPa)*.5
  Paveg=(2.*PgIn-dPg)*.5
  Tfilmg=(Twall+Taveg)*.5
C
C.....Calculate the pressure loss on the gas-side.
C
  dPgl=PHXCF(MRg,ygCO2,ygH2O,ygO2,ygN2,ygAr,ygCO,Taveg,Tfilmg,
>           Paveg,length,OD,type,SnD,SpD,npn,npp)
C
C.....Pressure loss in bends.
C
  dPbg=0.
  dPg=dPgl*noPg+dPbg*(noPg-1.)
C
C.....Calculate the pressure loss inside the pipe.
C
  call PINPIP(MRpip,yaCO2,yaH2O,yaO2,yaN2,yaAr,yaCO,Tavea,Pavea,
>           ID,rough,dPfric,fric)
  if(noU.eq.0.)then
    dPfric=dPfric*totalL
  else
    dPfric=dPfric*totalL*2.*noU
  end if
C
C.....Pressure loss at entrance and exit.
C
  Roavea=ROGAS(Tavea,Pavea,yaCO2,yaH2O,yaO2,yaN2,yaAr,yaCO)

```

```

Vpip=MRpip/ROavea/PI/((ID/12./2.)**2)
dPloss=(Vpip**2)/2.*ROavea*(0.78+1.)/32.174/144.
C
C.....Total pressure loss in pipe.
C
      dPa=dPfric+dPloss
C
C.....Calculate inside heat transfer coefficient.
C
      hincnv=HINCON(MRpip,yaCO2,yaH2O,yaO2,yaN2,yaAr,yaCO,Tavea,
>                Pavea,ID,totalL)
      hin  =hincnv
C
C.....Calculate the outside heat transfer coefficient.
C
      hout=HHXCF(MRg,ygCO2,ygH2O,ygO2,ygN2,ygAr,ygCO,Taveg,Twall,
>                Paveg,length,OD,type,SnD,SpD,npn,npp,noU)
C
C.....Calculate U and UA
C
      U=1./(1./((ID/OD)*hin)+1./hout+OD/(2.*K*12.)*alog(OD/ID)+foul)
      UA=U*area
C
C.....Find the correction factor F.
C
      if(noPg.gt.1.)then
        Fcfhx=1.
      else
        Fcfhx=CORRHX(Tain,Tao,Tgin,Tgo,noU)
      end if
C
C.....Calculate the LMTD,Cp and UAreq.
C
      dt1=Tgin-Tao
      dt2=Tgo-Tain
      LMTD=(dt1-dt2)/alog(dt1/dt2)
C
C.....Calculate the total heat transfer and enthalpy of air at outlet.
C
      Qua=UA*Fcfhx*LMTD/3600.
      Q=(Qua+Qa)/2.
      if(1.gt.1.)then
        Q2=(Q+Q1)/2.
      else
        Q2=Q
      end if
      Hao=Q2/MRa+Hain
C
C.....Calculate the outlet temperature of air.
C
      Tao1=Tao
      Tao =TGASH(Hao,yaCO2,yaH2O,yaO2,yaN2,yaAr,yaCO)
C
C.....Check for convergence.
C

```

```

        if(abs(Q1/Q-1.)<.001)goto 40
        Q1=Q
10 continue
40 continue
C
C.....Check the velocity for erosion.
C
        Pao=Pain-dPa
        Pgo=Pgin-dPg
        call VEROSN(Paveg,Taveg,MRg,length,OD,SnD,SpD,nnp,Derosn,ROash,
>                ygCO2,ygH2O,ygO2,ygN2,ygAr,ygCO,Vmax,Versn)
C
C.....Make adjustments for leakage .
C
        call HXMIX(MRain,yaCO2,yaH2O,yaO2,yaN2,yaAr,yaCO,Tao,Pao,
>                MRgin,ygCO2,ygH2O,ygO2,ygN2,ygAr,ygCO,Tgo,
>                MRgo,yoCO2,yoH2O,yoO2,yoN2,yoAr,yoCO,To)
C
C.....Calculate the exergies and irreversibility.
C
        Pginab= 14.696 + .03613*Pgin
        Pgoab = 14.696 + .03613*Pgo
C
        Sain=SGASTP(Tain,Pain,yaCO2,yaH2O,yaO2,yaN2,yaAr,yaCO)
        Sao =SGASTP(Tao,Pao,yaCO2,yaH2O,yaO2,yaN2,yaAr,yaCO)
        Sgin=SGASTP(Tgin,Pginab,ygCO2,ygH2O,ygO2,ygN2,ygAr,ygCO)
        Sgo =SGASTP(To,Pgoab,yoCO2,yoH2O,yoO2,yoN2,yoAr,yoCO)
        Exain=(Hain-(Tds+459.67)*Sain)*MRain*1.0552
        Exao =(Hao-(Tds+459.67)*Sao)*MRao*1.0552
        Exgin=(Hgin-(Tds+459.67)*Sgin)*MRgin*1.0552
        Exgo =(Hgo-(Tds+459.67)*Sgo)*MRgo*1.0552
        IRR  = Exain+Exgin-Exao-Exgo
C
C.....Transport properties of both Streams.
C
        kg =KGASt (Taveg,ygCO2,ygH2O,ygO2,ygN2,ygAr,ygCO)
        ka =KGASt (Tavea,yaCO2,yaH2O,yaO2,yaN2,yaAr,yaCO)
        mua=MUGAST(Tavea,yaCO2,yaH2O,yaO2,yaN2,yaAr,yaCO)
        mug=MUGAST(Taveg,ygCO2,ygH2O,ygO2,ygN2,ygAr,ygCO)
C
C.....Print the results.
C
        write(8,1000)'....AIR GAS HEAT EXCHANGER...'
        txt1='flue gas'
        txt2='air'
        call HXPRIN(txt1,txt2,Tgin,Tain,Pginab,Pain,MRg,MRa,Tgo,Tao,
>                Pgoab,Pao,Cpg,Cpa,mug,mua,kg,ka,Exgin,
>                Exain,Exgo,Exao,type,SnD,SpD,nnp,npp,noPg,noU,OD,ID,K,rough,
>                length,lmax,height,width,area,Vmax,Versn,Fcfhx,hout,
>                hin,foul,U,UA,LMTD,Tfilmg,Twall,Q,IRR,dPa,dPamax,dPgmax,dPg)
1000 format(1x/10x,a)
        RETURN
        END

```

HEAT EXCHANGER SUBROUTINES

```

C*****
C
C   This subroutine calculates the pressure drop per unit
C   length and the friction factor inside the pipe. The
C   arguments in the subroutine are
C
C   MR      - Mass flow rate inside the pipe. (lbm/s)
C   y_      - Mole fractions of the gas flowing in the pipe.
C   Tave    - Average temperature inside the pipe. (F)
C   P       - Average pressure inside the pipe. (psia)
C   D       - Inside pipe diameter. (in)
C   ROUGH   - Roughness factor inside the pipe.
C   Pfric   - Frictional pressure drop per unit length. (psi/ft)
C   FRIC    - Friction factor inside the pipe.
C*****
C
C   SUBROUTINE PINPIP(MR,yCO2,yH2O,yO2,yN2,yAr,yCO,Tave,P,D,ROUGH,
C   > Pfric,FRIC)
C   REAL MU,MUGAST,MR
C   PI=ACOS(-1.)
C
C.....Properties of air.
C
C   RO= ROGAS(Tave,P,yCO2,yH2O,yO2,yN2,yAr,yCO)
C   MU=MUGAST(Tave,yCO2,yH2O,yO2,yN2,yAr,yCO)
C
C.....Calculate the Reynolds number.
C
C   AREA=PI*(D/12./2.)**2
C   VELOC=MR/RO/AREA
C   RE   =VELOC*RO*D/12./MU
C
C.....Calculate the friction factor.
C
C   FSM=0.316/RE**0.25
C   GUESS1=1./SQRT(FSM)
C   do 10 i=1,20
C     GUESS2=1.74-2.*ALOG10(2.*ROUGH+18.7*GUESS1/RE)
C     if(ABS(GUESS1/GUESS2-1.).LT.0.00001)goto 20
C     GUESS1=GUESS2
C 10 continue
C 20   FRIC=(1./GUESS2)**2
C
C.....Frictional pressure loss per unit length.
C
C   Pfric=FRIC/(D/12.)*RO*(VELOC**2)*0.5/32.174/144
C
C   return
C   end

```

```

*****
C
C   This function calculates the pressure drop on the gas-side
C   in a cross flow heat exchanger. The arguments in the function
C   are,
C
C   MR      - Mass flow rate of the shell side gases. (lbm/s)
C   y_      - Mole fraction of the shell side gases.
C   Tave    - Average temperature on the shell side. (F)
C   Twall   - Wall temperature on the shell side. (F)
C   P       - Average pressure on the shell side. (w.c)
C   HEIGHT  - Tube length per pass. (ft)
C   D       - Outside tube diameter. (in)
C   TYPE    - Type of tube layout. (inline = 1., staggered =2.)
C   SnD     - Normalized pipe spacing normal to the flow direction.
C   SpD     - Normalized pipe spacing parallel to the flow direction.
C   npn     - Number of pipes normal to the flow direction.
C   npp     - Number of pipes parallel to the flow direction.
C
*****
C
C   FUNCTION PHXCF(MR,yCO2,yH2O,yO2,yN2,yAr,yCO,Tave,Twall,P,HEIGHT,
C   >              D,TYPE,SnD,SpD,npn,npp)
C   REAL MR,MUwall,MUave,MUGAST,npn,npp
C
C.....Calculate the gas properties.
C
C   Pabs =14.696+.03613*P
C   MUwall=MUGAST(Twall,yCO2,yH2O,yO2,yN2,yAr,yCO)
C   MUave =MUGAST(Tave,yCO2,yH2O,yO2,yN2,yAr,yCO)
C   RO   =ROGAS(Tave,Pabs,yCO2,yH2O,yO2,yN2,yAr,yCO)
C
C.....Calculate the velocity of the gas in.
C
C   AREA=SnD*D/12.*(npn+1.)*HEIGHT
C   Vbulk=MR/RO/AREA
C
C.....Calculate the max velocity and Reynolds number.
C
C   if(SnD.LE.(2.*(SpD**2)-0.5))then
C     Vmax=Vbulk*SnD/(SnD-1.)
C   else
C     Vmax=Vbulk*SnD/(2.*SQRT((SnD**2)/4.+SpD**2)-1.)
C   end if
C
C
C   RE=RO*Vmax*D/12./MUave
C
C.....Friction coefficient(1:inline/2:Staggered)
C
C   if (TYPE.EQ.1.)then
C     TEMP=(SnD-1.)*(0.43+1.13/SpD)
C     FRIC=(0.044+0.08*SpD/TEMP)/RE**0.15
C   else
C     TEMP=(SnD-1.)*1.08

```

```

          FRIC=(0.25+0.118/TEMP)/RE**0.16
        end if
C
C.....Correction for temperature variation.
C
      y=.776*exp(-.545*RE**.256)
C
C.....Pressure loss
C
      PHXCF=FRIC*(Vmax**2)*RO*npp*((MUwall/MUave)**y)*.03613
C
      return
      end
C*****
C
C      This function calculates the convective heat transfer
C      coefficient inside the pipe surface. The arguments used
C      in the function are,
C
C      MR      - Mass flow rate inside the pipe. (lbm/s)
C      y_      - Mole fraction of the gas inside the pipe.
C      T      - Average temperature inside the pipe. (F)
C      P      - Average pressure inside the pipe. (psia)
C      D      - Inside diameter of the pipe. (in)
C      L      - Total length of a pipe. (ft)
C*****
C
      FUNCTION HINCON(MR,yCO2,yH2O,yO2,yN2,yAr,yCO,T,P,D,L)
      REAL K,MR,MU,MUGAST,KGAST,NU
      PI=ACOS(-1.)
C
C.....Properties of fluid at average temperature and pressure.
C
      Pr=PrGAST(T,yCO2,yH2O,yO2,yN2,yAr,yCO)
      MU=MUGAST(T,yCO2,yH2O,yO2,yN2,yAr,yCO)
      K = KGAST(T,yCO2,yH2O,yO2,yN2,yAr,yCO)
      RO= ROGAST(T,P,yCO2,yH2O,yO2,yN2,yAr,yCO)
C
C.....Reynolds number,
C
      AREA=PI*(D/12./2.)**2
      VELOC=MR/RO/AREA
      RE=VELOC*RO*D/12./MU
C
C.....Heat Transfer due to convection
C
      if((Pr.GT.0.5).AND.(Pr.LE.1.5))then
      NU=.0214*(RE**0.8-100.)*(Pr**0.4)*(1.+(D/12./L)**(2./3.))
      else
      NU=.012*(RE**0.87-280.)*(Pr**0.4)*(1.+(D/12./L)**(2./3.))
      end if
C
      HINCON=NU*K/D*12.
      end

```

```

C*****
C
C   This function calculates the heat transfer coefficient on
C   the outside surface of the pipe, in a cross-flow arrangement.
C   The arguments in the function are,
C
C   MR      - Mass flow rate of gas. (lbm/s)
C   y_      - Mole fraction of the shell side gas.
C   Tave    - Average shell side gas temperature. (F)
C   Twall   - Wall temperature on the shell side. (F)
C   P       - Average pressure on the shell side. (w.c)
C   HEIGHT  - Tube length per pass. (ft)
C   D       - Outside tube diameter. (in)
C   TYPE    - Type of tube arrangement.(inline=1., staggered=2.)
C   SnD     - Normalized pipe spacing normal to the flow.
C   SpD     - Normalized pipe spacing parallel to the flow.
C   npn     - Number of pipes normal to the flow.
C   npp     - Number of pipes parallel to the flow.
C   noU     - Number of U bends in a tube.
C
C*****
C
C   FUNCTION HHXCF(MR,yCO2,yH2O,yO2,yN2,yAr,yCO,Tave,Twall,P,HEIGHT,
C   >               D,TYPE,SnD,SpD,npn,npp,noU)
C
C   REAL MR,K,MU,MUGAST,KGAST,NULAM,NUTURB,NUROW,NUBANK,
C   >       NROWS,NPN,NPP,NOU
C
C   PI=ACOS(-1.)
C
C.....Calculate the gas properties.
C
C   Pabs=14.696+.0316*P
C   RO= ROGAS(Tave,Pabs,yCO2,yH2O,yO2,yN2,yAr,yCO)
C   K= KGAST(Tave,yCO2,yH2O,yO2,yN2,yAr,yCO)
C   MU=MUGAST(Tave,yCO2,yH2O,yO2,yN2,yAr,yCO)
C   Pr=PrGAST(Tave,yCO2,yH2O,yO2,yN2,yAr,yCO)
C
C.....Calculate the velocity of gas at the inlet.
C
C   AREA=SnD*D/12.*(npn+1.)*HEIGHT
C   Vgin=MR/RO/AREA
C
C.....Calculate the void fraction.
C
C   if(SpD.GE.1.)then
C     PSY=1.-PI/4./SnD
C   else
C     PSY=1.-PI/4./SnD/SpD
C   end if
C
C.....Calculate the Reynolds number.
C
C   RE=Vgin*(PI*D/12./2.)*RO/MU/PSY
C

```

```

C.....Calculate the temperature dependance of fluid properties.
C
  FK=(Tave/Twall)**0.12
C
C.....Calculate the arrangement factor.
C
  if(TYPE.EQ.1.)then
    f=1.+7*(SpD/SnD-0.3)/((PSY**1.5)*((SpD/SnD+0.7)**2))
  else
    f=1.+2./3./SpD
  end if
C
C.....Calculate the Nusselt number for the tube bank.
C
  NULAM=.664*(RE**0.5)*(Pr**(1./3.))
  NUTURB=.037*(RE**0.8)*Pr/(1.+2.443*(RE**(-0.1))*(Pr**(2./3.)-1.))
  NUROW =FK*(0.3+(NULAM**2+NUTURB**2)**0.5)
C
  if(noU.NE.0.)then
    NROWS=npp+2.*noU
  else
    NROWS=npp
  end if
C
  if(NROWS.GE.10.)then
    NUBANK=f*NUROW
  else
    NUBANK=(1.+(NROWS-1.)*f)*NUROW/NROWS
  end if
C
C.....Calculate the heat transfer coefficient.
C
  HHXCF=NUBANK*K/PI/D*12.*2.
C
  return
end
C
C*****
C
C  This function calculates the correction factor F in a cross
C  flow heat exchanger. The arguments used in the function are,
C
C  Tcfin - Inlet temperature of the cold gas. (F)
C  Tcfo  - Outlet temperature of the cold gas. (F)
C  Thfin - Inlet temperature of the hot gas. (F)
C  Thfo  - Outlet temperature of the hot gas. (F)
C  noU   - Number of 'U' bends in a tube.
C
C*****
C
FUNCTION CORRHX(Tcfin,Tcfo,Thfin,Thfo,noU)
C
REAL K,Knew,noU
f(K)  =exp(K*X)*(cosh(K*X)+(1-K)*sinh(K*X))-1./(1.-p)
fprm(K)=exp(K*X)*((2.-K)*X*cosh(K*X)+(2.*X-K*X-1.)*sinh(K*X))

```

```

C
  p=(Tcfin-Tcfo)/(Tcfin-Thfin)
  q=(Thfo-Thfin)/(Tcfin-Thfin)
  if(p.EQ.q)then
    r0=1.-p
  else
    r0=(p-q)/alog((1.-q)/(1.-p))
  end if
C
  if(noU.NE.0.)then
C
  X=p/q
  K=1.-exp(-q/2./r0)
  do 10 i=1,20
    Knew=K-f(K)/Fprm(K)
    if(abs(1.-K/Knew).LT.0.001)gotol00
    K=Knew
  10 continue
C
  100 r=-q/alog(1.-Knew)*0.5
  else
    r=q/alog(1./(1.-q/p*alog(1./(1.-p))))
  end if
C
  CORRHX=r/r0
C
  return
end
C
C*****
C
C   This subroutine calculates the maximum velocity on the shell
C   side and the maximum allowable velocity on the shell side to
C   prevent tube erosion.  The arguments in the subroutine are,
C
C   Pave   - Average pressure on the shell side. (w.c)
C   Tave   - Average temperature on the shell side. (F)
C   MR     - Mass flow rate of the shell side gases. (lbm/s)
C   length - Tube length per pass. (ft)
C   OD     - Outside tube diameter. (in)
C   SnD    - Normalized pipe spacing normal to the flow.
C   SpD    - Normalized pipe spacing parallel to the flow.
C   npn    - Number of pipes normal to the flow.
C   Dash   - Maximum diameter of the hardest particulate
C           material in the gas stream. (microns)
C   ROash  - The density of the above particles. (lbm/cu.ft)
C   y_     - Mole fraction of the shell side gases.
C   Vmax   - Maximum velocity on the shell side. (ft/s)
C   Versn  - Maximum allowable velocity on the shell side. (ft/s)
C
C*****
C
C   SUBROUTINE VEROSN(Pave,Tave,MR,length,OD,SnD,SpD,npn,Dash,ROash,
>   yCO2,yH2O,yO2,yN2,yAr,yCO,Vmax,Versn)
C

```

```

      real Mash,MR,length,npn
      PI=acos(-1.)
C
      Pabs=14.696+.03613*Pave
      RO=ROGAS(Tave,Pabs,yCO2,yH2O,yO2,yN2,yAr,yCO)
      Area=SnD*OD/12.*(npn+1.)*length
      Vbulk=MR/RO/AREA
C
C.....Calculate the maximum velocity.
C
      if(SnD.LE.(2.*(SpD**2)-0.5))then
          Vmax=Vbulk*SnD/(SnD-1.)
      else
          Vmax=Vbulk*SnD/(2.*sqrt((SnD**2)/4.+SpD**2)-1.)
      end if
C
C.....Calculate the velocity of erosion.
C
      Mash=PI*((Dash/1.E 6)**3)/6.*ROash*16.018
      Versn=.005382*.7*3.2808/(Mash**.5)
C
      return
      end
C
C.....*****
C
C.....This subroutine prints the heat exchanger data.
C
C      ----- Printing heat exchanger data -----
C
      subroutine HXPRIN (txt1,txt2,Tgin,Tpin,Pginab,Ppin,
      /      MRg,MRp,Tgo,Tpo,Pgoab,Ppo,Cpg,Cpp,mug,mup,kg,kp,EXgin,
      >      EXpin,EXgo,EXpo,type,SnD,SpD,npn,npp,noPg,nu,OD,ID,k,
      /      rough,length,lmax,height,width,area,VMAX,versn,
      >      Fcfhx,hout,hin,foul,U,UA,LMTD,Twmax,Tw,
      >      Q,IRR,dPp,dPpmax,dPgmax,dPg)
C
      character*10 txt1,txt2,arngm
      real MRg,MRp,length,lmax,ID,LMTD,IRR,mug,mup,kg,kp,f,npn,npp,nu
C
      if ( type .eq. 1.) then
          arngm = 'in-line'
      else
          arngm = 'staggered'
      endif
      write(8,1000) 'Flow conditions:',txt1,txt2
      write(8,1200) 'Temperature at inlet, F      ',Tgin,Tpin
      write(8,1200) 'Pressure at inlet, psia     ',Pginab,Ppin
      write(8,1200) 'Massflow, lbm/sec :           ',MRg,MRp
      write(8,1200) 'Temperature at exit, F      ',Tgo,Tpo
      write(8,1200) 'Pressure at exit, psia     ',Pgoab,Ppo
      write(8,1200)
      write(8,1200) 'Cp - values, btu/lbm F      ',Cpg,Cpp
      write(8,1250) 'Viscosity, lbm/s ft      ',mug,mup
      write(8,1250) 'Conductivity, btu/h ft R      ',kg,kp

```

```

write(8,1200) 'Exergy at inlet, KW      :',EXgin,EXpin
write(8,1200) 'Exergy at exit, KW     :',EXgo,EXpo

C
write(8,1100) 'Specifications of Heat Exchanger:'
write(8,1300)
write(8,1500) 'Tube arrangement:           ',arrngm
write(8,1300) 'Spacing of tubes normal to flow, Sn/d:   ',SnD
write(8,1300) 'Spacing of tubes parallel to flow, Sp/d:  ',SpD
write(8,1300) 'Number of tubes normal to flow:          ',npn
write(8,1300) 'Number of tubes parallel to flow:        ',npp
write(8,1300) 'Number of passes on the gas-side:        ',noPg
write(8,1300) 'Number of U's:                          ',nu
write(8,1300) 'Outside diameter of pipes:              ',OD
>   ',inches'
write(8,1300) 'Inside diameter of pipes:                ',ID
>   ',inches'
write(8,1300) 'Thermal conductivity of the tubes:      ',k
>   ',btuh/ft/F'
write(8,1300) 'Roughness factor inside the tubes (k/D): ',rough
write(8,1300) 'Length of the tubes:                     ',length
>   ',ft'
write(8,1300) 'Maximum allowable length of tubes:       ',lmax
>   ',ft'
write(8,1300) 'Height of the heat exchanger:            ',height
>   ',ft'
write(8,1300) 'Width of the heat exchanger:              ',width
>   ',ft'
write(8,1300) 'Total heat transfer area:                 ',area
>   ',sqft'
write(8,1300) 'Maximum velocity:                         ',VMAX
>   ',ft/sec'
write(8,1300) 'Maximum velocity for erosion             ',versn
>   ',ft/sec'

C
write(8,1100) 'Heat Transfer Data:'
write(8,1300)
write(8,1300) 'Correction factor due to cross-flow: ',Fcfhx
write(8,1300) 'H out - heat transfer coefficient:  ',hout,
>   'btu/h/sqft/F'
write(8,1300) 'H in - heat transfer coefficient:   ',hin,
>   'btu/h/sqft/F'
write(8,1300) 'Fouling in heat exchanger:           ',foul
write(8,1300) 'U - Overall heat transfer coefficient',U,
>   'btu/h/sqft/F'
write(8,1300) 'UA - value:                           ',UA,'btu/h/F'
write(8,1300) 'Log-Mean-Temperature-Difference :     ',LMTD,'F'
write(8,1300) 'Maximum wall temperature:             ',Tmax,'F'
write(8,1300) 'Average wall temperature:             ',Tw,'F'
write(8,1300) 'Total heat transfer:                   ',Q*1.0552,
>   'kW'
write(8,1300) 'Irreversibility:                          ',IRR,'kW'

C
C
write(8,1100) 'Pressure drops:'
write(8,1300)

```

```

write(8,1300) 'Pressure drop inside pipes           : ',dPp
>      , 'psi'
write(8,1300) 'Allowable Pressure drop in pipe:     : ',dPpmax
>      , 'psi'
write(8,1300) 'Pressure drop on gas side           : ',dPg
>      , 'in W.C.'
write(8,1300) 'Allowable pressure drop on gas side : ',dPgmax
>      , 'in W.C.'
write(8,1300)

C
1000  format(1x/10x,a,22x,a,11x,a)
1100  format(1x/10x,a)
1200  format(15x,a,2f16.3)
1250  format(15x,a,2e16.5)
1300  format(15x,a,f14.3,2x,a)
1500  format(15x,a,14x,a)
1600  format(15x,a,i14,2x,a)

C
      end

C
C*****
C
C      This subroutine calculates the mole fractions of the gas
C      stream resulting from the mixing of two gas streams. The
C      arguments used in the subroutine are,
C
C      MRi_   - Mass flow rate of an incoming gas stream. (lbm/s)
C      yi_    - Mole fractions of an incoming gas stream
C      yo_    - Mole fractions of the resulting gas stream.
C
C*****
C
C      subroutine MOLFRA(MRi1,yi1CO2,yi1H2O,yi1O2,yi1N2,yi1Ar,yi1CO,
>      MRi2,yi2CO2,yi2H2O,yi2O2,yi2N2,yi2Ar,yi2CO,
>      yoCO2,yoH2O,yoO2,yoN2,yoAr,yoCO)

C
C      real MRi1,MRi2,MRo,mO2,mN2,mCO2,mH2O,mAr,mCO,MOLi1,MOLi2,MOLo,
>      Mi1,Mi2

C
C      data mO2,mCO2,mN2,mH2O,mAr/32.,44.01,28.015,18.016,39.944/
C      data mCO/28.01/

C
C.....molar mass of inlet streams.
C
C      Mi1=yi1O2*mO2+yi1N2*mN2+yi1CO2*mCO2+yi1Ar*mAr+yi1H2O*mH2O+
>      yi1CO*mCO
C      Mi2=yi2O2*mO2+yi2N2*mN2+yi2CO2*mCO2+yi2Ar*mAr+yi2H2O*mH2O+
>      yi2CO*mCO

C
C.....number of moles (pr.sec)
C
C      MOLi1=MRi1/Mi1
C      MOLi2=MRi2/Mi2
C      MOLo=MOLi1+MOLi2

C

```

```

yoCO2=(y11CO2*MOLi1+y12CO2*MOLi2)/MOLo
yoH2O=(y11H2O*MOLi1+y12H2O*MOLi2)/MOLo
yoO2 =(y11O2*MOLi1 +y12O2*MOLi2 )/MOLo
yoN2 =(y11N2*MOLi1 +y12N2*MOLi2 )/MOLo
yoAr =(y11Ar*MOLi1 +y12Ar*MOLi2 )/MOLo
yoCO =(y11CO*MOLi1 +y12CO*MOLi2 )/MOLo
C
  return
  end
C
C*****
C
C   This subroutine calculates the mole fractions, mass flow
C   rate and the temperature of a gas stream resulting from the
C   mixing of two gas streams. The arguments used in the subroutine
C   are,
C
C   MRi_   - Mass flow rate at the inlet. (lbm/s)
C   yi_    - Mole fractions at the inlet.
C   Ti_    - Temperature at the inlet. (F)
C   Pi_    - Pressure at the inlet. (psia)
C   MRo    - Mass flow rate at the outlet. (lbm/s)
C   yo_    - Mole fractions at the outlet.
C   To     - Temperature at the outlet. (F)
C
C*****
C
  subroutine HXMIX(MRi1,y11CO2,y11H2O,y11O2,y11N2,y11Ar,
>                 y11CO,Ti1,Pi1,MRi2,y12CO2,y12H2O,
>                 y12O2,y12N2,y12Ar,y12CO,Ti2,
>                 MRo,yoCO2,yoH2O,yoO2,yoN2,yoAr,yoCO,To)
C
  real MRi1,MRi2,MRo

  MRo=MRi1+MRi2
  Hi1=HGAST(Ti1,y11CO2,y11H2O,y11O2,y11N2,y11Ar,y11CO)
  Hi2=HGAST(Ti2,y12CO2,y12H2O,y12O2,y12N2,y12Ar,y12CO)
  Ho =(MRi1*Hi1 + MRi2*Hi2)/MRo
C
  call MOLFRA(MRi1,y11CO2,y11H2O,y11O2,y11N2,y11Ar,y11CO,
>            MRi2,y12CO2,y12H2O,y12O2,y12N2,y12Ar,y12CO,
>            yoCO2,yoH2O,yoO2,yoN2,yoAr,yoCO)
C
  To=TGASH(Ho ,yoCO2,yoH2O,yoO2,yoN2,yoAr,yoCO)
C
  return
  end

```

Appendix C

INPUT DATA TO HEAT EXCHANGER MODEL

Appendix C

INPUT DATA TO HEAT EXCHANGER MODEL

	Air	Flue Gas
Mass flow rate, (lbm/s)	: 36.6	44.0
Pressure (psi)	: 132.4	15.15
Temperature at inlet, (F)	: 597.53	2400.0
Temperature at exit, (F)	: 1730.	

Mole Fractions

CO2	: .003	.0627
H2O	: .0107	.1375
O2	: .2073	.1144
N2	: .7726	.6767
Ar	: .0092	.0081
CO	: .00001	.0006

Conductivity of pipe material 'K', (Btu/sq.ft F)	= 24.2
Roughness 'Rough'	= .002
Fouling in the heat exchanger 'foul'	= .005
Density of the dust particles 'ROash', (lbm/cu.ft)	= 44.
Diameter of the dust particles 'Derosn', (microns)	= 500
Percentage leakage 'leakge'	= 1.5
Inside pipe diameter 'ID', (in)	= .55
Outside pipe diameter 'OD', (in)	= 1.05
Number of pipes parallel to the flow 'npp'	= 20
Number of passes on gas-side 'noPg'	= 3
Number of passes on air side, 'noU'	= 0
Type of tube arrangement , (1=inline, 2=staggered)	= 1.
Maximum tube length 'lmax', (ft)	= 10.5
Maximum allowable pressure drop on air-side 'dPamax', (psi)	= 5.0
Maximum allowable pressure drop on gas-side 'dPgmax', (w.c)	= 12.0